

Developing a More Efficient Method of Space Propulsion for Mars Transport

Duke Mechanical Engineering Senior Design 2023-24

Monday, April 29, 2024

Alejandro Assael

Noah Falbaum

Dadmehr Ghasemfar

Derrick Roseman

Swetha Sekhar

Shane Simkin

Table of Contents

Executive Summary	7
Background.....	8
Potential Impacts of the Solution.....	8
Current Solutions and Limitations	8
Client Needs and Design Criteria.....	9
Client Needs.....	9
Design Criteria	10
Table 1: Propulsion System Primary Design Criteria	10
Table 2: Secondary Design Criteria – Small Scale ERT Specific	10
Function Analysis and Journey Map.....	12
Functions.....	12
Figure 1: Function FAST Diagram	13
Journey Map.....	13
Table 3: Journey Map, tabular form.....	15
Ideation and Design Selection	16
Idea Generation.....	16
Idea Selection.....	16
Idea Reflection and Refinement.....	17
Engineering Analysis	18
Full System Computational Model	18
Figure 2: Heating Section Simplified Model	19
Table 4: Values for Variables and Constants	20
Heating Analysis	21
Figure 3: Heating Section with Wire Wrap.....	21
Table 5: Summary of Heating Element Calculations.....	21
Structure Analysis	22
Testing.....	22
Preliminary Testing	22
Figure 4: Plot of the output volumetric flow rate at nozzle exit [m ³ /s]	23
Figure 5: Three plots of the output velocity at nozzle exit [in m/s]	24
Build 1 Testing	24
Table 6: Steady State Heated Tests – Build 1.....	25
Figure 6: Plots for input pressure [psi], output temperature [psi], and thrust [N] vs time [sec].	26

Table 7: Comparison between Theory and Experiment	26
Design and Design Components	27
How the System Works	27
Complete Assembly	28
Subsystem/Component 1: Nozzle	28
Figure 8: Annotated Cross Section Drawing of General Nozzle Shape.....	29
Subsystem/Component 2: Heating Section.....	30
Figure 10: CAD of Heating Section.....	30
Figure 11: Real-Life Image of Heating Section	30
Subsystem/Component 3: Inlet Section	31
Figure 12: CAD of Inlet Section.....	31
Figure 13: Real-Life Image of Image Section.....	31
Subsystem/Component 4: Thrust Stand	31
Figure 14: CAD of Thrust Stand.....	32
Design Implications	33
Holistic Impact of the Project and Design Process	33
Qualitative Life Cycle Analysis	34
Material Impact.....	34
Table 8: Material Impact for Physical Build.....	35
Total Energy Consumption	39
Emissions	40
Positive Environmental Impacts	40
Future Changes	41
Recommendations and Conclusions	42
Acknowledgements.....	42
References.....	43
Appendix.....	44
1. User Manual.....	44
Appendix A: Use Instructions	44
2. Fabrication Instructions	45
Appendix A: Parts Index	45
Table 1: Part Numbers and Descriptions.....	45
Appendix B: Part Manufacturing Instructions	47
Appendix C: Assembly Instructions	48

3.	Brainstorming Supplements.....	51
	Appendix A: Pictorial Journey Map.....	51
	Appendix B: Brainstorming Idea List.....	53
	Appendix C: Morph Chart	60
	Appendix D: Idea Selection – Filters 1 and 2	61
	Appendix E: Decision Weighting Plot and Pugh Matrices	64
4.Engineering Part Drawings	
67	
	Appendix A: Linear Rail Mating Plate	67
	Figure 1: Dimensioned Drawing.....	67
	Appendix B: T Slot Straight Linear Plate Connector.....	68
	Figure 1: Dimensioned Drawing.....	68
	Appendix C: T Slot	69
	Figure 1: Dimensioned Drawing.....	69
	Appendix D: Corner Gusset Bracket	70
	Figure 1: Dimensioned Drawing.....	70
	Appendix E: Linear Rail	71
	Figure 1: Dimensioned Drawing.....	71
	Appendix F: Linear Rail Bearings	72
	Figure 1: Dimensioned Drawing.....	72
	Appendix G: Stainless Steel Tube.....	73
	Figure 1: Dimensioned Drawing.....	73
	Appendix H: Ceramic Sleeve.....	74
	Figure 1: McMaster Product Detail Page.....	74
	Appendix I: Nozzle (100 psi Design)	75
	Figure 1: Dimensioned Drawing.....	75
	Appendix J: Force Sensor Mount.....	76
	Figure 1: Dimensioned Drawing.....	76
	Appendix K: Corner Bracket	77
	Figure 1: Dimensioned Drawing.....	77
5.Engineering Assembly Drawings	
78	
	Appendix A: Complete Assembly with Balloon Callouts.....	78
	Figure 1: Full Assembly Engineering Drawing	80

6.	Bill of Materials
	81
	Appendix A: As-Built Bill of Materials	81
	Table 1: Tabular Bill of Materials	81
7.	Specification Sheets	86
	Appendix A: Formlabs High Temp v2 Resin	86
	Appendix B: Formlabs Durable Resin	91
	Appendix C: Formlabs Nylon 12 Sintering Powder	94
	Appendix D: Stratasys ABS Filament.....	97
	Appendix E: Stratasys PC-ABS Filament.....	107
	Appendix F: Stratasys ABS-CF10 Filament	119
	Appendix G: Ceramic Sleeving	129
8.	Computational Model Code.....	130
	Appendix A: MATLAB Code	130
9.	Other Software Code.....	132
	Appendix A: Load Cell Arduino Code.....	132
	Appendix B: Load Cell Library	146
10.	Analysis Supplements.....	150
	Appendix A: MATLAB Plots.....	150
	Appendix B: Heating Calculations	154
	Appendix C: Computational Model Calculations	156
11.	Design Documentation.....	157
	Appendix A: Box Folder Access	157
	Appendix B: Meeting and Process Notes/Documentation.....	158
	Appendix C: Ideation Process CAD	176
	Figure 1: 13 Point Interpolation-Based Rao Nozzle	176
	Figure 2: Sketch Basis of 13 Point Rao Nozzle	177
	Figure 3: Draft Heater Structure	177
	Figure 4: Draft Nozzle with Cooling Channels.....	178
	Appendix D: Ideation Calculations.....	179
	Figure 1: Maple Worksheet.....	180
	181
	Figure 2: Nozzle Design Parameters – Spreadsheet Screenshots	184
12.	Final Budget
	187

Appendix A: Purchased Materials Budget.....	187
Table 1: Compiled Purchases	187
13. Client Provided Resources.....	190
Appendix A: Rocket Science 101	190
Appendix B: Rocket Science 101 Part 2	205
Appendix C: Atomic Rocket	210

Executive Summary

112 years ago, the Wright brothers first took flight in air. 55 years ago, mankind first step foot on the moon. In time, humans will set foot on the next frontier: Mars. There are many obstacles to overcome before such a journey can become reality. Existing rocket propulsion methods are both too inefficient and unreliable to fit the mission criteria for a potential Mars mission. New engines would not need to have such a large thrust, because it would be used only in the vacuum of space, but it would need to make the same amount of fuel last for far longer without issue.

The group determined several important design criteria for any given design. Firstly, it had to be safely constructed within the set budget and the tools readily available to the team. Designs that passed these criteria then had to be judged by the secondary criteria: an ISP of at least 150 s, a thrust of at least 0.1 N, and materials strong enough to withstand temperatures of 800 K as well as pressures of 1 Bar. As a potential solution to this dilemma, the team developed the Electric Resistive Thermal Propulsion (ERTP) engine, which converts electrical energy to thermal energy, thereby accelerating fuel and generating thrust. Theoretically, by avoiding combustion of the fuel, the resulting engine can be more reliable and efficient than traditional counterparts, despite emitting significantly less thrust.

To verify this the team created a mathematical model based on the underlying thermodynamic equations. From there a scaled down prototype was developed to compare the computational with experimental results. In the prototype, pressurized air was fed into a tube wrapped in nichrome wire. When a current flows through this wire, thermal energy is emitted and transferred to the air passing through the tube. The air then is accelerated by the thermal energy and moves through the converging-diverging nozzle to generate thrust.

Preliminary testing resulted in an ISP of ____ and a thrust of 1.6 N (highest values achieved reported here, see below for more detail). These results are promising as multiple compromises were made to maintain the safety criteria at the expense of thrust including using air as fuel, testing in normal atmospheric conditions, and limiting the power draw to the wire. Still, the results show that this design has maintains acceptable thrust numbers while having significantly greater efficiency and reliability than existing designs.

Background

Current propulsion technologies available for space missions are primarily chemical-based and are efficient for short distances like trips to the moon or satellites into orbit. However, these technologies fall short for long-duration missions, such as those required to reach Mars or explore deeper into our solar system. The limitations include high fuel requirements and the mass of the spacecraft, inefficiency over longer distances, and the environmental impact of launching and operating these systems. There is a pressing need for a more sustainable, efficient, and longer-lasting propulsion method to meet the future demands of interplanetary travel.

The Electric Resistive Thermal (ERT) propulsion system was proposed by the client Robert Hickman, a visionary in aerospace engineering with academic credentials from Stanford University and the University of Southern California, and professional experience at Aerospace Corporation. His involvement suggests a significant alignment with the interests of key industry players like NASA and the Space Force, indicating that the solution has potential industrial viability and could fulfill a critical role in future space programs.

The importance of developing an efficient long-duration space propulsion system cannot be overstated. As humanity's interest in exploring and possibly colonizing other planets grows, so does the need for technology that can economically and safely transport materials and people across vast distances in space. The ability to conduct prolonged missions would significantly enhance scientific research opportunities, allowing for more comprehensive studies of celestial bodies, and potentially pave the way for manned missions beyond the moon.

Potential Impacts of the Solution

Societal Impact: A successful solution like the ERTP could revolutionize space travel, making it more accessible and less costly. This accessibility could spur new industries and educational opportunities, fostering a broader public understanding of space and science.

Industry Impact: For the aerospace industry, the adoption of ERTP technology could lead to new standards in spacecraft design, focusing on sustainability and efficiency. This could catalyze further innovations in materials science, engineering, and energy utilization.

Environmental Impact: One of the significant advantages of the ERTP system, as evidenced in the project reports, is its minimal environmental impact compared to traditional propulsion methods. Using electricity to heat propellant and focusing on materials that are less harmful reduces the carbon footprint of launches and operations. Additionally, the technology aims to utilize hydrogen, a clean fuel, which only emits water vapor, thereby addressing the critical environmental concerns associated with current rocket fuels.

Current Solutions and Limitations

Presently, the most commonly used propulsion methods for space travel are chemical combustion rockets, which rely on the combustion of rocket fuel to generate thrust. While effective for short missions, they are less suitable for longer missions due to the vast amounts of fuel needed and the environmental toll of their emissions. Another method in use includes ion thrusters, which, although efficient and capable of running for extended periods, produce very low thrust, making them impractical for human transportation over long distances.

Client Needs and Design Criteria

Client Needs

The client has asked the team to develop the ERTP concept as a potential method of space propulsion. In addition, the client has asked the group to compile these findings into a deliverable for NASA's mission to Mars. Based on this framework, the client requires that the team design, build, and test a small-scale version of the ERTP engine as well as create an analytical model to validate the experimental results. The final design prototype is an engine that has the following specifications (which are also the design constraints for this project):

- Electrical Resistance Thermal Propulsion

The chief need of the client is a working model of the ERTP engine. This involves designing a heat exchanger to transform electrical energy into thermal energy stored in the fuel. The design prototype must also have measurable outputs to gather data from.

- System components: Heat exchanger to a converging-diverging nozzle

In addition to developing the ERTP mechanism, thrust will largely be derived from the design of a converging-diverging nozzle to accelerate the fuel as it exits the system. There are no specific target values for this device as long as it increases the velocity of the heated air.

- Analytical Model

The experimental findings from the ERTP must be validated by the underlying thermodynamic equations governing propulsion mechanisms. Developing a working analytical model is required by the client to support test data.

- NASA Report

The design specifications and output data must be compiled into a report for NASA by the end of the project. This includes comparisons between the analytical and experimental models as well as comparisons between the ERTP and other existing propulsion methods.

These specifications will allow the team to complete analysis of a small-scale version of the resistive heating rocket engine technology in the process of being patented by the client. The results will be used to verify models that will then be used to write a proposal to NASA during their mid-year proposal solicitations.

Design Criteria

Having defined the project goals, the team laid out the following design criteria, describing the small-scale ERTP thruster (Tables 1 and 2).

Table 1: Propulsion System Primary Design Criteria

ID	Criterion	Description	Specific Target
1	Physical Feasibility	Must be realistic, making use of existing materials and manufacturing methods	Y/N
2	Safety	The design must be developed with a focus on safety	Y/N
3	Budget	Prototyping must stay within budget	<\$2000

Table 2: Secondary Design Criteria – Small Scale ERT Specific

ID	Criterion	Description	Specific Target
4	Engine: Efficiency	Design must have an improved ISP from traditional chemical propulsion	$\text{ISP} \geq 150 \text{ s}$
5	Engine: Thrust	Amount of thrust produced by system	$F \geq 0.1 \text{ N}$
6	HX: Effectiveness	Design must be capable of transferring requisite heat for propulsion system	$\Delta T_{\text{fuel}} \in [100, 700] \text{ K}$
7	HX: Robustness	Design must be capable of withstanding the expected temperatures and pressures of the propulsion system (the inlet conditions of the nozzle)	$T = 800 \text{ K}$ $P = 1 \text{ bar}$

Below are explanations and supporting calculations for each of the design criteria listed in the table. They are addressed in the list below based on the IDs in Tables 1 and 2.

1. Feasibility
 - a. It is important that the small scale propulsion system proposal makes use of readily acquired materials and manufacturing processes so that it can be built and tested on Duke's campus. The full scale will not be feasible to build on campus, but should make physical sense and have avenues available for its development and manufacturing. By following this guideline, the team may ensure that the report submitted to NASA is as ready to produce as possible.
2. Safety
 - a. In physically developing the heat exchanger subsystem, it is essential that the team pays the utmost attention to physical safety and best practices of engineering. The team expects to be working with fluids at high temperatures and pressures, which, when improperly handled, can pose significant risks to the physical safety of team members.
3. Budget
 - a. The cost for the propulsion design should not exceed \$2000.
4. Efficiency
 - a. ISP is a measure of the amount of thrust produced by a rocket engine per unit of propellant mass. Generally, rocket engines making use of conventional chemical

propulsion methods achieve ISP values between 175s and 300s. The greatest ISP achieved by a conventional rocket engine is around 500s. In developing novel propulsion methods like the ERTP, the team hopes to achieve an ISP value greater than 500s (for the full scale model) to demonstrate its superiority. For the small scale, current calculations expect the ISP to be around 180 s, so the goal is to be able to reach ISP = 150 s with the physical prototype to verify the assumptions and calculations that have been done, which can then be used when doing analysis on the full scale model to get a better prediction of what the ISP for the full scale model would look like.

5. Thrust

- a. The two main types of propulsion methods used in rockets are ion propulsion and thermal propulsion. Ion propulsion is capable of producing very high ISPs, (1500 s to 6000 s) however it typically performs at very low thrust levels. In the latest ion propulsion test conducted by NASA in 2017, they were able to generate 1.1 lbf of thrust with an ISP of 1800 s using 102 kW of power. Scaling these ion thrusters has been very difficult to achieve and not much progress had been made since then. However, using the ERTP method that the client is proposing (thrust predictions pending for the resistive heating engine), the team could see an improvement of 3 to 6 times the thrust to electrical power ratio at a comparable power level. Using the knowledge available from the research and physical tests that have been conducted using similar propulsion methods, the team's goal is to have a full scale system that can produce a thrust of at least 1.5 lbf. For the small scale system, the goal is to get to 0.1 N since calculations predict 0.19 N of thrust given.

6. Effectiveness

- a. The numbers provided are for the small scale model, which will be a proof of concept for the electric resistance based heat exchanger, assuming an incoming flow with a temperature of at least 100 K and an inlet nozzle temperature of 800 K.

7. Robustness

- a. As listed above, the temperature requirement comes from a choice of inlet temperature that would not get too close to the melting point of Titanium (1000 K). The desired fuel temperature (3100 K) provided by the client will be used for the full scale model. For the pressure, the plan is to run the entire system at the same pressure so that auxiliary systems are not required to change pressure between processes (minimizes loss from transfers). The current nozzle calculations for both the H₂ nozzle (full scale) and the H₂O nozzle (small scale) are in the spreadsheet linked through Box under Appendix B.

Function Analysis and Journey Map

The system functions and accompanying journey map dictated the design process of the ERTP thruster. In particular, by creating a function list and journey map the group was able to determine the critical features of the ERTP when in deployment as well as extra features needed for testing. For example, the converging-diverging nozzle of the thruster must be shaped differently for use in space versus Earth's atmosphere. In addition, it became clear that the Earth based prototype required a special testing bed in order to record certain system outputs (e.g. thrust, pressure, etc.). When the project constraints limited the choices the group could make, the design analysis helped order the functions of the project to help with idea generation and application.

Functions

To meet the client's needs, the team identified several main functions of the design concept, each with subfunctions. These are listed in verb-noun form, below:

1. Propellant Flow
 - 1.1. Prevent Backflow
 - 1.2. Control Flow Rate
 - 1.3. Measure Pressure
 - 1.4. Report and Record Pressure data
2. Propellant Heating
 - 2.1. Contain Gas
 - 2.2. Release Excess Pressure
 - 2.3. Prevent Leaking
 - 2.4. Prevent burst tank
 - 2.5. Measure temperature
 - 2.6. Report and Record temperature data
 - 2.7. Prevent thermal backwash
3. Convert electrical energy to heat
 - 3.1. Control heat input
 - 3.2. Prevent heating element damage
 - 3.3. Reduce wasted heat
 - 3.4. Prevent fire
 - 3.5. Limit voltage and current
4. Generate thrust
 - 4.1. Measure thrust
 - 4.2. Report and Record thrust data

All of these functions are critical to the function of the ERTP system. The primary ERTP system requirements are thrust, ISP, and burn time. All functions must work in harmony to accomplish these objectives. As such, it does not make sense to assign specific functions to individual client needs. Rather, the team simply must build out all listed functions to produce an operational engine that satisfies the requirements.

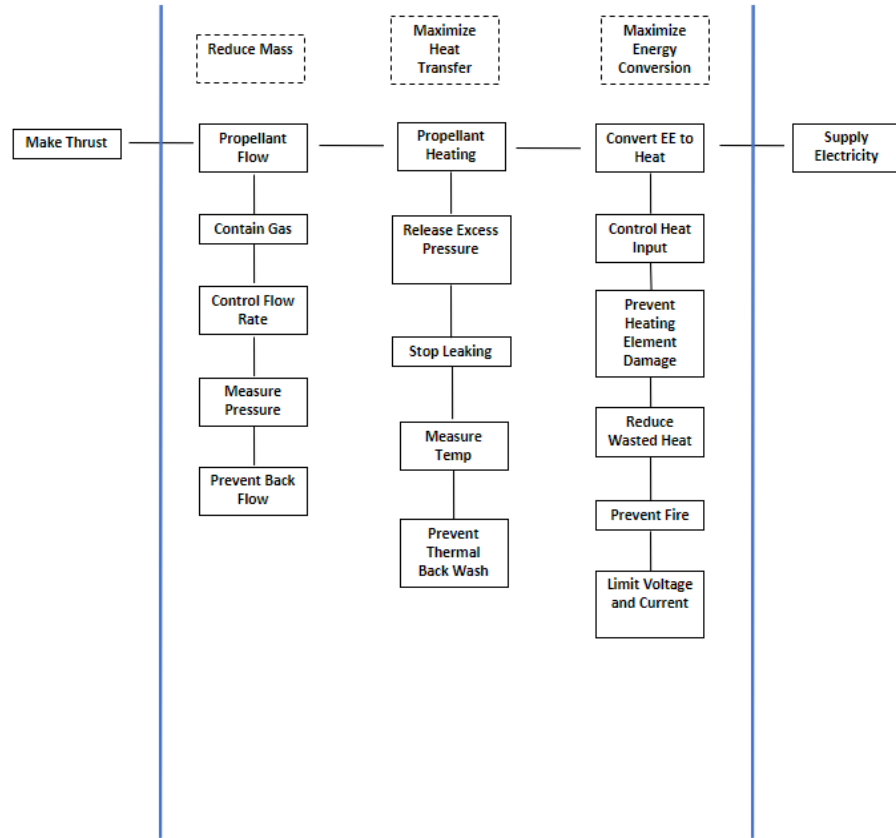


Figure 1: Function FAST Diagram

Journey Map

For this journey map of the system, the team chose a propulsion system user (person or controller) as the actor. The journey map itself is below in table form. A pictorial version is provided in the appendix. As a result of this journey, the actor should theoretically gain the ability to generate thrust when the system is at steady state. Each of the touchpoints represent a step in which the user or electronic main controller would have to intervene with the operation of the system. Most of the process is automated and does not require any input from the person in control, however, the tasks outlined in the journey map provide the user with certain checkpoints to ensure safe operation. Each point on the map was chosen because it would be a point where a person or electronic main controller would have to intervene with the operation of the system. Operation of the system may be divided into three sections – startup, operation, and shut down. Within each of these sections, there are certain key actions the operator must take to ensure safety and functionality. During startup, these include initiating fluid flow, turning on the heating element, and identifying steady state conditions. During operation, the operator must evaluate system temperatures and measure system output. During shutdown, the operator must disable heating and propellant flow, and check for part integrity. As the critical touch points of the operators during engine use, the team felt that these were essential to include in the journey map.

Below is a list of the top opportunities found for the system, listed based on whether they're positive or negative:

Positive Cues

- Improve heat transfer to fluid
- Improve cooling and insulation
- Ensure reliable data measurement capabilities

Negative Cues

- Prevent unsafe flow conditions
- Minimize startup irregularities
- Prevent leaks and mechanical failure

The journey map in its tabular form is included below (Table 3). The pictorial journey map is available in Appendix 3A (Figure 1).

Table 3: Journey Map, tabular form

Journey phase	Scenario, expectations	Actions, emotions	Outcomes	Opportunities
Startup	Start fluid flow and confirm initial pressure and temperature values	+/-, easy to check	<ul style="list-style-type: none"> Working fluid flow through system Consumes fluid Reasonable initial condition measurements 	<ul style="list-style-type: none"> Ensure fluid can flow without any heat in the system Reduce fluid consumed during startup
	Turn on heating element, set to specific heat power across the steel tube	+/-, easy to check	<ul style="list-style-type: none"> Heat transfer to fluid Increase in flow output 	<ul style="list-style-type: none"> Improve heat transfer to fluid Minimize startup irregularities
	Determine when steady state conditions are reached	+/-, SS conditions may not be reachable in certain cases	<ul style="list-style-type: none"> Thrust output maximized Optimal usage conditions reached 	<ul style="list-style-type: none"> Prevent unsafe flow conditions Prevent leaks and mechanical failure
Evaluation	Manage cooling of system	+/-, If run at lower temperatures cooling may be unnecessary	<ul style="list-style-type: none"> Preserve material, system, and seal integrity 	<ul style="list-style-type: none"> Improve cooling and insulation Substitute more cost-effective materials with better cooling methods
	Collect measurements needed for ISP and thrust	+/-, Read and interpret from instrumentation	<ul style="list-style-type: none"> Data for analysis 	<ul style="list-style-type: none"> Reduce error in measurements Increase readability Decrease measurement time
Shut down	Turn off heating section	+/-, Switching off electrical components	<ul style="list-style-type: none"> System completes use Fuel and tube return to safe temperatures 	<ul style="list-style-type: none"> Reduce cooling time Alert system for when system is dangerous for interaction
	Shut off air	+/-, easy to do	<ul style="list-style-type: none"> No more fuel in the system 	<ul style="list-style-type: none"> Shut down complete Can manually check integrity of the system
	Check integrity of parts	+/-, should be done visually or via noticing unusual fluctuations in values	<ul style="list-style-type: none"> Increase system lifetime Ensure safe use for future tests 	<ul style="list-style-type: none"> Increase visibility of deformations

Ideation and Design Selection

To begin, the team completed some preliminary research using resources provided by the client (Appendix 13). Based on this preliminary information, some basic CAD was completed to get an idea of how to build optimized nozzles in Solidworks (optimized being Rao nozzles, which are essentially nozzles with a parabolic expanding section, see Appendix 11C). Supplementary calculations were also completed in a spreadsheet to get an idea of geometric and other build parameters for a hypothetical design (Appendix 11D). After getting more clarity on the specifics of the project through this process, the team began to look at how the small scale system would work and how it would be built. Through a couple of meetings (Appendix 11B), the team decided to build a thruster by using a stainless steel tube with a heating coil around it to mimic the actual full scale design. From here, as shown in the section above, functional analysis was done and a journey map were created to find the strengths and weaknesses in the planned design. These opportunities were used as a basis to begin our final design selections.

Idea Generation

Based on the opportunities identified in the section above, the team brainstormed ideas to improve the current project standing, as can be seen in Appendix 3B. This list is annotated so that ideas generated based on different methods can be identified quickly. After ideas were generated, subpoints were added as part of idea evaluation, to be discussed in the next section.

The three different methods used for brainstorming were a morph chart, flash cards, and taking inspiration from parallel systems. The morph chart was used as a starting point as a way to reframe the different places or subfunctions where we could make gains and address inadequacies. This gave the team a good place to start, as intended, but the team also noted a tendency towards becoming fixated on specific issues due to the questions themselves. For the next round, the team tried using flashcards to generate a large amount of ideas quickly without being constrained by specific subfunctions. Even though the vast majority of ideas generated were not pursued, this method helped provide new ideas that did fit in the original deign structure, but still provided helpful functions. Finally, the group looked into parallel systems that used the same sub functions as the propulsion design. Some of the key categories of ideas generated were the following:

- Cooling methods
- Alternate fuels, data collection methods, heating methods
- Controls for automated control of the system
- Controlling heat loss

Idea Selection

The first action the team took to evaluate ideas was to go through the idea list and write down every concern, negative, or possible sticking point in each idea to evaluate them all for feasibility. These results are noted in Appendix 3B as the indented notes under each idea when applicable. These notes also include printed part properties, as shown in Appendices 7A-F. These considerations were then used as a preliminary filter for ideas so that everything that would end up being infeasible within the team's constraints (time, budget, expertise available within the team, etc) was removed from consideration. Other feasibility constraints that were used in the first filter were noted where the resulting idea list is shown (Appendix 3D). This pared down the field substantially, but there were still enough ideas available that another set of filtering was deemed necessary. For the second filter, the team removed any ideas that did not address key functions/issues or did not address more than one concern at once, deeming those ideas as

less immediate functionality for the prototype. The resulting idea lists from these two filters can be seen in Appendix 3D.

Filter 2 resulted in 14 candidate ideas, which would be too many for a scoring matrix. Therefore, these ideas were mapped onto a decision weighting plot (from Prof. Twiss' slides) to decide which ones would be best placed in the Pugh Screening matrix. This work is shown in Appendix 3E.

From here, the team set up a Pugh scoring matrix (shown below in Appendix 3E, Table 2) as a way of evaluating ideas further (all ideas were weighted the same, so both matrices have no weighting column). Each score was determined through voting and unanimous consensus (team members with contrasting views debated everything out until everyone could agree on a score). This was a very clean way to get numerical backing for idea selection while also making sure that everyone was heard, at least as much as possible within time constraints. The ideas that were selected to move forward are listed below:

1. Thrust Measurement – Weight Scale

To measure thrust, place the entire testing setup on a very accurate scale. By positioning the system such that the nozzle fires hot gas in the upward direction, operators may observe an increase in the “mass” of the system. This results from upward thrust forcing the system down into the scale. This shows promise as a direct way to measure thrust without the uncertainties and difficulty associated with test setups like the pendulum method.

2. Nozzle Manufacturing - 3D printing: DMLS

To make the nozzle, the team wanted to consider alternative methods to machining due to the lead time. DMLS (direct metal laser sintering) 3D printing is laser sintered powder, available through the Gall Lab's Titanium printer. This uses a laser to precisely melt each layer of the material and create a cohesive part. This is extremely useful as there are basically no geometric constraints for printing due to the fact that the print is self-supported by the un-sintered powder in each layer. Due to the expected size of our nozzle, we can also print multiple iterations on one build plate, saving time on making iterations.

3. Nozzle Manufacturing - 3D printing: Nylon 12 SLS

Selective laser sintering (SLS) uses the same idea as DMLS to manufacture parts, but is instead for plastics. The printer that has this capability, the Formlabs Fuse 1, is set up for Nylon 12. It has the same lack of geometric constraints on design and ability to print multiple iterations per build chamber. These is also an added bonus in that one of the team members is a lab manager for the service that provides access to the Fuse 1, Bluesmith, which can decrease turnaround time even further.

Idea Reflection and Refinement

All of the ideas that ended up selected relate directly back to the journey map (Table 3), while at the same time addressing key issues/challenges that had been identified earlier in the design process.

1. Thrust Measurement – Weight Scale

This solution is key to the evaluation phase of the journey map. By creating an accurate testing setup, operators may ensure that the system is producing adequate thrust to fulfill the requirements of the project. Additionally, by designing a test setup that is cheap, simple to implement, and accurate, the team may be certain that quality test data is collected without devoting an overly significant amount of time to the test setup itself, which therefore means this solution addresses the quality instrumentation opportunity.

2. Nozzle Manufacturing - 3D printing: DMLS

This relates to the journey map objectives by allowing the team to test out multiple nozzles quickly. Since the nozzle geometry is calculated based on flow conditions which are measured (and will therefore have inconsistencies), it's important to be able to have multiple configs of nozzle available based on flow condition changes. The only concern is that right now the team does not have numbers for the tensile strength of DMLS Titanium off of the Gall Lab's printer, and therefore can not do checks for failure based on stress yet. However, this is easily mitigated as the Gall Lab should have this information (they manufacture tensile test specimens from this printer relatively often).

3. Nozzle Manufacturing - 3D printing: Nylon 12 SLS

This is the same as the DMLS manufacturing technique, but printing in Nylon 12 allows the team to have multiple nozzles available and therefore helps addresses the opportunities of preventing unsafe flow conditions and minimizing startup irregularities. The concern for this method of manufacture is that the heat deflection temperature of Nylon 12 is only 87 C at 1.8 MPa (Appendix 7C), which is too low for our test case. However, the team might be able to implement sufficient cooling by putting in cooling channels, which will be easy to add on an SLS print, and by adding cooling jackets and other external cooling methods (this will be further evaluated as the time comes, as the plan is to go forward with DMLS since it scored higher on the Pugh Matrix, in Appendix 3E).

As can be seen in the next section, it turns out that all of these selected ideas had to be modified when applied in practice. The weight scale was replaced with a force gauge for more precision of measurement as well as more flexibility in placement. The nozzle ended up being made out of resin based on the higher heat deflection temperature of 238 C at 0.4 MPa (Appendix 7A) when post processed with both a UV and thermal cure (fabrication details in Appendix 2B).

Engineering Analysis

The engineering analysis is largely conducted through the full system computational model explained below. Further analysis of the heating section and the prototype structure is done in the Heating Analysis and Structure Analysis sections.

Full System Computational Model

Because the entire system is interconnected with co-dependent sections, a computational model of the entire system was developed to analyze the system simultaneously. The two main sections of the system are the heating section (see Figure 2) and the nozzle. The fluid inside is assumed to be an ideal gas with constant specific heat, and pressure losses, thermal losses, and other energy losses are currently not accounted for.

The heating section begins with an input pressure p_0 , an input temperature T_0 , and an input density ρ_0 . These are all values that we select and can control for in the real-life prototype. It is assumed that these values are constant at steady-state. The heating section is modeled as internal convection through a cylindrical tube of radius r_{tube} and length L (as well as surface area $A_s = 2\pi r_{tube}L$ and cross-sectional area $A_c = \pi r_{tube}^2$) with constant surface heat flux q'' . Here, we assume 1D steady state convection and neglect insulative losses and transient effects. A more detailed heating analysis is done in the Heating Model section.

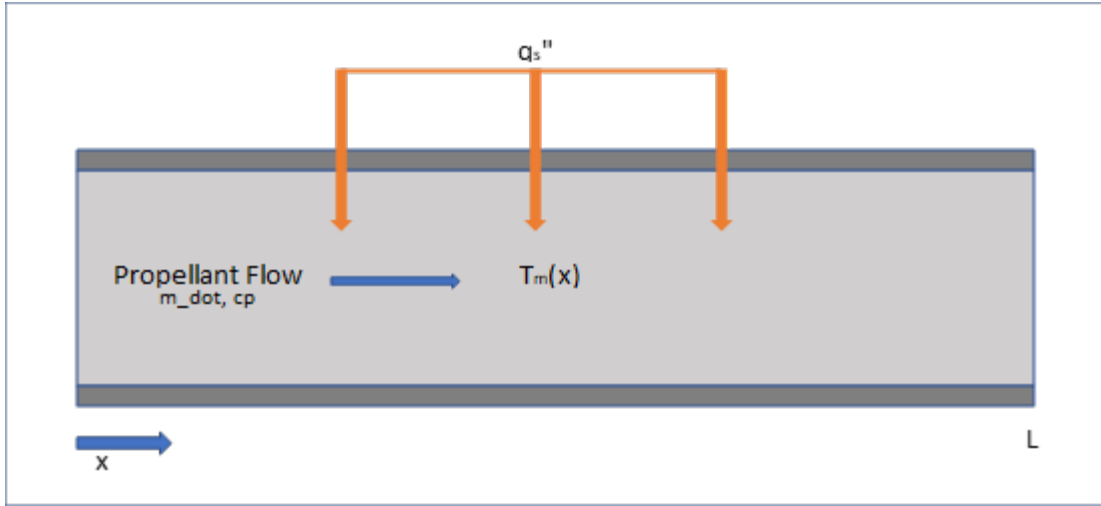


Figure 2: Heating Section Simplified Model

The nozzle inlet begins where the heating section ends (in the real-life prototype there is a small section between the heating section and nozzle inlet, but that is neglected in the model). The nozzle inlet pressure, temperature, and density are p_i , T_i , ρ_i respectively. The nozzle throat pressure, temperature, and density are p_t , T_t , ρ_t , and the nozzle exit pressure, temperature, and density are p_e , T_e , ρ_e . The nozzle throat radius is r_{throat} and the mass flowrate is \dot{m} (which is constant everywhere due to conservation of mass at steady-state). The area ratio $A_r = \frac{A_e}{A_t}$ is the ratio of exit area A_e to throat area A_t .

The mass flowrate through the nozzle can be described by (1), where γ is the ratio of specific heats and R is the specific gas constant. This is a commonly known equation in aeronautics. It is derived from the relationship between mass flow rate and velocity, the speed of sound of an ideal gas, the fact that the nozzle throat is choked at Mach 1, and the simple relationship between throat and inlet temperatures and densities for perfectly expanded flow [2].

$$\dot{m} = \frac{\rho_i A_t}{1.577} \sqrt{\gamma R \frac{T_i}{1.2}} \quad (1)$$

The next equation used is the conservation of energy equation (2), where c_v is the constant volume heat capacity (assumed to be constant) and q is the input heat power. It is assumed that heating is constant pressure and head losses are negligible. This equation is typically expressed in terms of specific volume, velocity, and internal energy but density, mass flowrate, and temperature are used instead since they appear in the other equation.

$$q = \dot{m} \left[c_v (T_i - T_0) + \frac{p_i}{\rho_i} - \frac{p_0}{\rho_0} \right] + \frac{\dot{m}^3}{2A_c^2} \left(\frac{1}{\rho_i^2} - \frac{1}{\rho_0^2} \right) \quad (2)$$

Since there are three unknowns (the throat area and tube cross-sectional area can be assumed given and several values are selected for testing), we need one more equation to solve the system: the ideal gas law (3). This equation is applied to both the initial and nozzle inlet values.

$$p = \rho RT \quad (3)$$

With lots and lots (and lots) of algebra and using the thermodynamic relation $c_p = c_v + R$ (where c_p is the constant pressure heat capacity) an equation for the nozzle inlet temperature can be solved (this step is shown in Appendix 10C). With a substitution from nozzle inlet temperature T_i to a new variable $\chi = \sqrt{T_i}$, we are left with a quartic equation (4). Once this quartic equation is solved, T_i can be solved through its relation to χ , while ρ_i and \dot{m} can be found through (1) and (3). The nozzle inlet pressure p_i does not need to be found since pressure is assumed to be constant. Because of the size of this quartic equation, a few new variables are defined (5-12). Furthermore, the solution to the quartic equation is infamously long, so this equation is solved numerically in MATLAB with the use of the fzero function (see Appendix 8A).

Once the quartic equation is solved finding the thrust and ISP is simple. First, nozzle exit conditions need to be found. Equations for this exist (such as the Area-Mach number relation), however, tabulated values are chosen instead [2]. With the exit conditions now known and the assumption of perfectly expanded flow, the thrust is simply $\dot{m}v_e$ and the ISP is $\frac{v_e}{g}$, where v_e is the exit velocity and g is the acceleration due to gravity. The burn time is found by dividing the initial mass by the mass flowrate. The initial mass is calculated by multiplying the tank density (assumed to be input density ρ_0) by the tank volume V .

The results from these calculations are displayed through several MATLAB plots in Appendix 10A. The calculations are performed for both the prototype and the theoretical full-scale system. The values used for both are tabulated in Table 4. It should be noted that the theoretical full-scale system is operating under more extreme conditions and a vacuum, so assumptions such as perfectly expanded flow are less justified but still give a good estimate of expected values.

Table 4: Values for Variables and Constants

Variable/Constant	Prototype Value	Theoretical Full-Scale Value	Units
Propellant	Air	Hydrogen	NA
Specific Heat Ratio (γ)	1.4	1.4	NA
Specific Gas Constant (R)	287	4124	$J/kg \cdot K$
Constant Pressure Heat Capacity (c_p)	1010	18,390	$J/kg \cdot K$
Constant Volume Heat Capacity (c_v)	700	12,260	$J/kg \cdot K$
Heating Tube Radius (r_{tube})	$2.67 (10^{-3})$	0.01	m
Heating Tube Length (L)	1	1	m
Nozzle Throat Radius (r_{throat})	$1 (10^{-3})$	$1 (10^{-4})$	m
Nozzle Area Ratio (A_r)	1.57	100	NA
Heating Power (q)	150	$2 (10^6)$	W
Input Pressure (p_0)	$1.03 (10^6)$	$5 (10^7)$	Pa
Input Temperature (T_0)	295	295	K
Input Density (ρ_0)	12.2	41.1	kg/m^3
Tank Volume (V)	0.028	10	m^3

The calculations in MATLAB allowed testing of different parameters, until the ones in Table 4 were selected. These calculations drove the design of the physical prototype by giving reasonable and optimal numbers for the prototype values. The key performance predicting results for the prototype are a max temperature of 400K, a burn time of 4 minutes, an ISP of 65s, and a thrust of 1N. The theoretical full-scale calculations resulted in a max temperature of 3700K, a burn time of 2 days, an ISP of 950s, and a thrust of 10N. More optimization of the theoretical full-scale parameters is needed to achieve better results. Even more, a more thorough analysis is needed for the theoretical full-scale setup that accounts for the dissociation of hydrogen, under-expanded flow, and extreme conditions in temperature and pressures.

Heating Analysis

The full system computational model assumes constant surface heat flux q'' and 1-D steady state convection, while neglecting insulative losses and transient effects. These assumptions are analyzed here.

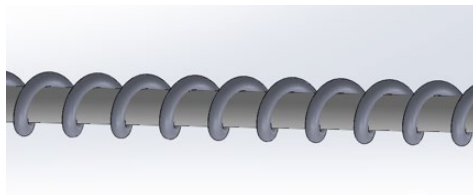


Figure 3: Heating Section with Wire Wrap

To start, the heating is coming from a thin wire wrapped around the heating section with current running through it (see Figure 3). This is known as Electric Resistive Heating. We assume lossless power conversion from electrical to heating. The necessary equations for analysis are Ohm's Law (13), the Electrical Resistivity Equation (14), and the Electrical Power Equation (15). Here, V is the voltage across the wire, I is the current across the wire, R is the resistance of the wire, ρ is the resistivity of the wire, L is the length of the wire, and A is the cross-sectional area of the wire.

$$V = IR \quad (13)$$

$$R = \frac{\rho L}{A} \quad (14)$$

$$P = I^2 R \quad (15)$$

With the equations above, we are able to evaluate a few potential wire materials (see Table 5). We want to maximize power while limiting current for safety reasons. The power can also be controlled through a variac that limits the voltage across the wire (from the equations above it can be seen that doubling the voltage quadruples the power). The aluminum wire is ruled out because the current is too high, and it is found that the best power output with reasonable current is the Nichrome 80 Wire Wrap. This is the wire used in the prototype, and it is wrapped around the propellant tube 300 times to produce the desired heating. Because of how tightly woven the wire is, it is reasonable to assume constant surface heat flux. Furthermore, the wire is electrically insulated from the steel tube through a ceramic woven sleeve.

Table 5: Summary of Heating Element Calculations

Material	Resistivity (Ohm*m)	OD (m)	Thickness (m)	Area (m ²)	Length (m)	Resistance (Ohm)	Voltage	Power (W)	Current (A)
304L Stainless Steel	7.00E-07	0.00635	0.000508	9.32342E-06	30	2.252392939	30	399.5750407	13.31916802
Nichrome 40-20	9.60E-03	0.00635	0.000508	9.32342E-06	1	1029.665343	110	11.75139095	0.106830827
Aluminum 6061-T6	4.07E-08	0.00635	0.000508	9.32342E-06	1	0.004361062	110	2774553.693	25223.21539
Nichrome 80 Wire Wrap	1.10E-06	0.00065	0.000325	3.31831E-07	4	13.25977277	110	912.5344911	8.295768101
Quartz with Nichrome 80 Wrap	1.10E-06	0.00081	0.000405	5.153E-07	9.1	19.42558732	110	622.8897896	5.662634451

Next, the assumption of 1-D convection and no insulative losses is analyzed. Since the computational model only looks at the fluid temperature, an analysis of the wall temperature is done as well to ensure that temperature do not skyrocket. These calculations can be found in Appendix 10B. To summarize, a resistor network is employed along with the Dittus-Boelter Correlation for internal convection to get an estimate of wall temperatures and conduction through the ends of the steel pipe, and it is found that wall temperatures and conduction through the sides are all within a reasonable range. Free convective losses are found to be minimal as well with the help of correlations in [3].

Structure Analysis

A structure was built around the prototype to calculate the thrust in testing. However, the method devised for calculating the thrust in the testing setup ran into a problem – friction. The thrust generated is not enough to overcome the friction of the structure, and thus the force sensor does not register a measurement. As a solution, the structure is tilted to allow gravity to assist in overcoming friction. For this to be successful, we need assistance from gravity to be exactly equal to the frictional force.

The dry lubricant used has a coefficient of friction $\mu_s = 0.19$. From basic engineering dynamics, we know that the force of friction will be $\mu_s mg \cos\theta$, where mg is the weight of the structure and θ is the angle that the structure is tilted. Similarly, the assistance by gravity will be $mg \sin\theta$. If we set these two equations equal to each other, we find that $\theta = \tan^{-1} \mu_s = 0.19 = 10.9^\circ$. Thus, the entire setup is tilted by exactly 10.9° to get an accurate force measurement.

Testing

Preliminary Testing

The testing and modelling in this project work together side-by-side, corroborating each other's results from the start of the build phase to the conclusion. Heuristic and qualitative testing started informally the moment the system was initially assembled (before the addition of a nozzle section or a heater). From estimating the exhaust velocity by feeling the output stream by hand, to listening for air leaks and sounds originating anywhere except from the exit, to hovering our palms over sections of tubing during heated tests to roughly estimate heating power, such informal tests accelerated the build phase and facilitated early prototyping.

Once the team had selected the final components and layout for the heated section, air source, and input pressure regulator, true quantitative testing began. The first two tests were “quick and easy” rough measures of the system volumetric flow rate and unheated pressure difference from input to nozzle. Prior to these early tests, the team truly had no concept of the true flow rate. It was evident from the first day that the rate was too high for the rotameter-style flow meters found at Duke Labs. To get even a rough estimate of the thrust and ISP (using the model discussed in *full system computational model*) the flow rate must be determined. The team brainstormed numerous rough measures of flow rate, including measuring the mass difference in a source tank (this concept returns in future testing), purchasing an electronic flow meter, and using very basic PIV at the nozzle exit. In the end, the team chose to simply use balloons. Allowing the system to run at some pressure for some number of seconds with a balloon attached to the exit, the volumetric flow rate and mass flow rates can both be estimated from the size of the balloons. After inflation the balloon is imaged, imported into SolidWorks, and modelled to find volume.

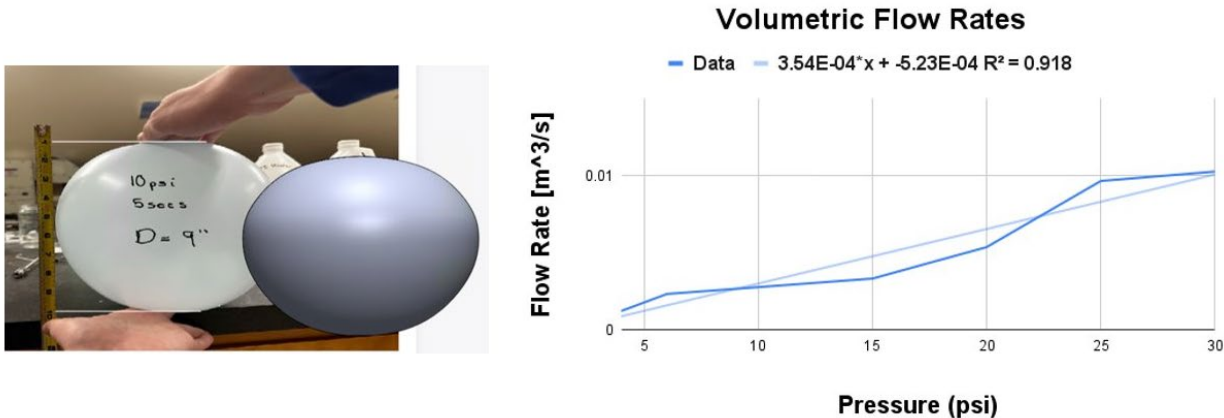


Figure 4: Plot of the output volumetric flow rate at nozzle exit [m^3/s]

(measured with balloon method) vs the source pressure from the regulator [psi] (measured with an analog gauge). To the left of that is an image of a test balloon, fiducial marker, and the SolidWorks 3D recreation of the balloon.

This test gave an estimate of the ranges of flow magnitudes the team would come to expect from the systems. Greater pressure results in greater flow as expected. In theory, the curve should behave like a square root relationship (since volumetric flowrate is linearly proportional to exit velocity which is proportional to the square of the pressure difference from Bernoulli's principle). In reality no balloon was large enough to contain all the air for pressures higher than 30 [psi].

The pressure difference prior to any heating was more straightforward to measure. Two standard 3-way junctions, two $\frac{1}{4}$ " NPT threaded pressure gauges (see *BOM* in Appendix 6A), and some Teflon tape (to seal cracks) are added in series before and after the heating element. These can accurately measure relative pressures from 0 psi to 300 psi with an error of around ± 2 psi. They are also rated to work up to 55 C. With these installed, pressure data is collected (system input vs nozzle input) for two unique nozzles (see Figure 6 caption for dimensions of nozzles A and B) and without a nozzle. The dimension of these nozzles is approximated with the model and from the flow rate measurements above. Furthermore, flow velocity at the nozzle exit is simultaneously also measured with a standard digital anemometer. The results are shown below:

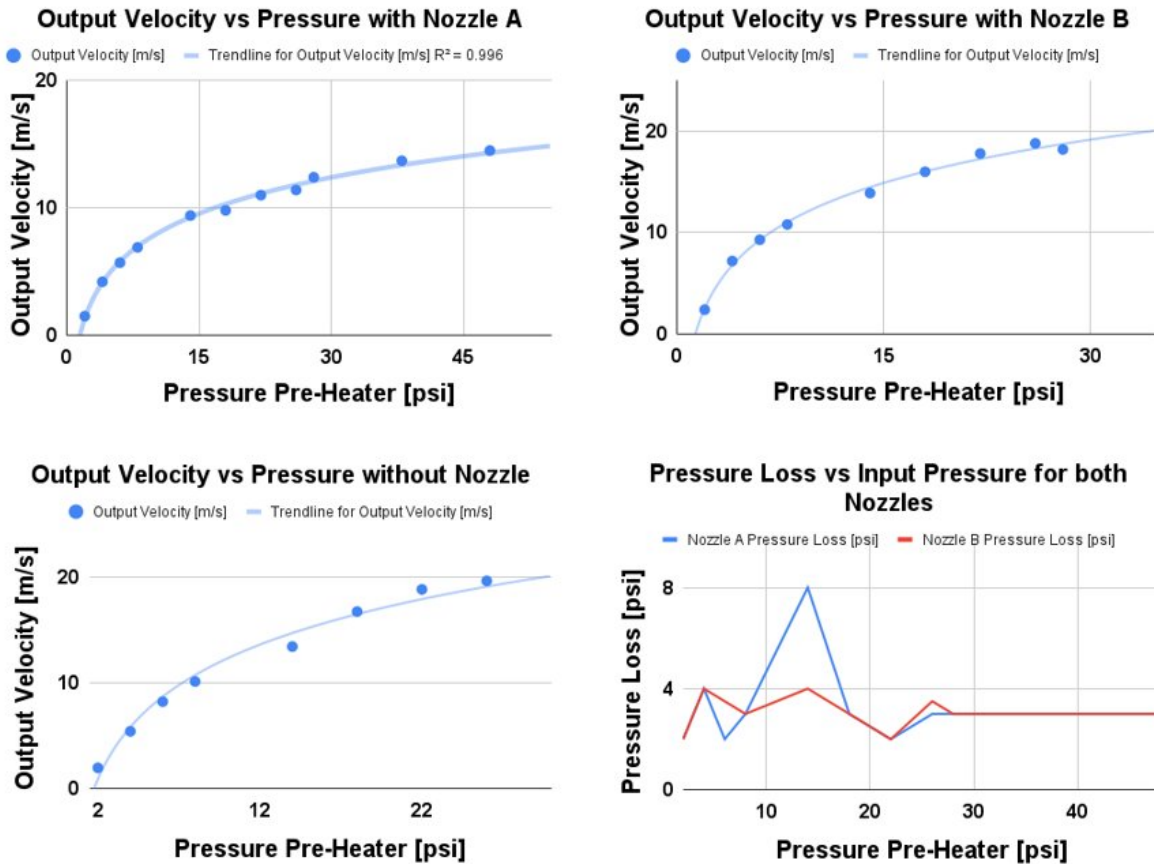


Figure 5: Three plots of the output velocity at nozzle exit [in m/s]

(as measured with a digital anemometer) against the nozzle input pressure [psi] (as measured with an analog gauge) for different nozzle shapes. Nozzle A has an inlet diameter of 5.3 mm, a throat diameter of 0.6 mm, and an exit diameter of 5.3 mm. Nozzle B has an inlet diameter of 5.3 mm, a throat diameter of 1 mm, and an exit diameter of 6 mm. Units are kept in a mix of imperial and metric for ease of reading and consistency with physical setup.

As expected, and explained above, the output velocity follows the expected square root relationship with regards to input pressure. Although pressures above 50 [psi] max out the anemometer, the data-fit is strong enough to reliably predict velocities at higher pressure. The pressure lost due to major and minor head loss is a constant 3-5 [psi], which matches expectations. This loss is due to a curved section of rubber hosing and due to micro-leaks at every junction.

Build 1 Testing

The next natural parameter/subsystem to test would be the heating section. To do this much of the system had to be replaced to withstand higher temperatures. In this time: new thermocouples were ordered and installed, the nichrome wire and ceramic insulation were added, a variable and regulated power source is hooked up with high temperature ceramic connectors, and a force gauge is connected. To calculate the mass flow rate, the overall mass of propellant used is divided by burn time. To find the overall mass of propellant used, the initial and final tank pressure is recorded. The ideal gas law is used to go from tank pressure to tank mass (temperature and volume are constant). With this all set up, the team was ready to run initial heating tests. Results are shown below:

Table 6: Steady State Heated Tests – Build 1

Variac Power	20%	30%	40%
Temp. In (C)	27.4	27.4	27.7
Temp. Out (C)	49.8	54	82.4
Thrust (N)	0.270	0.330	0.401
Heater Power (W)	26	58	103
ISP (sec)	109.3	133.6	162.3

Data collected from the steady-state heating tests. As explained above ISP is calculated from the change in tank pressure, heater power is calculated from the variac power and AC grid voltage, everything else is measured directly. All tests are at 58 [psi] input pressure. The nozzle for these has input diameter of 5.3 mm, throat diameter of 1 mm, and an exit diameter of 6 mm.

Again, results match expectation. More power in the nichrome heating wire results in a higher output temperature and also in higher ISP and thrust. With these results, the team felt confident adding a pressure gauge and moving up to 60% maximum variac power (anything higher slowly burned the ceramic insulation). The final series of tests were the same, but with a new and improved set of bearings and a new and improved force gauge. The results are plotted below:

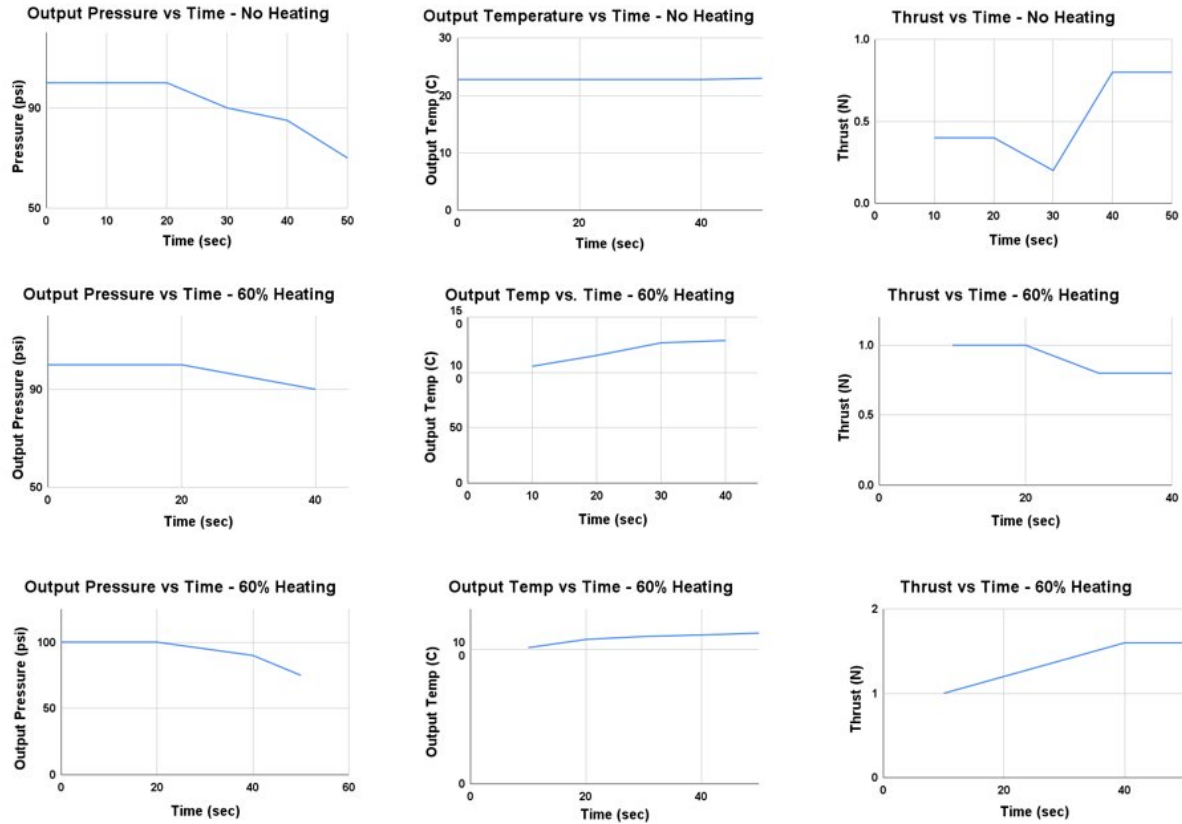


Figure 6: Plots for input pressure [psi], output temperature [psi], and thrust [N] vs time [sec]. The first row is performed at a nominal 100 [psi], with no heating, and with a burn time of 55 seconds. The second row is performed at a nominal 130 [psi], with 60% heating, and with a burn time of 45 seconds. The last row is performed at a nominal 130 [psi], with 60% heating, and with a burn time of 55 seconds. The last two rows took the source tank from 180 [psi] to 140 [psi].

As before, the results both match theoretical expectations as well as matching the values from the mathematical model. The three tests had average thrusts of 0.52 N, 0.9 N, and 1.36 N respectively (going from the 1st row to the 3rd). By using the ideal gas law at a constant atmospheric temperature of 23 C and at a volume of 15 gallons, along with the changing source tank pressure, the team calculates the test ISP. The three tests had average ISP's of 13.12 sec, 23.4 sec, and finally 41.4 sec respectively (from 1st row to the 3rd).

Experimental results are compared to theoretical predictions in Table 7. We see close matches for some data points, while others are more different. The tests marked in red are from the previous iteration of the thrust stand, while the tests marked in green are from the new version of the thrust stand.

Table 7: Comparison between Theory and Experiment

Heating	Pressure	Theoretical Thrust	Theoretical ISP	Experimental Thrust	Experimental ISP
0W	100psi	0.64N	51.0s	0.52N	13.12s

26W	58psi	0.32N	47.4s	0.27N	109.3
58W	58psi	0.32N	51.0s	0.33	133.6
103W	58psi	0.32N	58.4s	0.401	162.3
232W	130psi	0.87N	67.4s	0.9N	23.4s
232W	130psi	0.87N	67.4s	1.36N	41.4s

There are countless sources of error in such an experiment, both from the measurement side and from simplifications and assumptions in the model. There are two major sources of error in experimentation. The most significant source of error in the test stand was the static friction inherent to the system. Although the original t-slot linear sleeve bearings were swapped out for linear ball bearings, this error remained significant. To help with this issue, the setup was inclined to an angle of around 10 degrees to aid the slipping on the incline. At times, the force gauge would still read a positive value even with the device off. Another very significant source of error was air leaks; although this was not an issue until around 60 [psi] input pressure, higher pressures often result in leaks and bursts. A repeated issue came up with one of the thermocouples (it was faulty and had a leak) so it was scrapped.

Other less significant sources of error include measuring and setting all pressures using manual dial gauges. Not only does this mean that there is error in time-series data, which must be collected manually by hand, but it also results in at least ± 2 [psi] error. The gauge on the storage tank was particularly problematic, with a deviation precision of around ± 8 [psi] due to the tiny dial and markings. In addition, all output velocity measurements had an inherent error. Bringing the anemometer too close to the nozzle would affect the pressure up stream. Bringing the anemometer too far results in numbers that are too small.

Design and Design Components

Before beginning, calculations were all done in metric, but build parameters were converted to imperial due to the fact that all of the sourced components for the physical build were designed and rated in imperial.

How the System Works

Detailed usage instructions can be found in Appendix 1. To summarize, the system takes compressed air from a compressor unit (allowed into the system by a ball valve), regulates the input pressure down to the setting desired (normally 100 psi by the end of testing), and then allows the fuel to flow through the heating section and gain thermal energy from conduction and internal convection from the pipe wall (being heated by a Nichrome wire coil). This heated flow is then pushed through a converging-diverging conical nozzle to generate thrust at the end of the thruster.

Complete Assembly

Below is an image of the complete assembly as build in SolidWorks. Assembly drawings for this are shown in Appendix 5. Detailed fabrication instructions are provided in Appendix 2, with a table provided to index all relevant parts in Appendix 2A, pre-manufacturing steps explained in 2B, and the full assembly process explained in 2C.



Figure 7: Full Assembly Screenshot

Subsystem/Component 1: Nozzle

To start, a cross section of the nozzle design in use right now is shown below. A complete drawing of the nozzle is shown in Appendix 4I, which also includes the threads used to connect the nozzle to the Swagelok at the very end of the system.

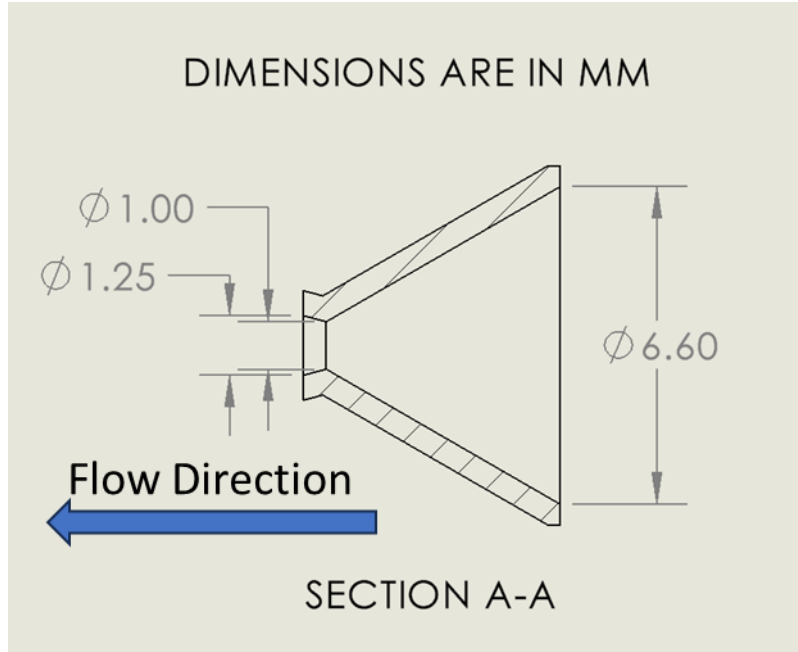


Figure 8: Annotated Cross Section Drawing of General Nozzle Shape

For the geometry of the nozzle, the team decided to use a simple conical nozzle, with geometry constrained by the following parameters:

- Converging section half angle: 30 degrees
- Diverging section half angle: 15 degrees
- Throat radius: Equation input, ranging between 0.5-1 mm
- Epsilon (expansion ratio): Equation input, ranging from 1.1 to 1.3

The equation input refers to dimensions controlled via the Equations interface in SolidWorks, screenshotted below. Another nozzle iteration is that could be considered instead fixes the length of the diverging section via an equation used for Rao nozzles (an optimized nozzle shape, normally associated with a traditional Bell nozzle shape).

Equations, Global Variables, and Dimensions			
<input type="checkbox"/> Filter All Fields			
Name	Value / Equation	Evaluates to	C
<input checked="" type="checkbox"/> Global Variables			
"r_outlet"	= "r_throat" * sqr ("epsilon")	0.022444	
"r_throat"	= 0.5mm	0.019685in	
"r_inlet"	= 0.13	0.130000	
"epsilon"	= 1.3	1.300000	
Add global variable			
<input checked="" type="checkbox"/> Features			
Add feature suppression			
<input checked="" type="checkbox"/> Equations			
"D2@Sketch1"	= "r_throat"	0.019685in	
"D1@Sketch1"	= "r_inlet"	0.13in	
Add equation			

Figure 9: SolidWorks Equations Interface (cropped and resized for clarity)

Subsystem/Component 2: Heating Section

The heating section is composed of the stainless steel tubing, wrapped in ceramic sleeving, and then wrapped with Nichrome 80 wire (20 gauge). The tubing itself is 6 ft long, but the heated area (area with Nichrome coil) is 5 ft. This section is where the fuel is heated before entering the nozzle explained above. The figures below show both a CAD and real-life view of the sections respectively.

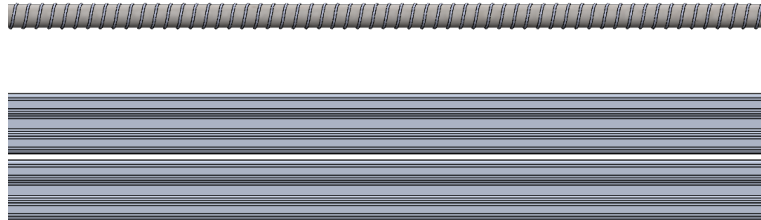


Figure 10: CAD of Heating Section

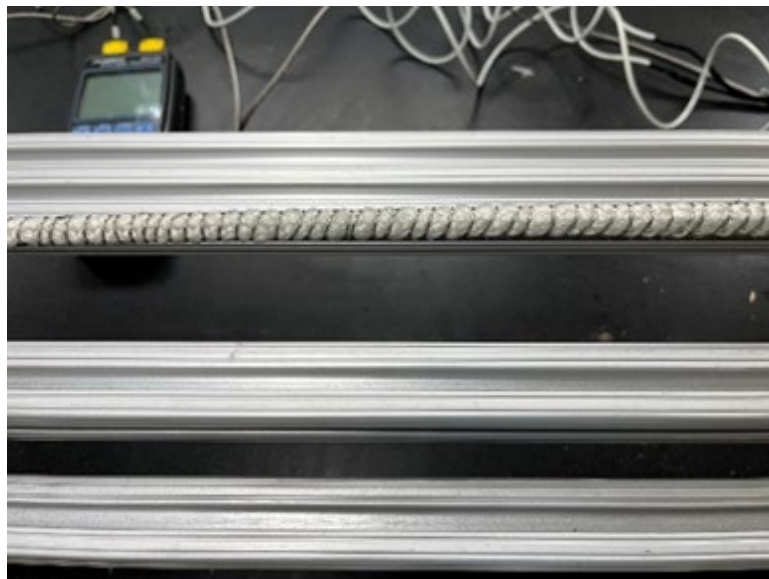


Figure 11: Real-Life Image of Heating Section

The ceramic sleeving was chosen for its low electrical conductivity, as its primary function was to stop the Nichrome wire from shorting through the conductive steel pipe, which would render the coil itself useless. The coils were chosen so that the length of wire used would have a resistance high enough that even if the variac were set to 100%, the Nichrome wire would not burn out. The basis for these calculations is shown in Table 5; the total length shown under the Nichrome 80 entry was divided by the circumference of the ceramic wrap to get the total number of turns needed in the coil (300).

Subsystem/Component 3: Inlet Section

This is where compressed air comes into the system and the pressure is regulated down to the desired heating section input pressure (set to 100 psi). From here, the flow goes into the heating section. The figures below show CAD and the real-life version of the inlet section.

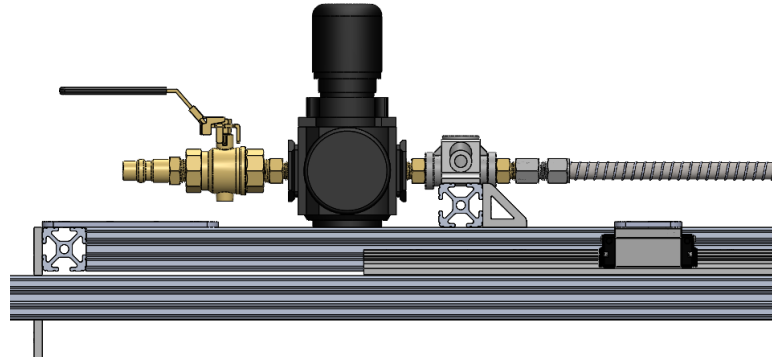


Figure 12: CAD of Inlet Section

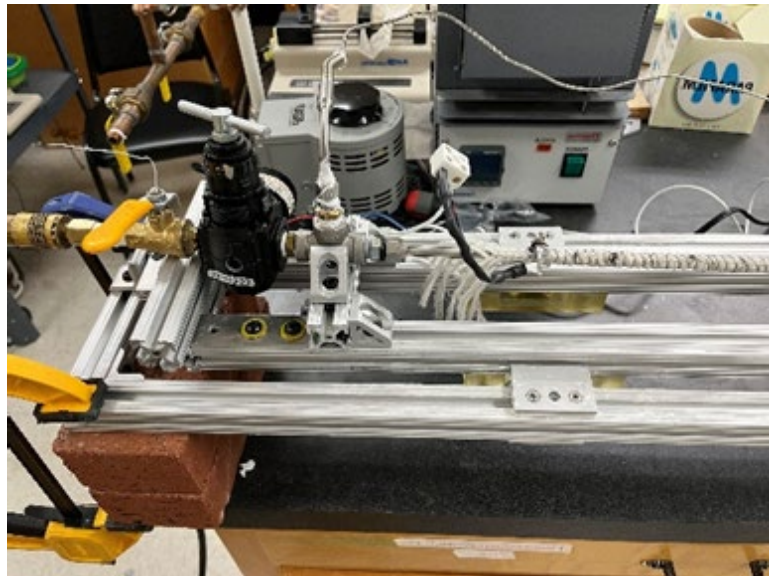


Figure 13: Real-Life Image of Image Section

The regulator shown was chosen for its ability to handle pressure up to 200 psi since the compressor the team used could supply up to 200 psi. The valve was rated for 500 psi, and the QuickConnect was chosen for its compatibility with the ARO Automotive female fitting on the compressor hose.

Subsystem/Component 4: Thrust Stand

The thrust stand was designed to allow accurate measurement of the thrust produced by the electric resistance propulsion system. The team utilized T-Slot framing for the main structure due to its low cost, structural rigidity, and flexibility as a prototyping material.

The design includes two major regions – the stationary region, and the dynamic region. The stationary region rests on the workbench and does not move throughout the duration of a test. A load cell is mounted to the stationary region to measure thrust. The dynamic region supports the entire thrust system – the air inlet, heating section, and nozzle assemblies. It rests on four linear bearings which allow it to slide along the length of the stationary section. As the system generates thrust, the dynamic section slides into the load cell, which records the applied compressive force. The test stand was originally designed to operate horizontally. However, to overcome sliding resistance, the team elected to angle the test stand such that the dynamic region slid down the rails under its own weight. Using the tare button on the load cell after this initial motion allowed the team to only measure the thrust applied.

An image of the test stand with the propulsion system hidden is included below (Figure 14).



Figure 14: CAD of Thrust Stand

Design Implications

Holistic Impact of the Project and Design Process

The Mars Propulsion Team has been carefully focused on the project's impacts on society and industry and has taken steps to ensure public safety measures. This section will address the teams' cultural, economic, and environmental considerations. The team's design holds transformative potential for both society and industry. It supports the broader goal of interplanetary travel and Mars colonization, which can lead to significant advancements in science, technology, and infrastructure. The technology developed could lead to new industrial applications and enhance the capabilities of current aerospace technologies. This could foster a new era of space exploration, potentially leading to economic expansion into new markets and sectors, such as space tourism and planetary resource extraction.

Public safety has also been a paramount concern throughout the project. The propulsion system design incorporates multiple safeguards to protect against the inherent risks associated with rocket thrust testing. For instance, the use of compressed air in initial testing phases significantly reduced potential hazards.

Rigorous safety protocols were adhered to, ensuring that all testing was conducted under strict supervision and within controlled environments to mitigate any risk to the project team and the general public. There were other measures taken such as wrapping a ceramic sleeve around the stainless-steel tube the team used to test the propulsion system in order to prevent any burning or potential fires. Moreover, the team looked into the heat deflection specifications of each of the components in the test setup to figure out what would be limiting factor for how much the temperature could be raised. As a result, the team could continually run trials without worrying about the system overheating.

Furthermore, accessibility and inclusivity were central to the design process. Culturally sensitive practices were adopted to respect diverse norms and customs, which is critical in a project with global implications. One of the considerations already made was to do all of the calculations in metric instead of imperial. The only switch to imperial occurred when building out of necessity since the available parts were manufactured and designed using imperial units. One future consideration would be to make technical documentation available in multiple languages to ensure that the project is accessible to individuals regardless of socioeconomic background or physical capabilities.

From an economic standpoint, the project was designed to be cost-effective, adhering to a strict budget of at most \$2000. This constraint fostered innovative solutions such as the choice of propulsion testing methods and materials. Already available sensors and other measurement devices on campus made it possible for the team to make astute observations and gather data that wouldn't have been possible otherwise. The potential economic impact of this design is significant, promising to lower the costs of space travel and make it more accessible to a broader range of customers.

Finally, the Mars Propulsion Team ensured that the rocket propulsion system effectively addressed any environmental concerns and continually worked on mitigating environmental harm. The materials and processes selected were chosen to minimize environmental harm, such as using eco-friendly filament and ensuing sustainable practices during testing phases. However, some environmental risks and considerations were beyond the scope of the initial project phase. These include the long-term impacts of increased launches on the Earth's atmosphere and potential debris in space. Future phases of the project will need to address these broader environmental concerns as part of a comprehensive sustainability strategy.

Qualitative Life Cycle Analysis

Material Impact

Our consideration of the material impacts for the physical build are shown in the table below. Considerations for the hypothetical full-scale system cannot be shown here since the system has not been developed, and therefore any consideration of materials used would be purely conjecture.

Table 8: Material Impact for Physical Build

Material	Use case	Toxicity	Scarcity	Other environmental concerns	Set up processing concerns	Disassembly process concerns
Steel	Main tube, Swagelok connectors, bushings, and pipe adapters	X	X	Manufacturing process unknown	Every junction must be sealed with Teflon tape or high-temp Loctite	Parts will be returned to MEMS stock for other students to use
Ceramic sleeving	Electrical insulation for heating section	Possible if we start to melt the ceramic wrap, but very unlikely	X	Manufacturing process unknown	Cut to length and slide on, some fibers will escape and are swept and trashed, impact expected to be negligible	Assuming integrity is maintained, material will be donated for other students' use, otherwise will be trashed unless faculty notes that this would require chem disposal processes
Nichrome 80 wire	Heating element	X	X	Manufacturing process unknown	Wire must not touch itself to avoid short circuits (not a major safety concern but reduces efficiency)	Wire will be trashed, assuming it is worn enough to not be worth saving for others; no expected issues here

Teflon tape	Threaded element sealing	N/A, unless it melts	X	Manufacturing process unknown	Hand wound along each threaded fitting, no power or installation environmental cost	Cut off and trashed, unless melted no issues expected
JB Weld	Thermal insulator for the heating section	No after full cure, but problematic before if placed into trash	X	Manufacturing process unknown	Hand placed with gloves, no power or installation environmental cost	Broken off and trashed, should be fully cured so no environmental concerns past landfills here
Formlabs High Temp v2 Resin	Preliminary nozzle manufacturing due to metal printer issues	Yes, before curing, but thermal and post cure should keep this from becoming an issue during testing	Only Formlabs sells this specific resin, but there does not seem to be any reason for concern related to component scarcity, also all materials noted in the data sheet as going into the resin are not	Uncured resin must be disposed of properly, but this is handled by the printing service itself and Duke's Chem Waste management system	Uncured resin gets on gloves during print setup, and these gloves must be thrown out after each use (went through ~4 pairs of nitrile gloves per successful print), that uncured resin goes into the trash as it is not enough	Fully cured parts are completely safe for handling as long as they do not melt and release fumes, so simply trashing the parts will be fine for the purposes of the physical set up being built right now.

			particularly scarce		to merit chem disposal. Therefore, that resin is in trash bags that eventually get to landfills.	
O-ring	Sealant for wood to threaded fittings	Unless it melts, but unlikely	X	Production methods unknown, and therefore cannot be adequately considered from an environmental standpoint	Slide in, press fit	Pull off, hopefully is reusable
T slot, screws and nuts, and associated brackets (Aluminum)	To build a robust test stand structure to hold all parts in place and measure thrust	X	X	N/A	Cost during material sourcing and machining, both before acquiring the t slot and after the team uses power tools to cut it down to the correct lengths	All fixtures will be hand tightened with Allen keys, so undoing them requires no power and therefore the only cost would be in making sure that the material gets reused, which is not expected to be an issue since the team

						can donate the material back to MEMS for other students to use
16- and 22-gauge wiring	For getting electrical power into the nichrome wire to use for heating	Unless insulation melts, N/A	X	Sourcing for insulation material, any byproducts created in its construction	Stripped sections have a small bit of insulation that was cut off and thrown in the main trash, which will go into landfills	Will have the stripped ends clipped and thrown out in main trash; the rest will be returned for other students to use
Non lead based solder	For securing and tinning wires	X	X	Unknown production methods, therefore, cannot be evaluated for environmental concerns	Fan used to filter the fumes coming off the soldering iron while the solder was being used	Use desoldering tools to remove and throw out directly, but is not toxic so should not cause issues when placed in main trash

Total Energy Consumption

For the lab test setup, there are two primary energy sinks in the system – the compressor and the heater. Although the exact make and model of the lab compressor is unknown, comparisons to similarly rated compressors¹ reveal an energy usage of around 120 W (12V DC and 10A) at 70 psi. The approximately 5 meters of 20-gauge nichrome-80 wire will use around 380W (60V AC and 6A)² when at a goal temperature of 400C. So, when running the test setup at the maximum settings, the expected power consumption is around 500 W, or half that of a standard microwave oven. So, for a three-minute test the expected electric energy consumption is 90 kJ.

Assuming a completed final form of this thruster generates similar thrust but at a higher pressure and temperature (and hence a higher ISP and efficiency), a higher energy consumption will be expected. At 1000 psi, a specialized 3-stage air compressor uses around 3.7 kW of power³. Similarly, assuming double the heated length (the longer the heated section the more effective the heat transfer) and goal temperatures closer to 700C, the nichrome-80 heating wire will use around 2.1 kW (213V AC at 10A) of power. The overall power consumption is then around 5.8 kW. This is an upper bound estimate as the thruster would run below the maximum steady state. Hence, a three-minute burn would burn through an expected 1044 kJ of electric energy.

The manufacturing process for each part will also contribute to the total energy consumption for this project. A horizontal bandsaw was used for the T slot cuts, and based on the 1 hp power rating of a similar model,⁴ and that the cuts were being run for 30 minutes, the energy used was approximately 1342 kJ. The Formlabs Form3 is rated to run at 220 W, and the prints were about 2 hours long each (printed twice in case of failures during post processing), so the energy use was about 1584 kJ. The post processing included 12 min in the Form Wash station (50 W power use, so 36 kJ energy used), 120 minutes in the Form Cure (post curing, 144 W for 2 hours is 1037 kJ of energy), and then 180 minutes in an oven at 160 C for the final thermal cure (using Projet Finishing Oven, so 1.2 kW over 3 hours yields 12970 kJ of energy).⁵

Based on all these numbers, the total energy consumption for the prototype build is somewhere around 16519 kJ of energy, which is 4.59 kWh.

The full-scale use case energy consumption differs significantly from testing. The thruster is designed to draw its energy from an onboard RTG (radioisotope thermoelectric generator), which is a small nuclear reactor. The energy consumption during a given burn should be similar to the testing values. The energy cost of successfully deploying the thruster must also be considered. The intended use case of the ERTP (electric resistance thermal propulsion) is to be in space, which means that the energy consumed during

deployment will be the energy required to lift the thruster from earth into orbit. At the end of its lifecycle, the rocket body will either be left to drift in space or will be burned up by entry into an atmosphere. In both cases the energy consumption is minimal.

Emissions

First, we consider the emissions of the electric resistance thermal propulsion thruster during its usage. The emissions of the thruster during a burn will depend on the chosen fuel. In testing air is used which does not release harmful pollutants when it is heated. During deployment, the designated fuel is liquid hydrogen, which burns clean by itself, releasing water vapor. A burn may result in carbon ash being released into the atmosphere as a pollutant, but launches in atmosphere are currently infrequent, with most burns occurring in space.

Another factor to consider is that, to deploy the thruster, it must be lifted into orbit. This is commonly done with solid fuel rockets, some of which do not burn cleanly and can release harmful chemicals into the atmosphere.

The energy plants used in testing and deployment will also generate emissions. In testing, the power will be drawn from a nearby wall socket. The emissions from local energy powerplants must be considered during testing. In deployment, the energy will be from an onboard nuclear reactor. This generates spent nuclear fuel waste, but this can be disposed of safely when the rocket body is retired either by burning it up into another planet's atmosphere or letting it drift off into space.

For the prototype build, using a 2022 EIA estimate of 0.86 lbs CO₂ per kWh generated, the estimated emissions are around 3.67 lbs CO₂.⁶

Positive Environmental Impacts

The use of compressed air in the lab setup has significantly reduced the project's negative impact on the environment. While monoatomic gases such as nitrogen can contaminate the atmosphere, air is already abundant and does not have any harmful side effects. This is an important consideration as nitrous oxide is 300 times more potent than methane and carbon dioxide as greenhouse gases. It is also the biggest human-made threat to the ozone layer.

Another place in which the team made positive environmental choices is avoiding melting any components. A lot of the environmental issues that are noted in the "Materials Impact" section are relevant if components start to melt. Therefore, the team's approach of verifying numbers and thoroughly modeling the system before making major build decisions and doing system runs stops the team from unintentionally releasing all sorts of possibly problematic fumes.

Other than these, the prototype build does not have many environmental concerns. For the full-scale system, there have been no specific design decisions made other than to rely on additive manufacturing instead of subtractive machining for both the ERT module and the nozzle. Assuming that both are manufactured with sintering methods, the waste generated would be in the form of metal powder which can hypothetically be reused (based on similar processes used for plastic sintering), which would be less wasteful. Even if the powder cannot be used, it would be less than the waste yield from subtractive manufacturing. Casting is another option, but there is a substantial amount more of energy required to make a body of metal molten instead of locally melting smaller bodies of metal.

Future Changes

Below is a bulleted list of the different ways the system would be made more sustainable and environmentally friendly.

- Energy Source for Resistive Heating: The ERT system relies on traditional resistive heating to heat hydrogen for propulsion. Considering the environmental impact, ensuring the electrical power source for resistive heating is derived from renewable energy (e.g., solar, wind) could significantly reduce the carbon footprint associated with testing and operating this system on Earth.
- Material Selection: The manufacturing process for the thruster system components could prioritize materials that are sustainable, recyclable, or have a lower environmental impact. For example, using recycled metals or materials with sustainable lifecycle management practices could minimize the environmental footprint.
- Computational Analysis: Given the limited time and resources available, the team was not able to analyze the air flow through the nozzle using computational fluid dynamics. In the future, running tests on a computer software program would reduce the amount of 3D printed nozzles needed to be used and minimize the amount of PLA wasted on trial nozzles (used before heated testing to assess for leaks, get an idea of dynamics, etc) throughout the experiment.
- Long-term Space Environmental Considerations: While not directly related to the Earth's environment, considering the broader implications of propulsion systems on space environments (e.g., space debris, planetary protection policies) is becoming increasingly important as space travel becomes more common and accessible to the public. The system should be designed to minimize its impact on celestial bodies or the space environment, ensuring it does not contribute to space debris.
- End-of-Life Recycling: Developing a plan for the end-of-life disposal or recycling of the ERT system and its components can ensure that environmental impacts are minimized once the system

is no longer in use. This might include designing the system for easy disassembly and recycling of materials. The team can put in place a protocol to dispose materials that are no longer needed.

Recommendations and Conclusions

To start, there are a few improvements that can be made to the current design. The first would be decreasing the weight of the structure. The structure's weight adds to the frictional force and makes it more difficult to accurately measure thrust. Next, the design should be better pressure-fitted. There are occasional pressure losses, specifically around the temperature sensors, and these can cause significant decreases in thrust and ISP. Furthermore, the system should ideally be tested in a vacuum to better emulate the conditions in space. If this design were to be used in mass production, further optimization should be done to maximize thrust and ISP. This includes testing different fluids, using more powerful heating, and using parts that are better pressure and temperature rated.

Through this experience, a few lessons have been learned. The first lesson learned was how to scope a project. The majority of the first semester was dedicated to picking a proper scope, and a lot of care went into this step. Improper scoping could have left us unsure of our goal. Next, a lot was learned about rocket science. The majority of the team lacked experience in this field, and a lot of time was spent learning more about this. Furthermore, many lessons were learned in structuring a team and delegating responsibility. With several members in our group, we worked most efficiently when everyone had a task and there was not too much overlap. Lastly, we learned to trust trial and error and not fall into too much "analysis paralysis." A lot of time was spent overthinking decisions, and a lot more progress was made when we started being decisive and going through the process of trial and error. Overall, a lot was learned in the two semesters spent working on this project, and many of these lessons will carry over into our future.

Acknowledgements

The design team would like to thank the client, Robert Hickman, for providing the opportunity and support to work on this project. The team would also like to thank the teaching staff of ME 421 and ME 424, especially Professor Greg Twiss and Harry Xu, the team's assigned point professor and TA respectively, and the Department of Mechanical Engineering for facilitating the team's work on the project.

References

- [1] “7 in x 12 in, 86 to 260, Band Saw.” *Grainger*, www.grainger.com/product/21C004?gclid=N%3AN%3APS%3APaid%3AGGL%3ACSM-2295%3A4P7A1P%3A20501231&gad_source=1&gclid=CjwKCAjwrr6wBhBcEiwAfMEQs76kIVMtvHopuBK7ap_HJ6dstY53X3vr-qSxmhYsz7Qzf9duqWJXWBoC_IkQAvD_BwE&gclsrc=aw.ds.
- [2] Anderson, John David. *Fundamentals of Aerodynamics*. 6th ed., McGraw-Hill Education, 2017.
- [3] Bergman, Theodore L., et al. *Fundamentals of Heat and Mass Transfer*. 7th ed., J. Wiley & Sons, 2011.
- [4] “Frequently Asked Questions (Faqs) - U.S. Energy Information Administration (EIA).” *Frequently Asked Questions (FAQs) - U.S. Energy Information Administration (EIA)*, www.eia.gov/tools/faqs/faq.php?id=74&t=11#:~:text=This%20equaled%20about%200.86%20pounds,efficiency%20of%20electric%20power%20plants.
- [5] “I-Series 3.” *7.5 SCFM Systems | Bauer Compressors*, www.bauercomp.com/products/industrial-air/400-1000-psi-systems/i-series-3.
- [6] *McMasterCarr*, www.mcmaster.com/6709K12/.
- [7] *McMasterCarr*, www.mcmaster.com/6709K33-6709K303/.
- [8] *McMasterCarr*, www.mcmaster.com/47065T663/.
- [9] *McMasterCarr*, www.mcmaster.com/47065T101-47065T122/.
- [10] *McMasterCarr*, www.mcmaster.com/88175K32-88175K52/.
- [11] *McMasterCarr*, www.mcmaster.com/47065T236/.
- [12] “Specific Impulse.” *Wikipedia*, Wikimedia Foundation, 21 Apr. 2024, https://en.wikipedia.org/wiki/Specific_impulse
- [13] *Viaircorp*, www.viaircorp.com/v/wp-content/uploads/2020/11/10010_10014_10016_10019_Manual_R2-122020.pdf. Accessed 30 Apr. 2024.

Appendix

1. User Manual

Appendix A: Use Instructions

- 1) Make sure all sensors are plugged in and reading, connect the compressor hose to the inlet of the system, and then take measurements to get baseline readings of sensors
- 2) Have people ready to read each of implemented gauges
- 3) Charge the compressor to 120 psi and then open the valve to check for leaks across the system, note where any open/are found and then turn off the airflow and plug the leaks. After letting plugs set, check again for leaks
- 4) Charge the compressor to between 170-180 psi
- 5) If using heating during the run, turn on the variac and set it to the desired input power (calculate the desired variac setting based on $P=V^2/R$, with R being the total resistance of the Nichrome wire section); let it heat for 60 s
- 6) Open the valve and start taking measurements in 10 s intervals across all sensors, note the starting regulator pressure
- 7) Close the valve when the regulator pressure starts to slip down from starting pressure
- 8) Transfer all measurements into one file and turn off the variac
- 9) If doing another run, recharge the compressor, otherwise begin disconnecting wires to pack up the system

2. Fabrication Instructions

Appendix A: Parts Index

Table 1: Part Numbers and Descriptions

Part Number	Part Description	Amount
1	T slot, 4.75" long	2
2	T slot, 12" long	2
3	T slot, 6' long	4
4	T slot, 6" long	4
5	T slot, 10" long	4
6	T slot, 4" long	2
7	Flat Plate Straight Connector, 4 holes	10
8	Flat Plate 90 degree Connector, 3 holes on each leg of the L	1
9	Gusset Corner Bracket	12
10	Corner Bracket	8
11	All Female Swagelok	2
12	Inline female to male, female on T Swagelok	1
13	½" male to 3/8" female reducer	2
14	Teflon tape	1
15	High pressure regulator	1
16	3/8" screw in plug	1
17	ARO Automotive Quick Connect Male Plug	1
18	S92 Ball Valve	1
19	Stainless Steel Tube, 6ft	1
20	Screw in thermocouples	2
21	High temperature pressure gauge	1
22	3D printed nozzle	2
23	Ceramic wrap, 10ft	1
24	Nichrome 80 wire, 10ft	1
25	Hose clamps	2
26	Linear rails with two bearings	4
27	M4x10 Socket Head Screws	8
28	¼"-20 x 1" Socket Head Screws	8
29	¼"-20 T Slot Nuts and Screw Pairs	84
30	200 psi Compressor with hose	1
31	¼" Washers	42
32	Ceramic screw terminals	2
33	Insulated 16 gauge wire	2

34	2x16 AWG wire with a wall plug	1
35	3D printed custom force sensor mount	1
36	Linear Rail Mating Plate	4

**Note: this table only has parts that need identification for product assembly purposes, for an exhaustive list of all parts needed for the build, see Appendix 6A, Table I*

Appendix B: Part Manufacturing Instructions

T Slot Plate Connectors

- 1) Find the dxf files provided in the Final Manufacturing folder, there should only be two
- 2) Import both dxf files into Fusion 360, and layout 10 of the straight connectors and 4 mating plates, making sure that they fit in the 1'x1' area of the Aluminum stock plate
- 3) Export the gcode for the OMAX waterjets, then go to the Colab and use the waterjets to cut all of the parts

T Slot Cuts

- 1) Take one 6' T slot and mark out 4 10 inch sections, 2 4 in sections, and 2 12 in sections
- 2) Take another 6' T slot and mark out 4 6 in sections and 2 4.75 in sections
- 3) Using either a miter saw or horizontal band saw, make cuts on each of the lines delineating the sections; take care to cut right on the lines since sections are adjacent to one another
- 4) File down the edges of each cut face

Nozzle 3D Printing

- 1) Find the STLs provided in the Box folder under Final Manufacturing named ...Simplified Nozzle Build 2 Threaded (there should be two files with other text before the Nozzle identifier which keeps track of the geometric properties of the nozzle STL)
- 2) If Preform is not downloaded, get Preform and open the software, set the printer type to Form 3, using High Temp v2 resin, and 0.100 mm layer height
- 3) Turn all models so that the face with text is sticking up, normal to the build plate
- 4) Do NOT generate support, but allow Preform to auto-layout the build plate after checking the box for optimizing for Build Plate 2; warnings will show for cups but attention during post processing should mitigate the effects, especially since they are small
- 5) Send to print, then before running in the Form Wash use a spray bottle to clear the tiny nozzle so that the flow path is clear, check to make sure it is by sticking the end of the spray bottle in right up to the throat of the nozzle and trying to get an IPA flow out of the other end of the nozzle (if this fails, REPRINT)
- 6) Set the Form Wash to run for 6 min maximum, then check for clear flow paths again in the same manner as done in step 5; leave the print to dry for approximately 10 minutes to make sure everything is clear (should be able to see if the path is clear)
- 7) After placing the prints in with the text facing up, start the UV cure using the Form Cure, run at 80 C for 120 minutes as recommended by Formlabs, check the flow path again after the UV cure (when the print is cold)
- 8) Preheat the post processing oven to 160 C, then put the prints in with the text facing up again (use thermal gloves for this!)
- 9) Run thermal cure for 180 minutes, take prints out IMMEDIATELY since excess thermal curing affects mechanical properties of the part and will cause even more thermal warping than the rest of the post processing

Force Sensor Holder 3D Printing

- 1) Find the STL provided in the Box folder under Final Manufacturing named Force Sensor Holder
- 2) Upload to 3DprinterOS and layout the file with the bottom face of the print slicking up in the air
- 3) Use standard slicing settings and generate a gcode, then run and collect the part

Appendix C: Assembly Instructions

- 1) After having manufactured all necessary parts according to Appendix 2B, collect and identify all necessary parts for assembly in accordance with Appendix 2A

Thruster support structure

- 2) Take two of the 6' T slots (part 4) and line them up perpendicular to one 4" T slot (part 6); the outer faces of part 4 should align with the end faces of part 6
- 3) Using two straight plate connectors (part 7), connect the 6' T slots and the 4" T slot from the top using 3 T-slot screw-nut pairs (part 29) and 3 washers (part 31) per side; one screw should end up in the 4" T slot and two should end up in the 6' T slot per side, and the face of the finished structure after this step will be the top face
- 4) Use two T slot screw-nut pairs (part 29) to attach the 90 degree flat plate connector (part 8) to the outside face of part 6 pointing away from the top face, this is now the front of the thruster support structure
- 5) Align the opposite end of each 6' T slot to a 6" T slot (part 4) and use four straight plate connectors (part 7) to connect the pairs together colinearly with connectors on the top face and bottom face of the structure
- 6) Take a 4" T slot (part 6) and a 6" T slot (part 4) and attach two corner gusset brackets (part 9) to them with t slot screw-nut pairs so that the brackets have coplanar free faces, do not tighten them in yet
- 7) Place both structures from step 6 on the top face of the main structure; the 4" T slot structure should go at the free end of part 7 at the front of the structure with the gussets facing away from part 7 and tightened down there and the 6" T slot structure should go on the free end and be tightened down while maintaining the spacing set at the front of the structure (4" total distance between the outer faces of the long section)
- 8) Attach two more corner gusset brackets (part 9) to the top of each structure attached in step 7, leave them with enough wiggle room so that their position on the T slots can be adjusted; this will be used to clamp onto the two Swageloks (part 11) that will mark the beginning and end of the heated section

Thruster

- 9) Place the steel tube (part 19, cut 2" off first) into the ceramic wrap (part 23, cut down to 6ft), and hold the ceramic wrap in place with two hose clamps (part 25) at each end, not tightened down fully
- 10) Attach a Swagelok (part 11) to each end of the stainless steel tubing (part 19), tighten down as much as possible and seal all screwed sections with Teflon tape (part 14)
- 11) Align the ends of the ceramic wrap (part 23) with the beginning of the Swageloks (part 11) as much as possible and tighten down the hose clamps (part 25)
- 12) Measure out 5 feet of the ceramic covered section, and mark each inch with a sharpie
- 13) Take the Nichrome wire (part 24) and wrap the demarked section, with 5 turns approximately evenly spaced per inch to get a total of 300 turns over 60 inches; tuck the ends of the Nichrome wire through the hose clamps (part 25) and tighten them down again, leaving a bit of slack outside of the hose clamps for wire attachments
- 14) Screw the free end of the Nichrome wire (part 24) on each side into a ceramic screw terminal (part 31)
- 15) Take the 2" section of the steel tube (part 19) and use it to attach the last Swagelok (part 12) to the end of the system

- 16) Take two approximately 8ft sections of insulated 16 gauge wire (part 33) and connect one end of each to one section of the wall plug cord (part 34), secure the connection with heat shrink and/or electrical tape; connect the free end of the insulated wire to the ceramic screw terminals so that power can go from the input into the Nichrome wire
- 17) On the opposite end from the side of the tube with two Swageloks, attach the high pressure regulator (part 15) using Teflon tape (part 14) to seal the screwed connection
- 18) Attach the ball valve on the free end of the regulator in the same way and then finally the compressor connection (part 17); at this point the inlet to the system should be the compressor quick connection and the end of the system should be the male end of a Swagelok (part 12)
- 19) Take the 3D printed nozzle (part 22) and tap the print open, then screw the print onto the end of the outlet Swagelok (part 12)
- 20) Using corner gusset brackets sticking up from the thruster support structure, clamp the thruster into the thruster support and then screw everything down tightly; check for any loose points and adjust as necessary to make the whole structure rigid so that a force at the nozzle will move the assembled structure together

Outer structure

- 21) Take the linear rails (part 26) and remove one bearing from each of them, then drill out both holes closest to the end of each rail so that they can fit $\frac{1}{4}$ " screws
- 22) Take two rails with one bearing on and install them 3 in away from a free end of a 6' T slot (part 4) each using part 28 and the nuts from part 29
- 23) Take the other two rails and install them the same way 6 in away from the opposite end of the 6' T slot (part 4); all of the rails should now be attached to the same face of their respective 6' T slot and this face is now the top face
- 24) Use corner brackets (part 10) to attach the two 6' T slots (part 4) to a 4.75" T slot (part 1), with the 6' T slots parallel to each other, and the inside face of each long T slot being coincident with the end faces of the 4.75" T slot
- 25) Use corner brackets (part 10) to attach two 12" T slots (part 2) to a 4.75" T slot (part 1), with the 12" T slots parallel to each other, and the inside face of each long T slot being coincident with the end faces of the 4.75" T slot
- 26) Pick a face perpendicular to the 4.75" T slot face that has the corner brackets (part 10) on it, and designate it the top face, then install two corner gussets (part 9) sticking up from the top face, centered with 0.5" space between them
- 27) Take the 3D printed force sensor mount (part 34) and attach two corner gussets (part 9) to it with the free faces coplanar to the base of the print (continuous face perpendicular to the holes left for the screws to mount in), then align the free faces to the top face of the 12" T slot (part 2) 1.5 inches away from the 4.75" T slot (part 1, the 3D print's long edge should be parallel to this) and screw in with the T slot nut-screw pairs (part 29)
- 28) Use four more straight plate connectors (part 7) to colinearly connect the 6' T slot last mentioned in step 24 to the 12" T slots while aligning the top and bottom faces; these plates should be installed on the top and bottom faces of both subassemblies with two screws used per subassembly and $\frac{1}{4}$ " washers (part 31) used with the T slot screw-nut pairs (part 29)
- 29) Using two M4x10 screws (part 27) placed diagonally from each other, attach the mating plate (part 35) to each linear rail bearing (sub part of 26); should have M4 washers sandwiching the mating plate
- 30) Flip the structure upside down and install the 10" T slots (part 5) perpendicular to the structure so that they stick up in the air at a slight angle; use corner brackets (part 10) and have the flat faces of the bracket face away from the rest of the structure

- 31) Use corner brackets on the outside faces of the 10" T slots (part 5) to attach another 10" T slot (part 5) perpendicularly so that the perpendicular bar would be resting on the ground when the structure is flipped right-side up; tighten everything in this structure down and make adjustments as needed so everything is rigid

Attaching subassemblies and instrumentation (WARNING: NEED AT LEAST 2 PEOPLE FOR THIS)

- 32) Flip the outer structure back up, it should be sloping down now at an angle of about 8 degrees
- 33) Place the force sensor into its mount, have the back of the sensor pressing against the corner gussets mounted pointing up from the top face and the compression force reading attachment on the reading end
- 34) Use the screws that come with the linear rails to place a placeholder screw at the first free hole in each rail, starting from the front of the outer structure (low point of the system), then bring each linear rail bearing to rest against the placeholder screw
- 35) Use two bricks on each end of the system to lift it up off of the table, then place the thruster support structure on top of the system and have one person hold it in place while another person uses ¼" washers and the T slot screw-nut pairs (2 of each per linear rail bearing) to secure the thruster support structure to the outer structure
- 36) Once everything is tightened into place and the person securing the screws in step 35 has moved, the placeholder screws should be removed and the thruster support should slide freely until it makes contact with the compression end of the force gauge; check if the contact is straight on and adjust as necessary
- 37) Use Teflon tape (part 14) on the screw ends of the thermocouples and then screw them in at the perpendicular opening in the Swageloks bracketing the heating section (part 11), then screw the pressure gauge (part 21) into part 12 in the same manner
- 38) Charge the compressor and connect it to the inlet of the system, then open the valve slowly and check/ID for leaks, sealing with Teflon tape, electrical tape, and hot glue as appropriate when the airflow is off (if using hot glue, the air at this leak can not go above 80 C!)
- 39) Plug the heating section wire into the variac and the variac into wall power, then check that the Nichrome wire is actually heating, turn off quickly once confirmed; for quicker cooling open the valve for some time

3. Brainstorming Supplements

Appendix A: Pictorial Journey Map

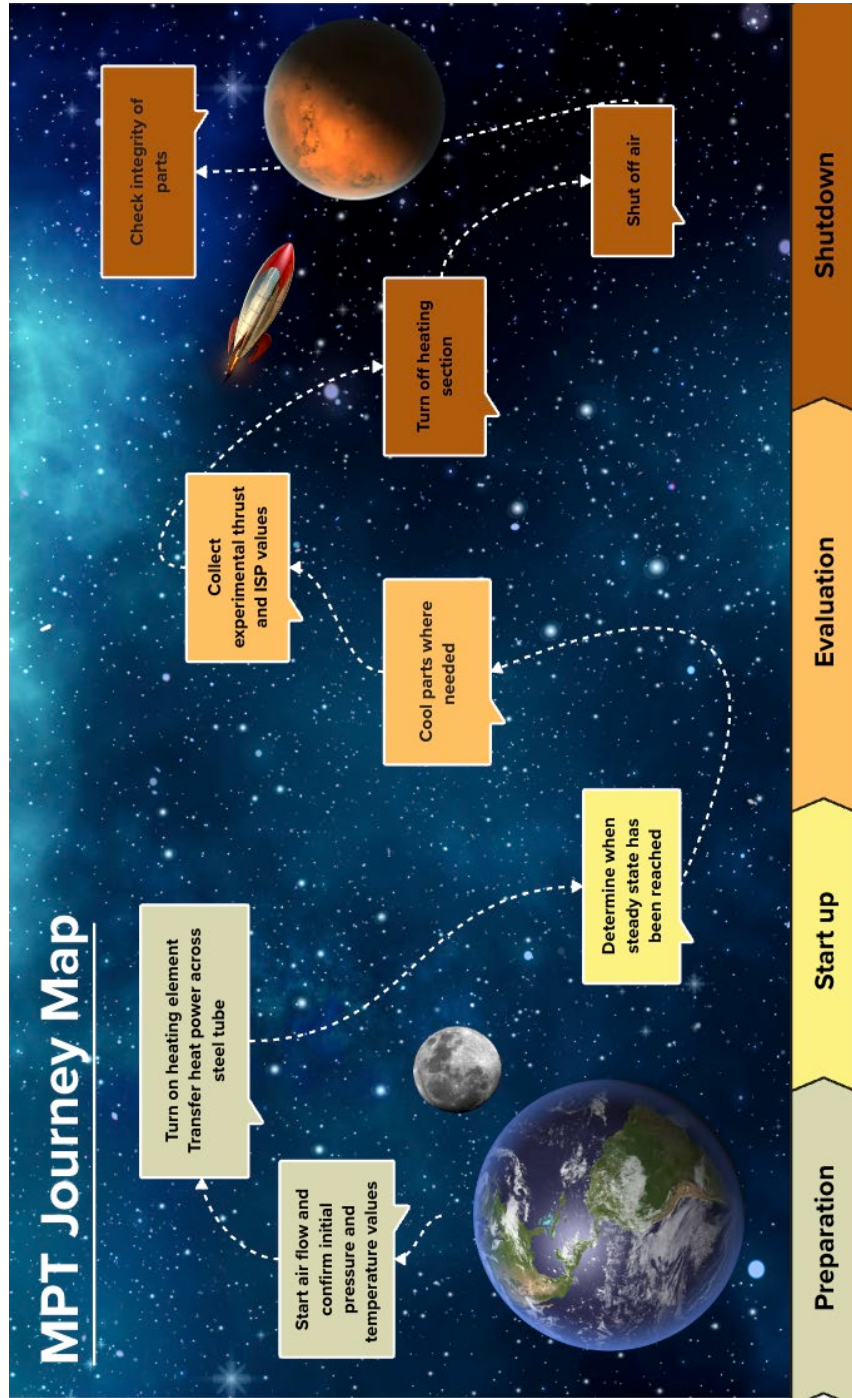


Figure 1: Journey Map Image

Appendix B: Brainstorming Idea List

Positive Cues

Flash cards

1. Have parts list with a spreadsheet, update condition of part each time test is run or change in the part is noted
2. Cooling channels in the nozzle, split some of the flow from the beginning of the system to go through the channels
 - Need pressure checks on the channels to make sure the walls of the channels are thick enough
3. Immerse the nozzle (excluding outlet) in cooling bath
4. Cooling jacket
5. Fire the nozzle into a bath of water?
6. Pendulum set up for thrust measurement à like aerospace corporation à proven
7. Weight scale for thrust measurement?
 - Need to be able to fire down/up
8. Flex tubing and excess length for initial flow sections to allow config changes for thrust measurement
9. Up power going into heating coil to increase flux going into the coils during start up, coarse adjustment by hand and then maintain via control system?
10. Use isothermal steel tube assumption to cool exposed areas of the tube outside of the heating section during shut down
11. External cooling jacket for the heating section
 - Temperature rating concern
 - Can we buy this? Design time to consider if not, running low as is
12. Flowmeters are expensive, can we make a cheaper version that will suit our needs?
 - Design lead time!
 - How exactly do they work
 - How precise can we get
 - Can this be made digital at the scale of available time and budget investment
13. Set up all sensors to be read from looking in the same direction? One person reads all measurements
14. Set up sensors to be read from different directions to get more simultaneous results
 - Easier to track long term behavior manually
15. Have parts on standby in case of breaks
16. Heat gas in stages to ensure accuracy and possibly allow for more overall heating
17. Throughout burn, change nozzle parameters actively to optimize thrust
 - How would we change geometry and maintain structural integrity?
18. Prevent heat loss using insulation
19. Boost performance by experimenting with different propellants (Argon, Helium, air, Nitrogen, etc)
20. Wrap stainless steel tube with nichrome wire as heating element

21. Run current directly through stainless steel tube as heating element
22. Run current directly through aluminum tube as heating element
23. Use quartz tube for air flow, wrap with nichrome wire
24. Use ceramic tube for air flow, wrap with nichrome wire
25. Wrap stainless steel tube with ceramic insulator, then wrap with nichrome wire
26. Active control of voltage source to control system temperature
27. Utilize induction heater
28. Closed loop control system to require less human actuation and faster (reduce overshoot and settling time of the control system for flow rate and heating)
29. Use Kalman filter instead of PID for the closed-loop control system
30. Use anemometer to measure output velocity
31. Use balloons inflated over a known time period to estimate the volumetric flow rate of the system
32. Preheating Method – take your time heating up the gas and building pressure, then release this pressure over a shorter period of time
33. Pulse Preheat Method – same as above, except the cycle is repeated n times per minute
34. Introduce a feedback thermodynamic cycle/loop (gas to heat exchanger, to heater, a portion back into the heat exchanger)
35. Optimize design parameters such that the pressure at the nozzle exit is as close to ambient pressure (but slightly above) as possible

Parallel Systems

36. Add variable thrust capabilities based on the wattage going into the heating coil – resistojet
37. Kilns use coils for resistive heating, maybe use a kiln coil for the heating section? -- kiln
38. Blow fuel directly over the heating coils – hairdryer
39. Regenerative cooling for all cooling jackets needed? -- combustion rocket engine
40. Ablation cooling: burn off insulation to get rid of heat – combustion rocket engine
41. Use water for fuel since it has a higher Cp and therefore can take more heat in – solar panel direct cooling
42. Use redundant sensor configs (TMR vs dual) to check for errors between sensors – industry standard from power generation gas turbines

Morph Chart

43. Compressed air through a heating coil, with measurements collected through a DAQ
44. Compressed air through a heating coil, with measurements collected through analog instrumentation
45. Compressed air through a heating coil, with measurements collected and recorded with a paper log
46. Compressed air heated because of microwaves, with measurements collected through a DAQ
47. Compressed air heated because of microwaves, with measurements collected through analog instrumentation
48. Compressed air heated because of microwaves, with measurements collected and recorded via paper log
49. Compressed air heated because of induction heating, with measurements collected through a DAQ
50. Compressed air heated because of induction heating, with measurements collected through analog instrumentation

51. Compressed air heated because of induction heating, with measurements collected and recorded via paper log
52. Compressed air heated because of solar heating, with measurements collected through a DAQ
53. Compressed air heated because of solar heating, with measurements collected through analog instrumentation
54. Compressed air heated because of solar heating, with measurements collected and recorded via paper log
55. Compressed air heated because of focused lasers, with measurements collected through a DAQ
56. Compressed air heated because of focused lasers, with measurements collected through analog instrumentation
57. Compressed helium heated because of focused lasers, with measurements collected and recorded via paper log
58. Compressed helium through a heating coil, with measurements collected through a DAQ
59. Compressed helium through a heating coil, with measurements collected through analog instrumentation
60. Compressed helium through a heating coil, with measurements collected and recorded with a paper log
61. Compressed helium heated because of microwaves, with measurements collected through a DAQ
62. Compressed helium heated because of microwaves, with measurements collected through analog instrumentation
63. Compressed helium heated because of microwaves, with measurements collected and recorded via paper log
64. Compressed helium heated because of induction heating, with measurements collected through a DAQ
65. Compressed helium heated because of induction heating, with measurements collected through analog instrumentation
66. Compressed helium heated because of induction heating, with measurements collected and recorded via paper log
67. Compressed helium heated because of solar heating, with measurements collected through a DAQ
68. Compressed helium heated because of solar heating, with measurements collected through analog instrumentation
69. Compressed helium heated because of solar heating, with measurements collected and recorded via paper log
70. Compressed helium heated because of focused lasers, with measurements collected through a DAQ
71. Compressed helium heated because of focused lasers, with measurements collected through analog instrumentation
72. Compressed helium heated because of focused lasers, with measurements collected and recorded via paper log
73. Compressed nitrogen through a heating coil, with measurements collected through a DAQ
74. Compressed nitrogen through a heating coil, with measurements collected through analog instrumentation
75. Compressed nitrogen through a heating coil, with measurements collected and recorded with a paper log
76. Compressed nitrogen heated because of microwaves, with measurements collected through a DAQ

77. Compressed nitrogen heated because of microwaves, with measurements collected through analog instrumentation
78. Compressed nitrogen heated because of microwaves, with measurements collected and recorded via paper log
79. Compressed nitrogen heated because of induction heating, with measurements collected through a DAQ
80. Compressed nitrogen heated because of induction heating, with measurements collected through analog instrumentation
81. Compressed nitrogen heated because of induction heating, with measurements collected and recorded via paper log
82. Compressed nitrogen heated because of solar heating, with measurements collected through a DAQ
83. Compressed nitrogen heated because of solar heating, with measurements collected through analog instrumentation
84. Compressed nitrogen heated because of solar heating, with measurements collected and recorded via paper log
85. Compressed nitrogen heated because of focused lasers, with measurements collected through a DAQ
86. Compressed nitrogen heated because of focused lasers, with measurements collected through analog instrumentation
87. Compressed nitrogen heated because of focused lasers, with measurements collected and recorded via paper log
88. Compressed hydrogen through a heating coil, with measurements collected through a DAQ
89. Compressed hydrogen through a heating coil, with measurements collected through analog instrumentation
90. Compressed hydrogen through a heating coil, with measurements collected and recorded with a paper log
91. Compressed hydrogen heated because of microwaves, with measurements collected through a DAQ
92. Compressed hydrogen heated because of microwaves, with measurements collected through analog instrumentation
93. Compressed hydrogen heated because of microwaves, with measurements collected and recorded via paper log
94. Compressed hydrogen heated because of induction heating, with measurements collected through a DAQ
95. Compressed hydrogen heated because of induction heating, with measurements collected through analog instrumentation
96. Compressed hydrogen heated because of induction heating, with measurements collected and recorded via paper log
97. Compressed hydrogen heated because of solar heating, with measurements collected through a DAQ
98. Compressed hydrogen heated because of solar heating, with measurements collected through analog instrumentation
99. Compressed hydrogen heated because of solar heating, with measurements collected and recorded via paper log
100. Compressed hydrogen heated because of focused lasers, with measurements collected through a DAQ

101. Compressed hydrogen heated because of focused lasers, with measurements collected through analog instrumentation
102. Compressed hydrogen heated because of focused lasers, with measurements collected and recorded via paper log

Negative Cues

Flash cards

1. Digitize sensors, use DAQ for information acquisition, make a VI to calculate system behavior in real time
2. Determine key points in operation (guesstimated in the journey map) to get model checks done
3. Have a valve to stop flow from going through nozzle during startup
 - Flow conditions are different with the nozzle attached, different enough that steady state would have to be reestablished
4. Specifically tuned control system for vent and nozzle valve actuations if valve present
5. Something in the nozzle to measure velocity of flow in there? Weird measurements would show presence of backflow
 - Need to be careful of compromising internal geometry of nozzle
6. Stick a strain gauge on the nozzle close to the outlet to get stress on the nozzle, back calculate what exit pressure is from this?
 - Need to be very precise in placing strain gauge
 - Design calculations required
 - NOT FRIENDLY TO NOZZLE ITERATION
7. 3D print the nozzle to make it easier to iterate, machining takes more time and energy from team
 - Nylon – 87 C heat deflection at 1.8 MPa, cooling NECESSARY, tensile strength when printed 50 MPa
 - Ti – need to find heat deflection for specific blend, cooling may be necessary (no idea of thermal conductivity in DMLS parts at present), tensile strength when printed unknown
 - ABS CF 10 via FDM (Stratasys) – 100 C heat deflection at 66 psi, cooling necessary, tensile strength at 21 MPa for upright print
 - PC ABS via FDM (Stratasys) – 112 C heat deflection at 66 psi, cooling necessary, tensile strength at 25.9 MPa
8. Sheet metal to make the throat and diverging sections?
 - Attachment issues even if the shape were to stay the same
9. Maybe fit into a flange and attach flange to the nozzle inlet?
 - More moving parts
10. Metal casting for nozzle manufacture
11. E stop by cutting off air flow first, then trigger heating circuit to turn off
 - If valve breaks, fitting loose, flow problem
12. Segment the set up so that problematic sections can be isolated
 - Add more vent to main flow set ups, like the one proposed for the nozzle, could be difficult to make this work
13. Units incongruity issues beginning to arise, make sure to provide all numbers in metric and do all calculations in metric
 - Keep note of the original customary dimension

14. Use an insulator to prevent shorting electricity through tube
15. Use high temperature insulation like ceramic to prevent burning
16. Ensure that every pipe fitting has Teflon tape wrapped clockwise at the threads so as to mitigate leaking of gas
17. Use steel/copper tubes and fittings so that the maximum allowed pressure (~100psi) will not be close to the failure pressure of the fitting (typical swagelok fittings go as high as 60k psi)
18. Prevent contact between thermocouple and pipe wall so that the measurement accurately represents the gas temperature not wall temperature
19. Match the current and voltage limits of the power source closely to the maximum allowable wattage of the heating element (prevent burnout and short circuits)
20. Mitigate thermal conduction upstream by using plastic/rubber tubing only upstream of the heating element
21. Cover the openings in the thermocouple plug to prevent air leakage in the system
22. Attach the nozzle inlet to the heated tube and ensure that it is sealed together
23. Generate a set of safety procedures to run through before testing

Parallel Systems

24. Closed loop fuel injection in automobile engines – based on air-fuel ratio in exhaust, pulses fuel injectors on/of for a different period of time to maintain engine combustion cycle
25. Complete calculations to ensure that system can withstand operating pressures – gas pressure vessel
26. Use SwageLok fittings for connections between tubes and sensors to prevent leaks - refrigerator
27. Buy check valve and place in front of the heating section to prevent backflow – Motorsports fuel system
28. Use Inconel, Monel, or Titanium alloys for nozzle to prevent mechanical failure under heavy heating – commercial aerospace parts
29. Conduct short duration tests to prove mechanical integrity of system prior to extended burn test – commercial aerospace testing
30. Flow visualization paint used in cars to see if flow direction is correct –Formula 1 racecar testing
31. Have stream indicator (tufts) to show direction of thrust, theoretically should show back pressure if occurring – Formula 1 racecar testing
32. Blowoff valve to bleed off excess/unsafe pressure – automobile turbocharger system
33. Use seals made of synthetic rubber or elastomers to reduce leakage– aircraft hydraulic systems
34. Employ a sophisticated control system to minimize startup issues – power plant startup
35. Implement an active cooling system using air cooling to prevent burning wire – high power electrical cables
36. Design a cool shot button that dispenses cold air to the wire for a brief period of time – hair dryer
 - Design time constraint
37. Set up a separate control room where the propulsion system can be monitored from in real time – commercial engine testing
 - Probably too big of a project for the team to deal with now, would be good for the actual full scale development
38. Design a clean room to prevent dust and other materials from interfering with measurements
39. Design a vacuum chamber so that there is no heat loss through the air and heat transfer is concentrated to the flow tube

40. Circuit breakers to limit levels of current through the wire for safety
41. Adding smell to the fluid so leaks can be noticed earlier
42. Submerge the tube so fluid leaks appear as bubbles
43. Design system to have interchangeable parts to extend test lifetime

Appendix C: Morph Chart

Solutions Subfunctions	1	2	3	4	5	Comments
Fuel Options	Compressed Air 	Compressed Helium 	Compressed Nitrogen 	Compressed Hydrogen 		Ideally use a gas with a high specific heat
Heat up gas	Heating Coil 	Microwaves 	Induction Heating 	Solar Heating 	Lasers 	Gas must be heated up quickly and temperature should be distributed evenly through tube
Instrumentation	DAQ 	Analog 	Paper Log 			Facilitate the method in which data is collected

Figure 2: Morph Chart

Appendix D: Idea Selection – Filters 1 and 2

Filter 1: ideas voted to move forward based on feasibility based on notes in Appendix B. Safety concerns with various fuels, material sourcing delays, etc, removed ideas that were good to think about but don't make sense at current scale

Positive

- Pendulum set up for thrust measurement à like aerospace corporation à proven
- Weight scale for thrust measurement?
 - Need to be able to fire down/up
- Cooling jacket for nozzle
- Heating gas in stages
- Wrap stainless steel tube with ceramic insulator, then wrap with nichrome wire
- Closed loop control system to require less human actuation and faster (reduce overshoot and settling time of the control system for flow rate and heating)
 - Maybe if we have more time
- Use balloons inflated over a known time period to estimate the volumetric flow rate of the system
 - Will be done as part of addressing sensing concerns
- Optimize design parameters such that the pressure at the nozzle exit is as close to ambient pressure (but slightly above) as possible
- - Maybe if we have more time
- Compressed air through a heating coil, with measurements collected through a DAQ
- Compressed air through a heating coil, with measurements collected through analog instrumentation

Negative

- Digitize sensors, use DAQ for information acquisition, make a VI to calculate system behavior in real time
 - Part of task that can be done based on another idea
- 3D print the nozzle to make it easier to iterate, machining takes more time and energy from team
 - Nylon – 87 C heat deflection at 1.8 MPa, cooling NECESSARY, tensile strength when printed 50 MPa
 - Ti – need to find heat deflection for specific blend, cooling may be necessary (no idea of thermal conductivity in DMLS parts at present), tensile strength when printed unknown
 - ABS CF 10 via FDM (Stratasys) – 100 C heat deflection at 66 psi, cooling necessary, tensile strength at 21 MPa for upright print
 - PC ABS via FDM (Stratasys) – 112 C heat deflection at 66 psi, cooling necessary, tensile strength at 25.9 MPa
- Metal casting for nozzle manufacture
- E stop by cutting off air flow first, then trigger heating circuit to turn off
 - If valve breaks, fitting loose, flow problem
 - Part of task that can be done based on another idea
- Use high temperature insulation like ceramic to prevent burning

- Generate a set of safety procedures to run through before testing (ideas nested to be added to safety documentation, pending)
 - Ensure that every pipe fitting has Teflon tape wrapped clockwise at the threads so as to mitigate leaking of gas
 - Use steel/copper tubes and fittings so that the maximum allowed pressure (~100psi) will not be close to the failure pressure of the fitting (typical swagelok fittings go as high as 60k psi)
 - Prevent contact between thermocouple and pipe wall so that the measurement accurately represents the gas temperature not wall temperature
 - Match the current and voltage limits of the power source closely to the maximum allowable wattage of the heating element (prevent burnout and short circuits)
 - Mitigate thermal conduction upstream by using plastic/rubber tubing only upstream of the heating element
 - Cover the openings in the thermocouple plug to prevent air leakage in the system
 - Attach the nozzle inlet to the heated tube and ensure that it is sealed together
 - Use seals made of synthetic rubber or elastomers to reduce leakage—aircraft hydraulic systems
 - Blowoff valve to bleed off excess/unsafe pressure – automobile turbocharger system
 - E stop by cutting off air flow first, then trigger heating circuit to turn off
- Buy check valve and place in front of the heating section to prevent backflow – Motorsports fuel system
- Flow visualization paint used in cars to see if flow direction is correct –Formula 1 racecar testing
- Have stream indicator (tufts) to show direction of thrust, theoretically should show back pressure if occurring – Formula 1 racecar testing

Filter 2: filter 1 pared down, idea lists combined since ideas should address positive and negative

- Pendulum set up for thrust measurement à like aerospace corporation à proven
- Weight scale for thrust measurement?
 - Need to be able to fire down/up
- Cooling jacket for nozzle
- Wrap stainless steel tube with ceramic insulator, then wrap with nichrome wire
- Optimize design parameters such that the pressure at the nozzle exit is as close to ambient pressure (but slightly above) as possible
- Compressed air through a heating coil, with measurements collected through a DAQ
- Digital sensors, use DAQ for information acquisition, make a VI to calculate system behavior in real time
- 3D print the nozzle to make it easier to iterate, machining takes more time and energy from team
 - Nylon – 87 C heat deflection at 1.8 MPa, cooling NECESSARY, tensile strength when printed 50 MPa
 - Ti – need to find heat deflection for specific blend, cooling may be necessary (no idea of thermal conductivity in DMLS parts at present), tensile strength when printed unknown
 - ABS CF 10 via FDM (Stratasys) – 100 C heat deflection at 66 psi, cooling necessary, tensile strength at 21 MPa for upright print
 - PC ABS via FDM (Stratasys) – 112 C heat deflection at 66 psi, cooling necessary, tensile strength at 25.9 MPa
- Metal casting for nozzle manufacture
- Use high temperature insulation like ceramic to prevent burning
- Buy check valve and place in front of the heating section to prevent backflow – Motorsports fuel system
- Flow visualization paint used in cars to see if flow direction is correct –Formula 1 racecar testing
- Have stream indicator (tufts) to show direction of thrust, theoretically should show back pressure if occurring – Formula 1 racecar testing

Appendix E: Decision Weighting Plot and Pugh Matrices

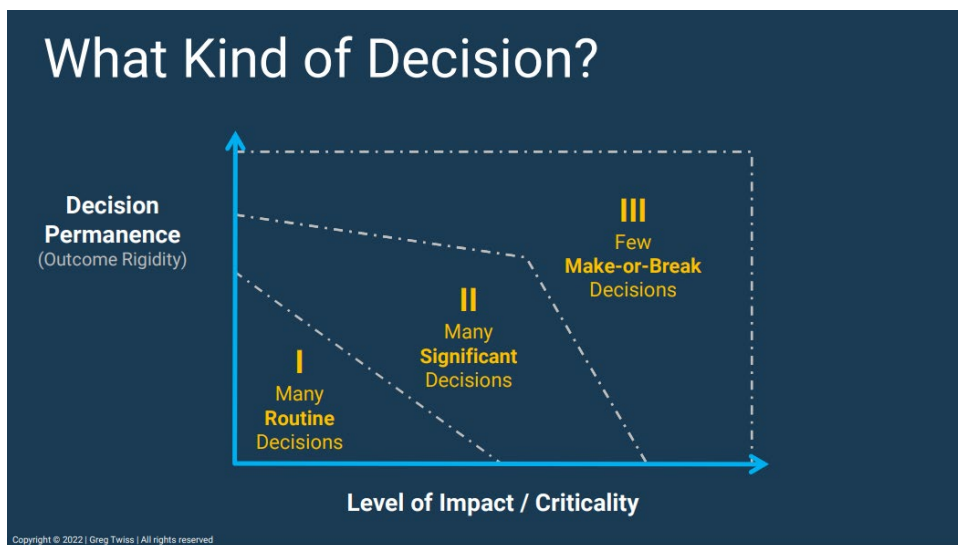


Figure 3: Decision Plot from Prof. Twiss' Slides

Section 1 Decisions

- Part integrity and set up specifics (these should all be done, so do not make sense for the Pugh matrix)
 - o Cooling jacket for nozzle
 - o Ceramic insulator between heating wire and heating section of pipe
 - o Compressed air through a heating coil, with measurements collected through a DAQ
 - o Buy check valve and place in front of the heating section to prevent backflow – Motorsports fuel system
 - o Flow direction checks (use option 1, 2, or 3)
 - Flow visualization paint used in cars to see if flow direction is correct –Formula 1 racecar testing
 - Have stream indicator (tufts) to show direction of thrust, theoretically should show back pressure if occurring – Formula 1 racecar testing
 - Integrated Flow Sensor (digital or analog)
- Sensing (analog and physical for first version, then digitize as the project moved forward)
 - o Digital sensors, use DAQ for information acquisition, make a VI to calculate system behavior in real time
 - o Analog/physical sensors
 - o Analog/electronic sensors

Section 2 Decisions

- Thrust measurement (needs to be decided)
 - o Pendulum
 - o Weight scale

Section 3 Decisions

- Part design (must be done anyway)
 - o Optimize design parameters such that the pressure at the nozzle exit is as close to ambient pressure (but slightly above) as possible
- 3D print the nozzle to make it easier to iterate, machining takes more time and energy from team (consider in matrix)
 - o Nylon – 87 C heat deflection at 1.8 MPa, cooling NECESSARY, tensile strength when printed 50 MPa
 - o Ti – need to find heat deflection for specific blend, cooling may be necessary (no idea of thermal conductivity in DMLS parts at present), tensile strength when printed unknown
 - o ABS CF 10 via FDM (Stratasys) – 100 C heat deflection at 66 psi, cooling necessary, tensile strength at 21 MPa for upright print
 - o PC ABS via FDM (Stratasys) – 112 C heat deflection at 66 psi, cooling necessary, tensile strength at 25.9 MPa
- Metal casting for nozzle manufacture (consider in matrix)

Pugh matrix idea list

- Nozzle mfg
 - o Metal casting
 - o 3D printing DMLS
 - o 3D printing Nylind 12 SLS
 - o 3D printing ABS CF 10 Stratasys FDM
 - o 3D printing PC ABS Stratasys FDM
 - o Machining (control, this was the originally planned method for manufacturing the nozzle)
- Thrust measurement
 - o Pendulum is held at a certain angle when on. Thrust is calculated based of mass.
 - o Weight scale just measures the change in mass of the physical setup when on vs off.
 - o Measuring the reaction force on a scale or pressure pad.
 - o Attaching nozzle to beam of know radius and material and allowing beam bending.

Table 1: Nozzle Manufacturing Pugh Matrix

Criteria	Metal Casting	3D printed DMLS	3D printed Nylon 12 SLS	3D printed PLA	Machining
Resolution	1	2	2	1	5
Strength	5	4	3	1	5
Heat Resistance	5	5	1	-2	5
Cost	-3	5	1	5	-3
Turnaround Time	-4	3	3	4	-3
Total	4	13	10	9	9

Table 2: Thrust Measurement Setup Pugh Matrix

Criteria	Pendulum	Weight Scale	Beam Bending
Accuracy	3	5	0
Precision	-1	5	-3
Difficulty	-3	-1	-3
Cost	-2	0	0
Design and Build Time	-1	3	0
Total	-2	12	-6

4. Engineering Part Drawings

The following section includes dimensioned drawings for all in-house designed and manufactured, or bought and modified components critical to the function of the final system. Purchased and un-modified components are not included in this section. Links to components not found in this section are available in the Bill of Materials (Appendix 6A).

Appendix A: Linear Rail Mating Plate

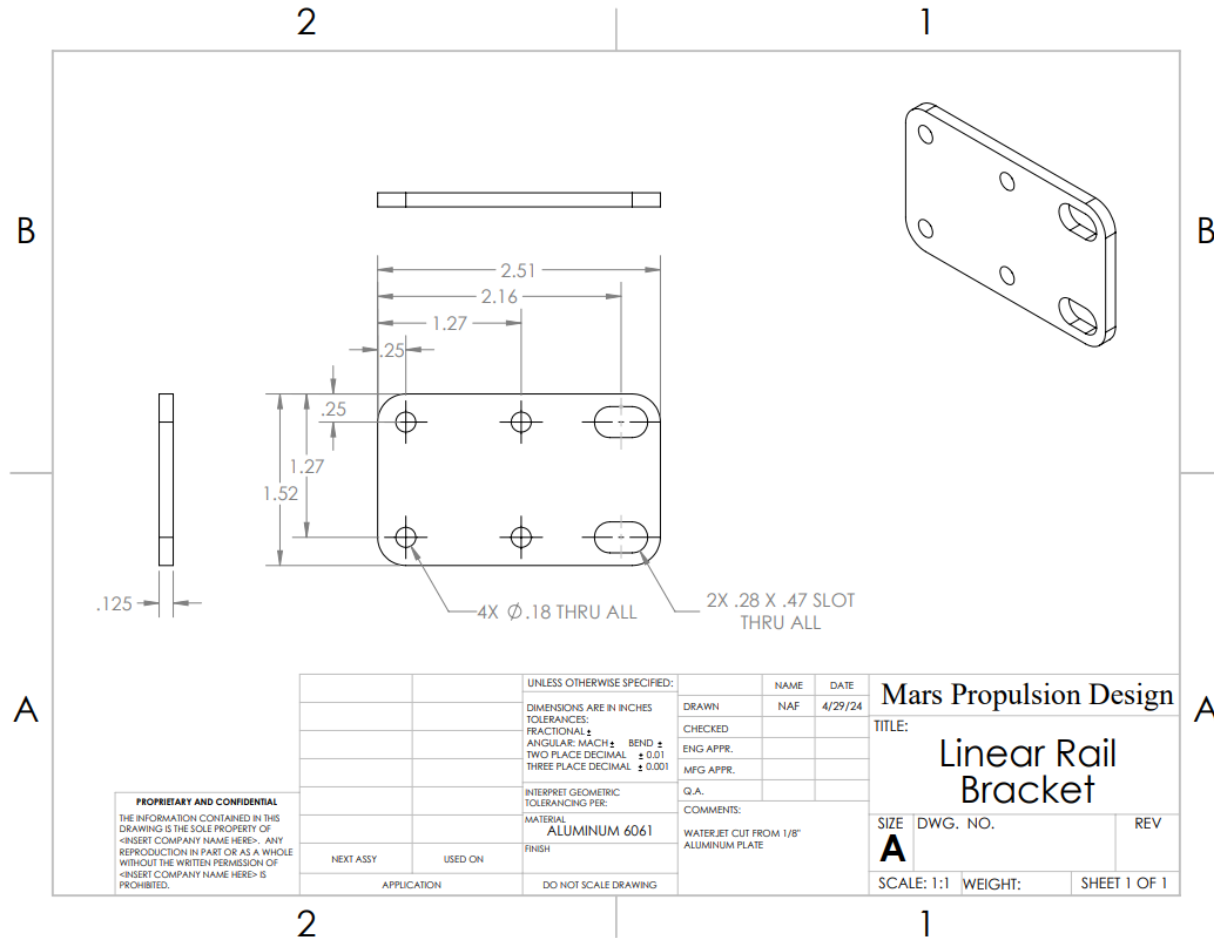


Figure 1: Dimensioned Drawing

Appendix B: T Slot Straight Linear Plate Connector

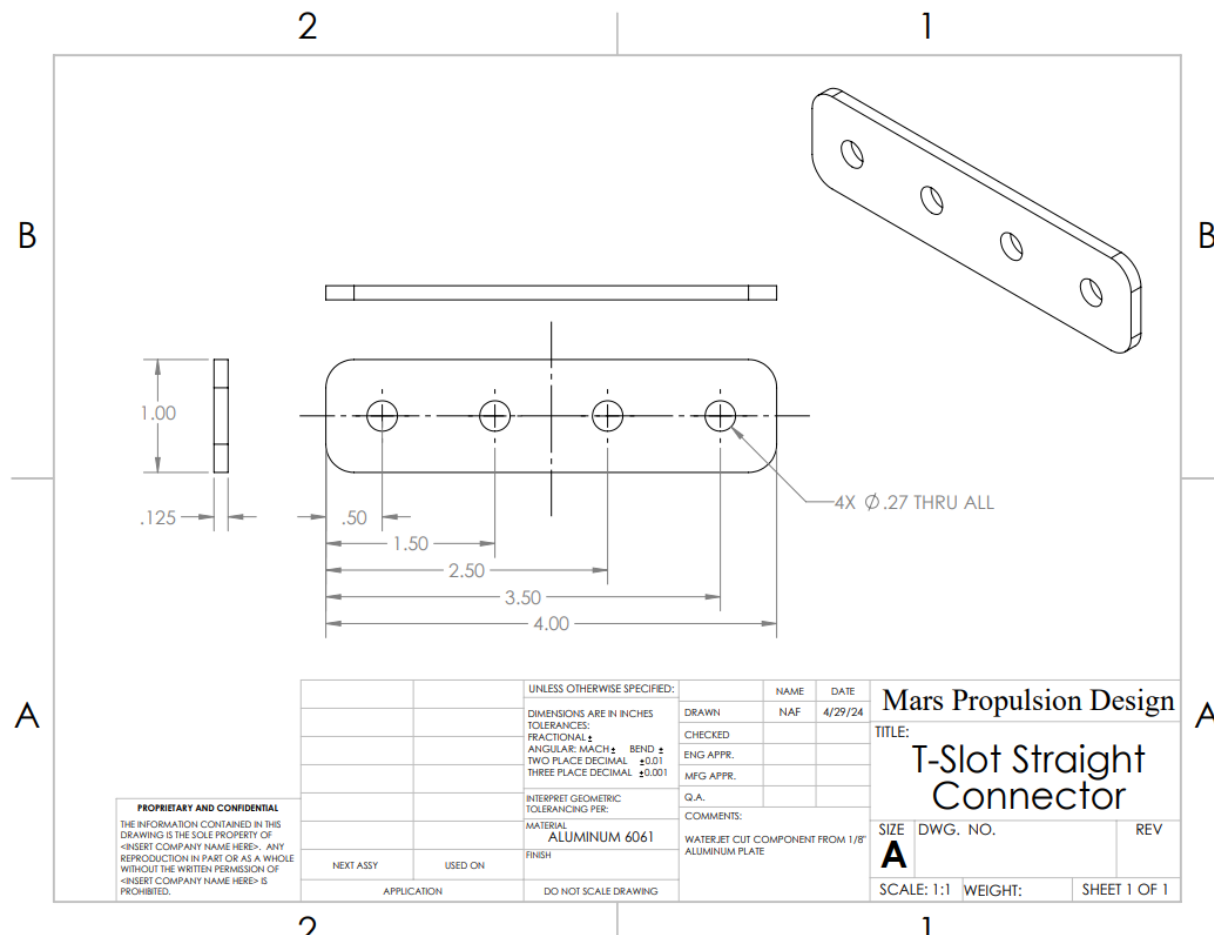


Figure 1: Dimensioned Drawing

Appendix C: T Slot

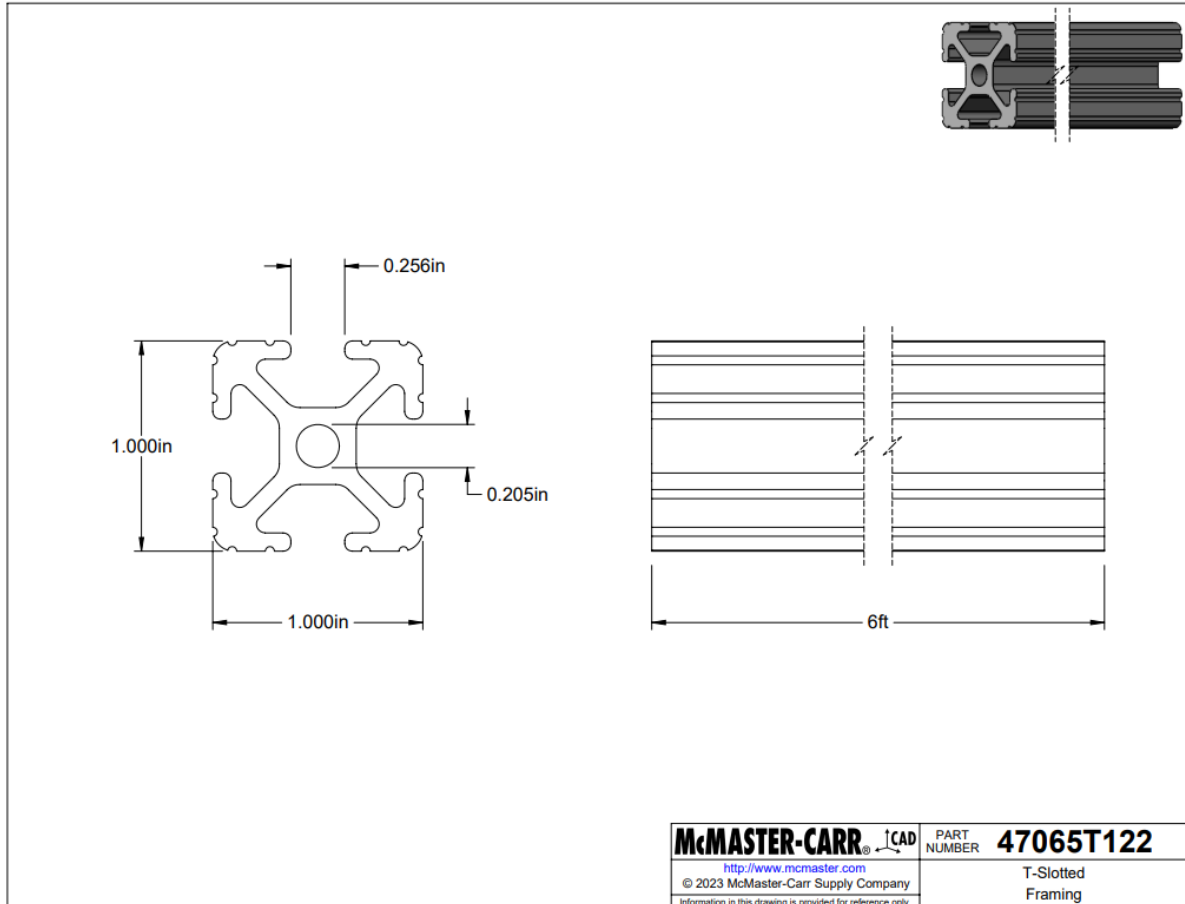


Figure 1: Dimensioned Drawing

Note: This drawing is for the T Slot purchased, it was cut down to the lengths needed as per the fabrication instructions in Appendix 2A

Appendix D: Corner Gusset Bracket

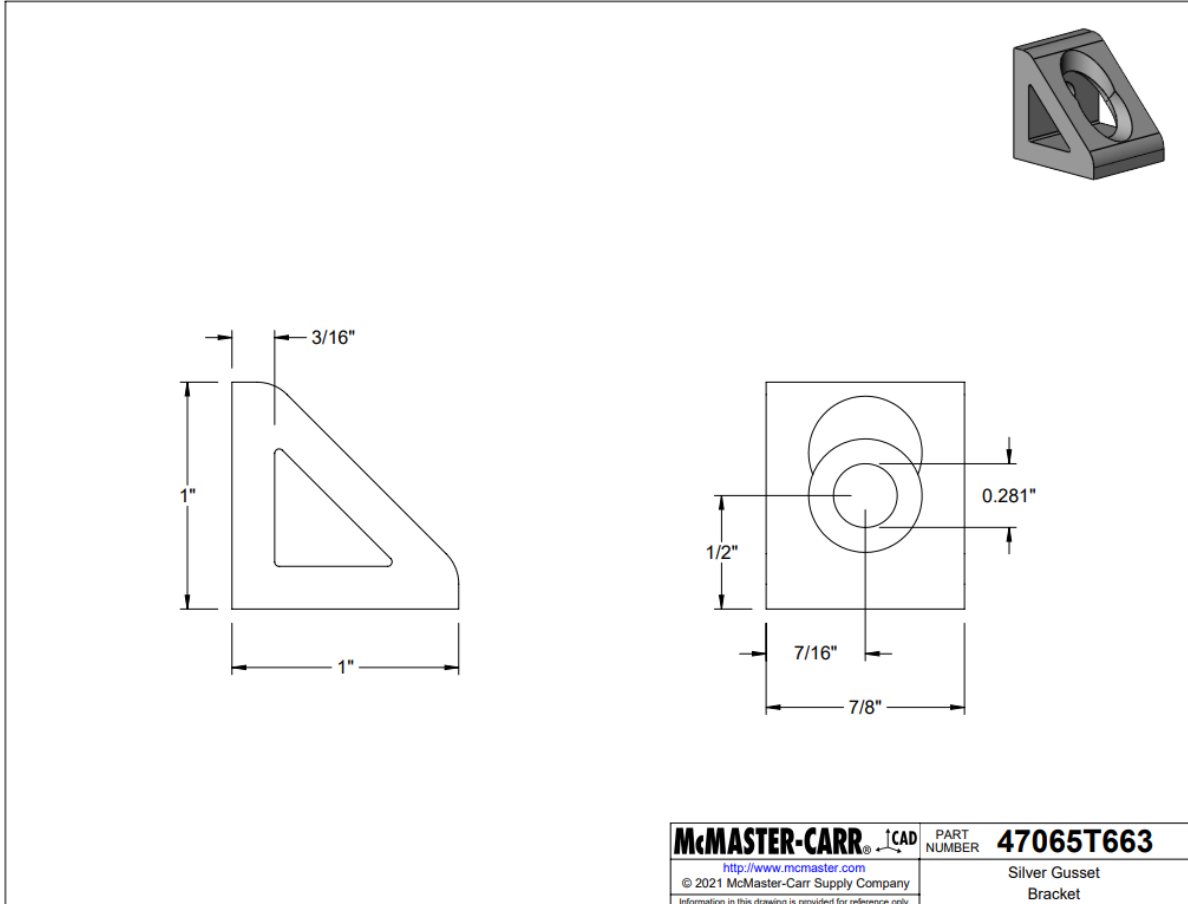


Figure 1: Dimensioned Drawing

Appendix E: Linear Rail

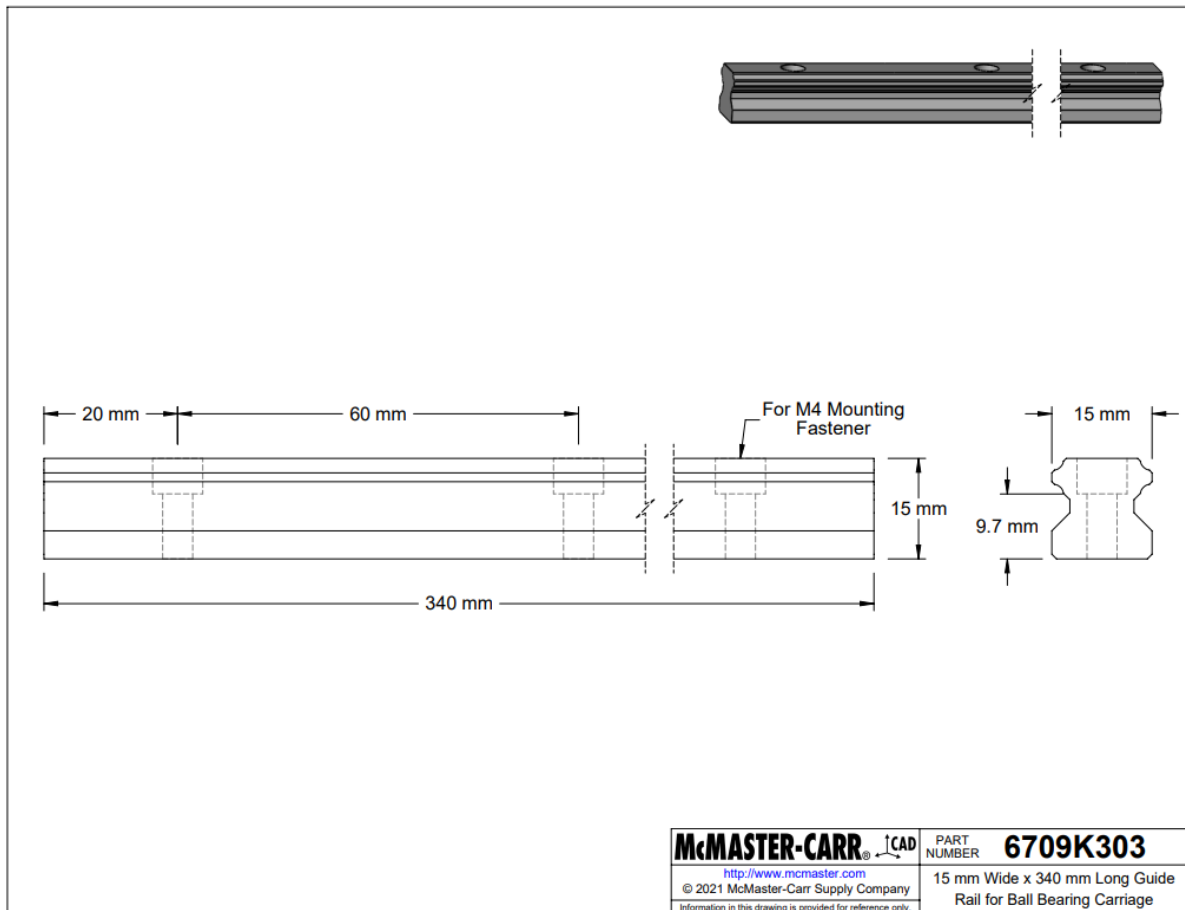


Figure 1: Dimensioned Drawing

Appendix F: Linear Rail Bearings

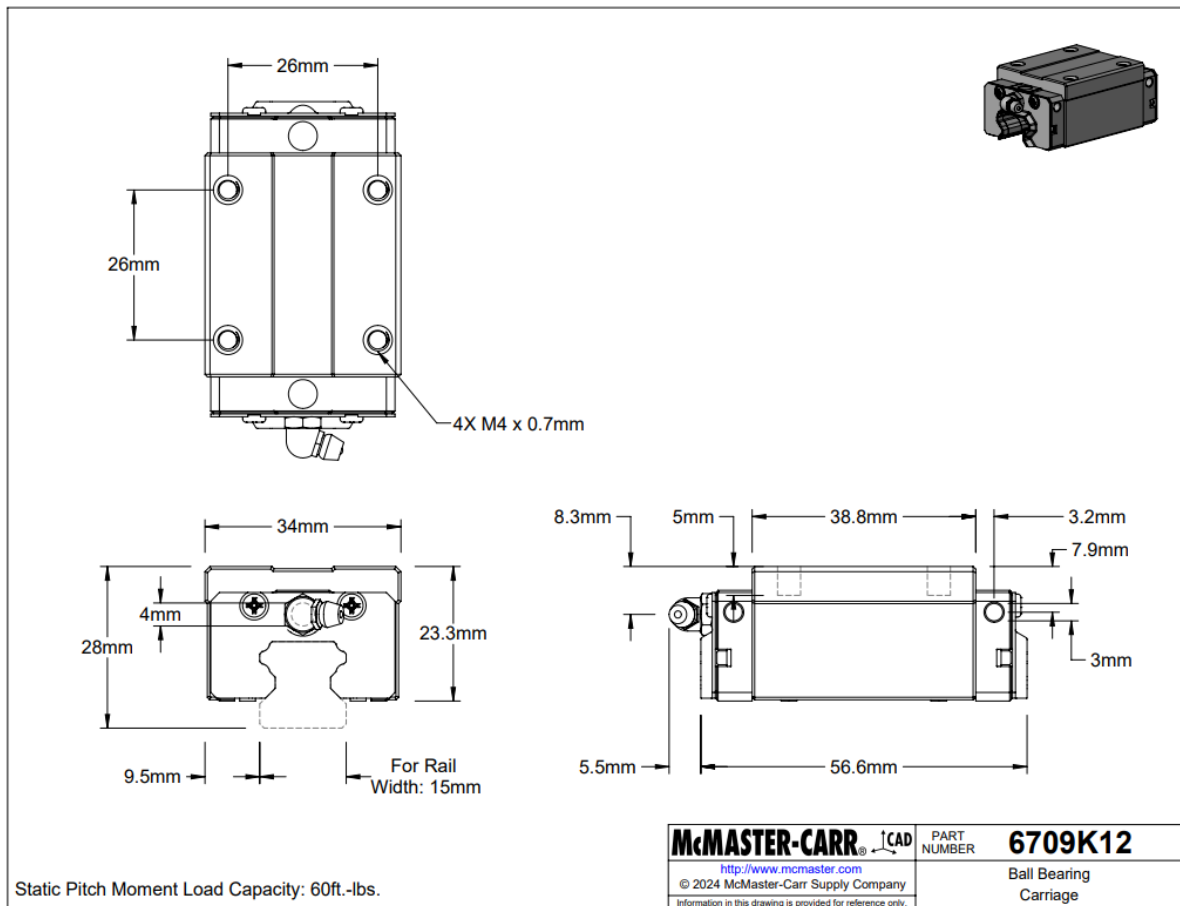


Figure 1: Dimensioned Drawing

Appendix G: Stainless Steel Tube

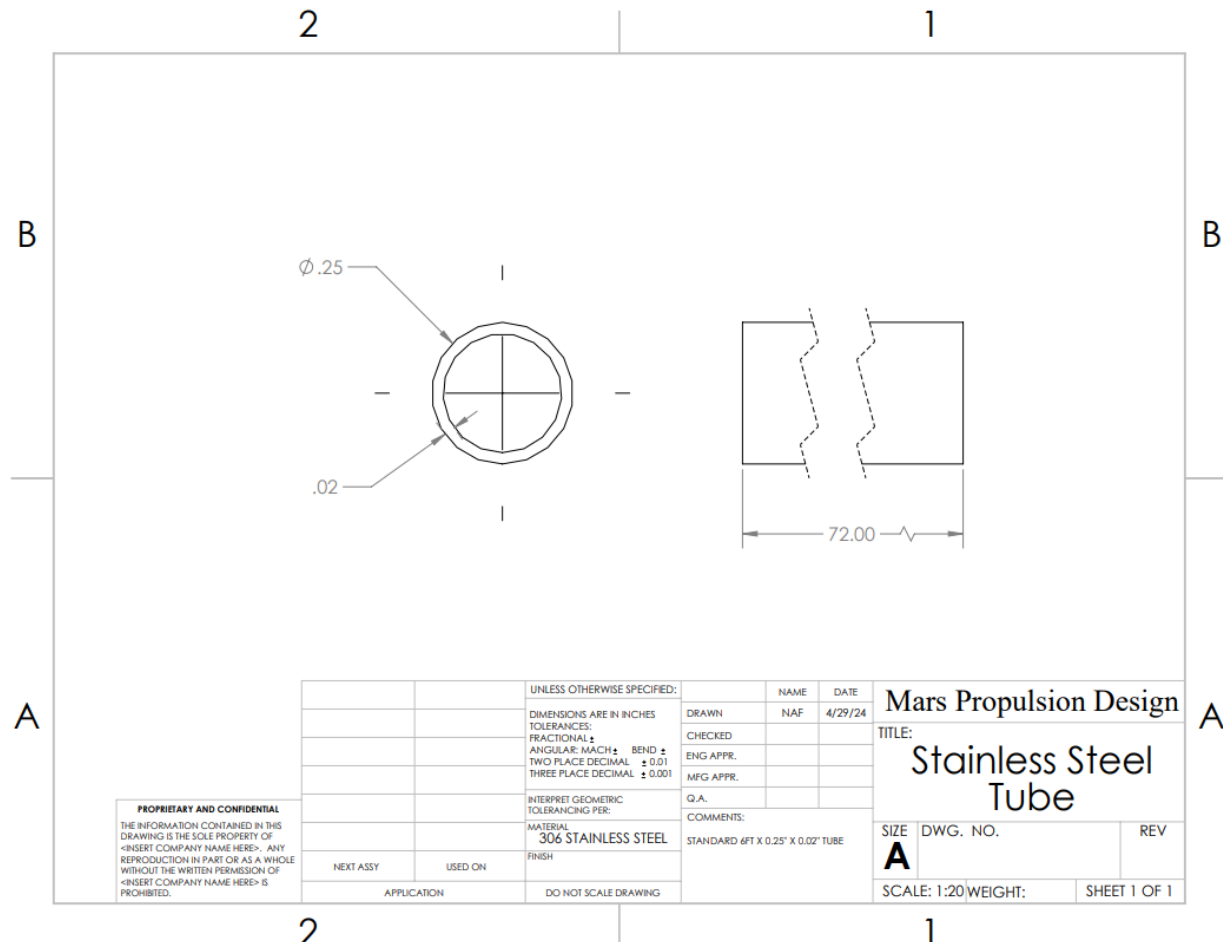


Figure 1: Dimensioned Drawing

Appendix H: Ceramic Sleeve

No-Irritation Ceramic High-Temperature Sleeving 1/4" ID



Length, ft.
✓ 10

Each

ADD TO ORDER

\$19.38 Each

In stock

88175K32

Sleeving Type	Non-Expandable
Sleeving Construction	Braided
Performance Properties	High Temperature
Material	Ceramic Fabric
ID	1/4"
Wall Thickness	1/16"
Minimum Temperature	Not Rated
Maximum Temperature	1100° F
Specifications Met	MIL-I-24244
Color	White
Length	10 ft.
RoHS	RoHS 3 (2015/863/EU) Compliant
REACH	REACH (EC 1907/2006) (01/17/2023, 233 SVHC) Compliant
DFARS	Specialty Metals COTS-Exempt
Country of Origin	United States
USMCA Qualifying	No
Schedule B	690320.0000
ECCN	EAR99

Unlike fiberglass and silica, this sleeving won't irritate skin, so it's easier to handle. It withstands open flame and molten metal splash, making it a good choice for welding applications. The ceramic fabric also resists acids, alkalies, alcohol, solvents, oil, and gasoline. Because this sleeving is non-expandable, it does not stretch, so it's best for applications where you know the exact diameter of the items you need to protect. It meets MIL-I-24244 for material quality.

Figure 1: McMaster Product Detail Page

Note: Dimensioned drawing not available for this part

Appendix I: Nozzle (100 psi Design)

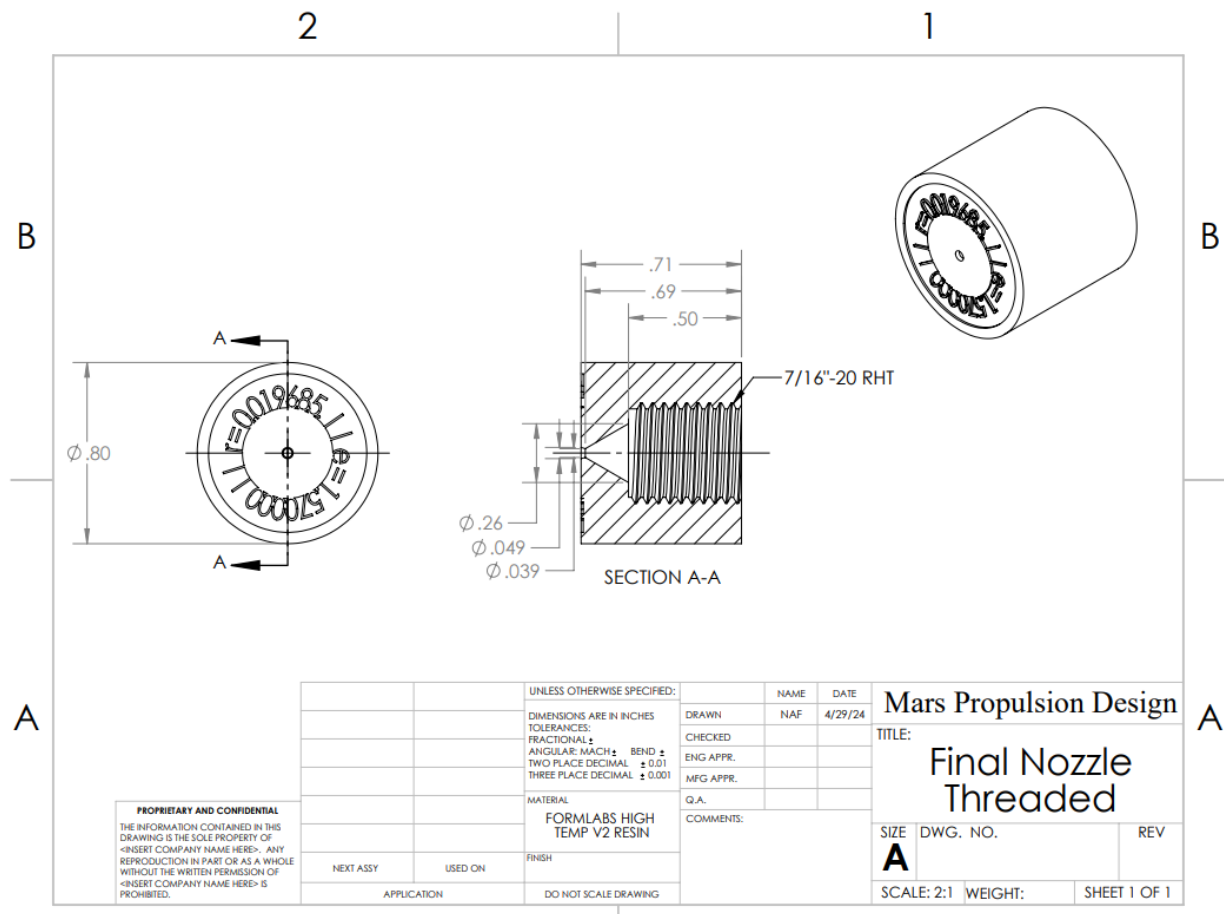


Figure 1: Dimensioned Drawing

Appendix J: Force Sensor Mount

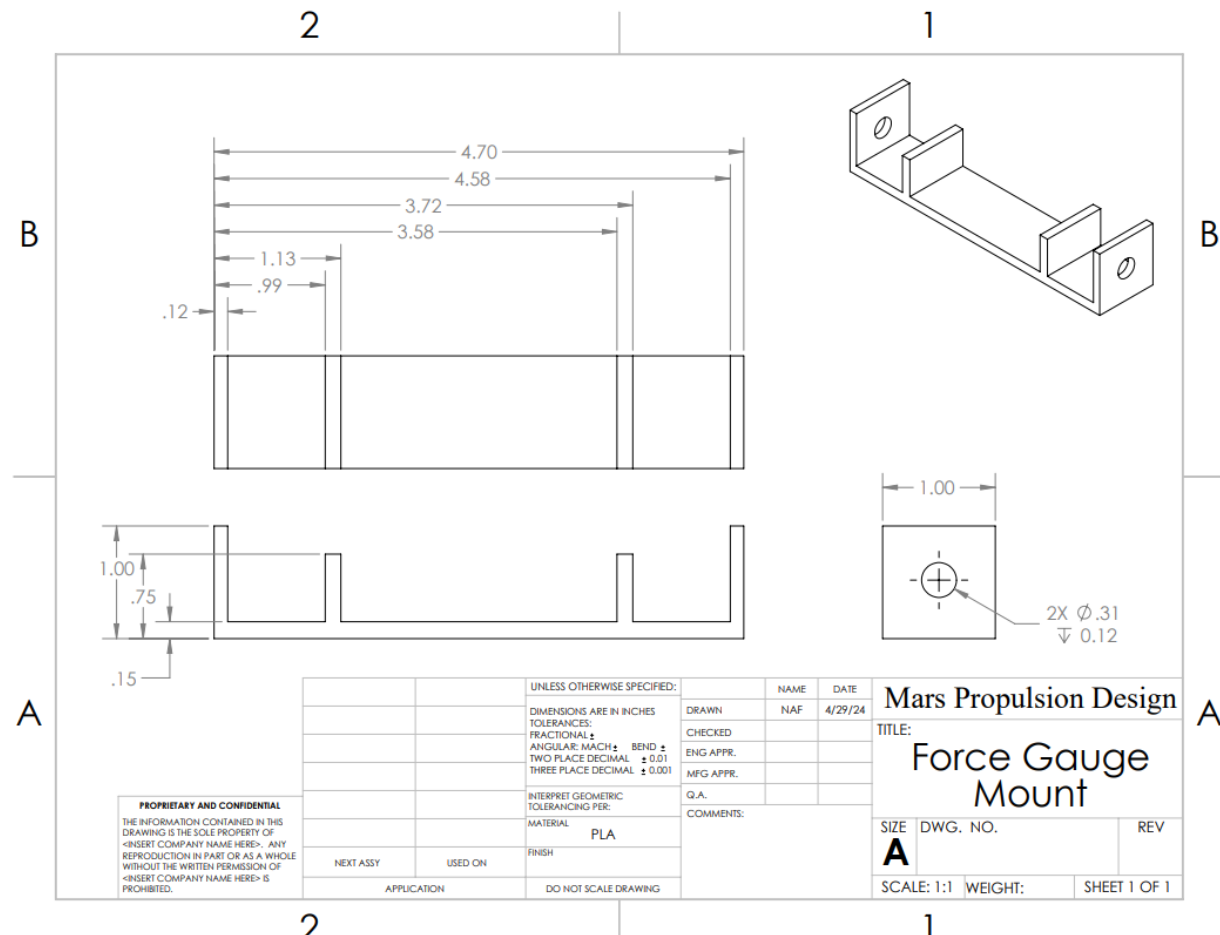


Figure 1: Dimensioned Drawing

Appendix K: Corner Bracket

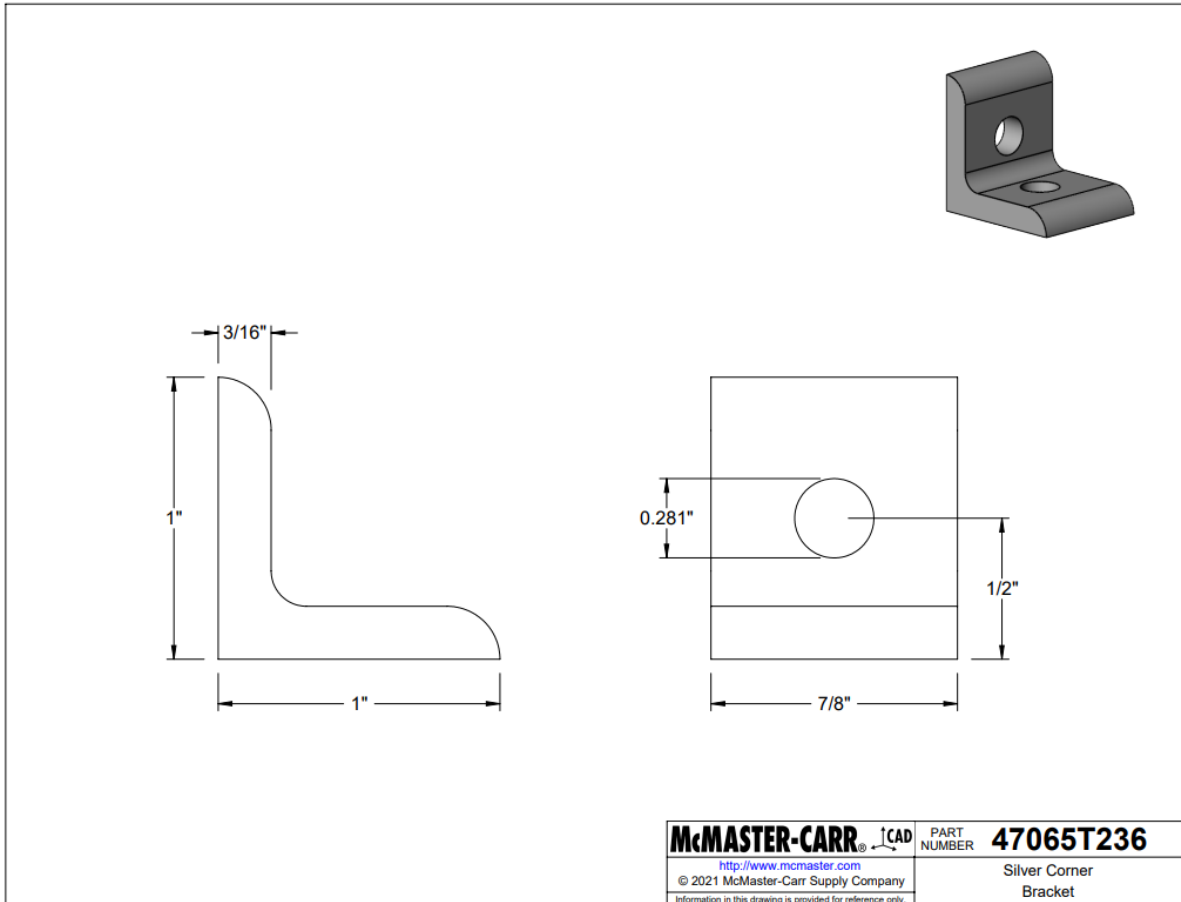


Figure 1: Dimensioned Drawing

5. Engineering Assembly Drawings

Appendix A: Complete Assembly with Balloon Callouts

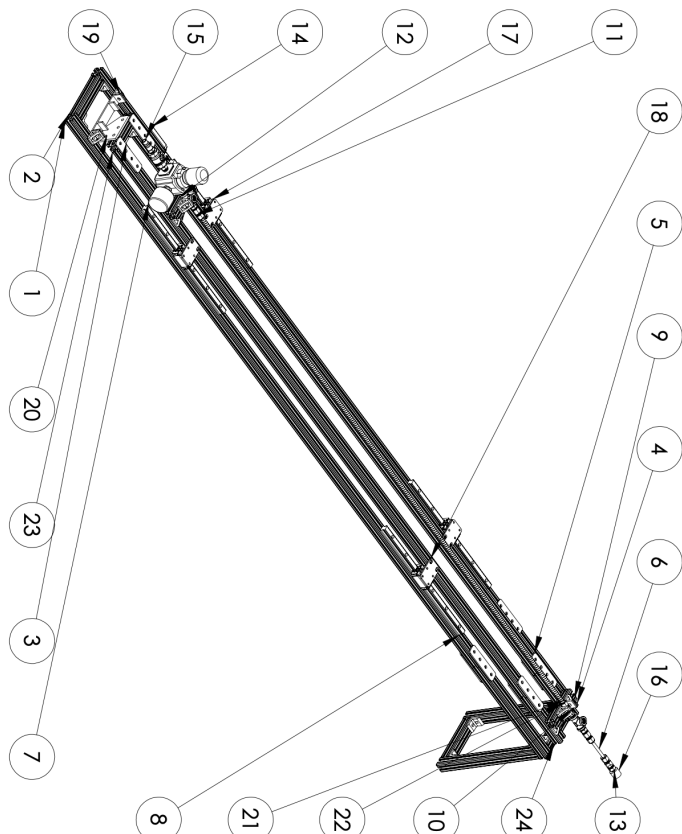
2

1

B

BILL OF MATERIALS

NO.	PART	DESCRIPTION	QTY.
1	47065T122	T-Slotted Framing	2
2	47065T011	T-Slotted Framing	3
3	47065T236	Silver Corner Bracket	10
4	47065T122	T-Slotted Framing	4
5		T-Slot Straight Connector	10
6		304L Stainless Steel Tube	1
7	7390K71	Norgren Air Regulator	1
8	6709K303	15 mm x 340 mm Guide Rail	4
9	47065T828	T-Slotted Framing	3
10	47065T663	Silver-Gusset Bracket	10
11	5943K284	Yor-Lok Fitting for Stainless Steel Tubing	4
12	4464K48	304 Stainless Steel Pipe Fitting	2
13	50715K162	Flared Fitting for Stainless Tubing	6
14	4628K81	Air-Exhaust On/Off Valve	1
15	5597K12	Quick-Disconnect Hose Coupling	1
16	6709K12	Final Nozzle Threaded	1
17	6709K12	Ball Bearing Carriage	4
18		Linear Rail Bracket	4
19		Force Gauge Mount	1
20	47065T267	T-Slotted Framing	1
21	88175K32	Ceramic High-Temp Sleeveing	1
22		Coll - Nichrome 80/20 Gauge	1
23	47065T413	T-Slotted Framing	2
24	47065T122	T-Slotted Framing	2



A

A

2

1

Figure 1: Full Assembly Engineering Drawing

6. Bill of Materials

Appendix A: As-Built Bill of Materials

Table 1: Tabular Bill of Materials

Item Description	Use Case	Price per unit	Amount	Total Cost	URL
1/4" Ceramic Sleeving	Used to insulate the coils from the pipe so that the current doesn't short straight through the stainless steel pipe	\$19.38	1	\$19.38	No-Irritation Ceramic High-Temperature Sleeving, 1/4" ID McMaster-Carr
Screw-in Thermocouples	To measure temperature at the beginning and end of the heating section, screw-in required to be able to effectively seal the joint where thermocouples are introduced to the system	\$52.74	1	\$52.74	EGT Thermocouple for Exhaust Gas Temp Probe with Exposed Tip & Connector K Type: Amazon.com: Industrial & Scientific
Nichrome 80 wire, 20 gauge	Used as a resistive heating element to convert electrical power supplied by the variac into thermal energy to be supplied to the fluid	\$9.99	1	\$9.99	Nichrome 80-50' - 20 Gauge Wire - 50ft - 0.81mm - 0.032in - Made in USA - Master Wire Supply: Amazon.com: Tools & Home Improvement
Gusset Corner Bracket	Used as a 90 degree connector for t-slots rails where the extra support from the gusset was needed	\$9.97	12	\$119.64	Silver Gusset Bracket, 1" Long for 1" High Rail T-Slotted Framing McMaster-Carr
Single T-Slot Rail, 1" x 1"x 6'	Actual t slot rails used to build the supporting structure for the heating rig and build the thrust stand	\$34.03	6	\$204.18	T-Slotted Framing, Single Four Slot Rail, Silver, 1" High x 1" Wide, Solid McMaster-Carr
Corner Bracket	Used as a 90 degree connector for t slot rails in tight fits as well as where the gusset wasn't needed	\$7.92	8	\$63.36	Silver Corner Bracket, 1" Long for 1" High Rail T-Slotted Framing McMaster-Carr
High Pressure Regulator	To be able to regulate pressure between 0 and 200 psi	\$43.50	1	\$43.50	Amazon.com: Viair Inline Air Pressure Regulator, 0-200 psi, Black, 90150 : Tools & Home Improvement
350 mm long Linear Rails	To allow the thruster apparatus to move linear independently of the rest of the thrust stand structure with low friction	\$21.50	4	\$85.98	350MM Linear Rail 2PCS HGR15 Linear Guide Rail HGH15 Linear Slide Rail with 4PCS HGH15CA Carriage Slider Block

					CNC Kit: Amazon.com: Industrial & Scientific
3D Printed Nozzles, 100psi and 150 psi versions	Printed using Formlabs High Temp v2 resin, cost is based on Bluesmith printing service charges	\$23.73	1	\$23.73	Bluesmith 3D Printing Service (duke.edu)
Aluminum Plate Stock	Used to make surface connectors for the thrust stand as well as the mating plate between the linear rails and the thruster structure	\$14.69	1	\$14.69	Amazon.com: 6061 T651 Aluminum Sheet Metal 12 x 12 x 1/8 (0.125") Inch Thickness Rectangle Metal Plate Covered with Protective Film, 3mm Aluminum Sheet Plate Flat Stock, Finely Polished and Deburred : Industrial & Scientific
200 psi compressor	Used to compress air to use in the thruster system	\$469.99	1	\$469.99	DEWALT 200 PSI 15 Gallon Air Compressor D55167 - Acme Tools
Compressor hose	Connects compressor to air inlet to the thruster	\$24.42	1	\$24.42	Estwing E1450PVCR 1/4" x 50' PVC / Rubber Hybrid Air Hose with Brass 1/4" NPT Industrial Fitting and Universal Quick Connect Coupler - Amazon.com
Teflon tape	Used for sealing screwed fittings	\$1.33	2	\$2.66	Harvey™ PTFE Thread Seal Tape - 1/2" x 520" at Menards®
3x3 Right Angle Surface Corner Bracket for T Slot	Used to create a flat surface for the force sensor to make contact with	\$11.60	1	\$11.60	T-Slotted Framing, Silver Corner Surface Bracket for 1" High Single Rail McMaster-Carr
Variac	Used to supply and control input electrical power to the resistive wire heating element	\$730.00	1	\$730.00	3PN1210B Staco Energy Products Company Test and Measurement DigiKey
PLA 3D Printed Force Sensor Mount	Used to hold the force sensor in place laterally when the thruster section engaged with it	\$0.00	1	\$0.00	N/A
Thermocouple Reader	Reads the thermocouples and reports them for manual data collection		1	\$0.00	Four-Channel Handheld Data Logger Thermometer (omega.com), discontinued
High Temperature Pressure Gauge	Pressure gauge used at the outlet of the system for manual data collection, capable of measuring 300 degrees F	\$99.99	1	\$99.99	Ashcroft Ammonia Pressure Gauge 45 1010S 02L 30-300PSI 1GA32921-009 4-1/2 eBay

Force sensor	Reads compressive force for manual data collection	\$1,106.33	1	\$1,106.33	Digital Force Gauge with USB Output Omega Engineering
16 gauge insulated wire (8ft)	Used to connect the nichrome wire to the variac, price per foot	\$0.61	16	\$9.76	TUOFENG 16 awg Wire Solid Core Hookup Wires- 6 Different Colored Jumper Wire 13.2ft or 4.m Each, 16 Gauge Tinned Copper Wire PVC (OD: 2.3mm) Hook up Wire Kit: Amazon.com: Tools & Home Improvement
Plug point ended wire (4ft long, 2x16 gauge)	Used to connect the nichrome wire to the variac	\$1.50	4	\$6.00	Amazon.com: Iron Forge Cable 16 AWG Replacement Power Cord with Open End - 10 Ft Black Extension Cable, 2 Wire 16/2 SJT : Tools & Home Improvement
1/4" Washers, yellow zinc	Extra engagement for flat plate straight t slot connectors	\$0.14	42	\$6.05	Grade 9 Steel Washer, Zinc Yellow-Chromate Plated, 1/4" Screw Size, 0.64" OD McMaster-Carr
1/4"-20 x 0.5" T Slot Screws and Nuts	Used to secure all t slot hardware to the t slot rails	\$0.76	84	\$64.05	T-Slotted Framing, End-Feed Single Nut with Button Head 1/4"-20 Thread Size McMaster-Carr
Valve	Allowed manual control of when flow is going through the system and when it is not	\$29.89	1	\$29.89	RuB S92 Ball Valve - 600 psi Max psi H J Kirby Corp
Compressor fitting	Used to connect compressor air flow to the inlet of the thruster	\$1.95	1	\$1.95	1/4 in. Male Brass Industrial Plug (harborfreight.com)
Hose Clamps	Used to keep the ceramic sleeve in place along the stainless steel tubing	\$1.05	2	\$2.10	Worm-Drive Clamps for Firm Hose and Tube, Steel Screw, 5/16" Wide Band, 7/32" to 5/8" Clamp ID McMaster-Carr
Stainless Steel Tubing, 6ft	Main tube of the thruster through which the gas flow moved while in heating section	\$51.88	1	\$51.88	Smooth-Bore Seamless 316 Stainless Steel Tubing, 1/4" OD, 0.02" Wall Thickness McMaster-Carr
Swagelok Tees	To connect between different in-line components, such as the regulator and instrumentation	\$26.00	2	\$52.00	Swagelok SS-400-3 Stainless Steel Tube Fitting, Union Tee, 1/4" Tube OD: Amazon.com: Industrial & Scientific
M4x10 socket head screws	To screw into the linear rail bearings	\$0.38	8	\$3.04	Amazon.com: M5 x 40mm Socket Head Cap Screws, Grade 12.9 Alloy Steel Black Oxide, Allen Socket

					<u>Drive, Full Thread, 25 PCS : Industrial & Scientific</u>
M4 washers	To connect mounting plate to linear rail bearings	\$0.13	16	\$2.11	<u>Hillman Stainless Steel Flat Washer (#6 Screw Size) 2226 - The Home Depot</u>
1/4"-20 x 1" socket heat screws	To connect linear rails to the t slot	\$1.10	8	\$8.76	<u>10Pcs 1/4-201" BSW Full Threaded Socket Head Cap Screws A2 304 Stainless Steel Allen Bolts (10Pcs, 1/4-201"):</u> <u>Amazon.com: Industrial & Scientific</u>
1/2" male to 3/8" female brass connector	To connect thermocouples into the swagelok tee	\$1.50	2	\$3.00	<u>T TANYA HARDWARE 1/8" x 1/4" Brass Hex Bushing, Female Pipe x Male Pipe, NPT, Pack of 10 - Amazon.com</u>
3/8" screw in plug	To plug unused swagelok openings	\$8.05	1	\$8.05	<u>304 Stainless Steel Threaded Pipe Fitting, High-Pressure, Plug with External Hex Drive, 3/8 NPT McMaster-Carr</u>
In line male ended Swagelok tee, other openings female	For connecting the nozzle at the end of the system	\$15.49	1	\$15.49	<u>Metalwork 316 Stainless Steel Forged Pipe Fitting Street Tee Male Run Tee, 1/4" NPT Male x 1/4" NPT Female x 1/4" NPT Female, 1pc:</u> <u>Amazon.com: Industrial & Scientific</u>
Ceramic screw terminals	For connecting between the nichrome wire and the electrical power supply wires	\$1.42	2	\$2.84	<u>uxcell 2 Way Ceramics Terminal Blocks High Temp Porcelain Ceramic Connectors 21.5x19.5x14.2mm for Electrical Wire Cable 5 Pcs: Amazon.com: Industrial & Scientific</u>
Electrical tape	For helping close leaks, price per roll	\$1.91	1	\$1.91	<u>Amazon Basics Electrical Tape, 3/4-inch by 60-feet, Black, 6-Pack, Model: DS-TPAMZ013 (Previously AmazonCommercial brand): Amazon.com: Industrial & Scientific</u>
Hot glue	For helping close leaks	\$8.27	1	\$8.27	<u>Amazon.com: Surebonder GM-160 Mini High Temperature Glue Gun, 10-watt, Green/Black & "Clear Stik" Hot Glue Sticks for All Temperatures - Mini Size</u>

					<u>4" L, 5/16" D - 25 Pack -</u> <u>All Purpose, Made in USA</u> <u>(DT-25) : Arts, Crafts &</u> <u>Sewing</u>
	Running Total			\$3,359.32	

7. Specification Sheets

Appendix A: Formlabs High Temp v2 Resin

MATERIAL DATA SHEET

High Temp

High Temp Resin for Heat Resistance**\$199 / L**

High Temp Resin offers a heat deflection temperature (HDT) of 238 °C @ 0.45 MPa, the highest among Formlabs resins. Use it to print detailed, precise prototypes with high temperature resistance.

Hot air, gas, and fluid flow**Molds and inserts****Heat resistant mounts, housings, and fixtures****FLHTAM02****formlabs**

Prepared 09 . 15 . 2016
Rev 02 . 12 . 05 . 2018

To the best of our knowledge the information contained herein is accurate. However, Formlabs, Inc. makes no warranty, expressed or implied, regarding the accuracy of these results to be obtained from the use thereof.

Material Properties Data Metric

	METRIC ¹			METHOD
	Green ²	Post-Cured ³	Post-Cured + Thermally Post-Cured ⁴	
Thermal Properties				
Heat Deflection Temp. @ 1.8 MPa	43.6 °C	99.2 °C	101 °C	ASTM D 648-16
Heat Deflection Temp. @ 0.45 MPa	49.3 °C	142 °C	238 °C	ASTM D 648-16

	METRIC ¹			METHOD
	Green ²	Post-Cured ³	Post-Cured + Thermally Post-Cured ⁴	
Mechanical Properties				
Ultimate Tensile Strength	20.9 MPa	58.3 MPa	51.1 MPa	ASTM D 638-14
Elongation at break	14 %	3.3 %	2.4 %	ASTM D 638-14
Tensile modulus	0.75 GPa	2.75 GPa	2.9 GPa	ASTM D 638-14
Flexural strength at break	24.1 MPa	94.5 MPa	93.8 MPa	ASTM D 790-15
Flexural modulus	0.69 GPa	2.62 GPa	2.62 GPa	ASTM D 790-15
Impact Properties				
Notched IZOD	32.8 J/m	18.2 J/m	24.2 J/m	ASTM D 256-10
Thermal Properties				
Thermal Expansion (0-150 °C)	118.1 (μm/m/°C)	79.6 (μm/m/°C)	74 (μm/m/°C)	ASTM E 831-13

¹ Material properties can vary with part geometry, print orientation, print settings, and temperature.

² Data was obtained from green parts, printed using Form 2, 100 μm, High Temp settings, washed for 5 minutes in Form Wash and air dried without post cure.

³ Data was obtained from parts printed using a Form 2, 100 micron, High Temp settings, and post-cured with Form Cure at 80 °C for 120 minutes.

⁴ Data was obtained from parts printed using a Form 2, 100 micron, High Temp settings, and post-cured with Form Cure at 80 °C for 120 minutes plus an additional thermal cure in a lab oven at 160 °C for 180 minutes.

⁵ Data was obtained from parts printed using a Form 2, 100 micron, High Temp settings, and post-cured with Form Cure at 60 °C for 60 minutes.

⁶ Data was obtained from parts printed using a Form 2, 100 micron, High Temp settings, and post-cured with Form Cure at 60 °C for 60 minutes plus an additional thermal cure in a lab oven at 160 °C for 90 minutes.

Material Properties Data Imperial

	IMPERIAL ¹			METHOD
	Green ²	Post-Cured ³	Post-Cured + Thermally Post-Cured ⁴	
Thermal Properties				
Heat Deflection Temp. @ 1.8 MPa	110.48 °F	210.56 °F	213.8 °F	ASTM D 648-16
Heat Deflection Temp. @ 0.45 MPa	120.74 °F	287.6 °F	460.4 °F	ASTM D 648-16

	IMPERIAL ¹			METHOD
	Green ²	Post-Cured ³	Post-Cured + Thermally Post-Cured ⁴	
Mechanical Properties				
Ultimate Tensile Strength	3031 psi	8456 psi	7411 psi	ASTM D 638-14
Elongation at break	14 %	3.3 %	2.4 %	ASTM D 638-14
Tensile modulus	109 ksi	399 ksi	421 ksi	ASTM D 638-14
Flexural strength at break	3495 psi	13706 psi	13605 psi	ASTM D 790-15
Flexural modulus	100 ksi	400 ksi	400 ksi	ASTM D 790-15
Impact Properties				
Notched IZOD	0.61 ft-lbf/in	0.34 ft-lbf/in	0.45 ft-lbf/in	ASTM D 256-10
Thermal Properties				
Thermal Expansion (0-150 °C)	65.6 µin/in/°F	44.2 µin/in/°F	41.1 µin/in/°F	41.1 µin/in/°F

¹ Material properties can vary with part geometry, print orientation, print settings, and temperature.

² Data was obtained from green parts, printed using Form 2, 100 µm, High Temp settings, washed for 5 minutes in Form Wash and air dried without post cure.

³ Data was obtained from parts printed using a Form 2, 100 micron, High Temp settings, and post-cured with Form Cure at 80 °C for 120 minutes.

⁴ Data was obtained from parts printed using a Form 2, 100 micron, High Temp settings, and post-cured with Form Cure at 80 °C for 120 minutes plus an additional thermal cure in a lab oven at 160 °C for 180 minutes.

⁵ Data was obtained from parts printed using a Form 2, 100 micron, High Temp settings, and post-cured with Form Cure at 60 °C for 60 minutes.

⁶ Data was obtained from parts printed using a Form 2, 100 micron, High Temp settings, and post-cured with Form Cure at 60 °C for 60 minutes plus an additional thermal cure in a lab oven at 160 °C for 90 minutes

Solvent Compatibility

Percent weight gain over 24 hours for a printed and post-cured 1x1x1 cm cube immersed in respective solvent:

Solvent	24 hr weight gain (%)	24 hr size gain (%)	Solvent	24 hr weight gain (%)	24 hr size gain (%)
Acetic Acid, 5 %	<1	<1	Hydrogen peroxide (3%)	<1	<1
Acetone	<1	<1	Isooctane (aka gasoline)	<1	<1
Isopropyl Alcohol	<1	<1	Mineral oil (light)	<1	<1
Bleach ~5% NaOCl	<1	<1	Mineral oil (Heavy)	<1	<1
Butyl Acetate	<1	<1	Salt Water (3.5% NaCl)	<1	<1
Diesel Fuel	<1	<1	Sodium Hydroxide solution	<1	<1
Diethyl glycol Monomethyl Ether	<1	<1	Water	<1	<1
Hydraulic Oil	<1	<1	Xylene	<1	<1
Skydrol 5	<1	<1	Strong Acid (HCl conc)	1.2	<1

Appendix B: Formlabs Durable Resin

MATERIAL DATA SHEET

Durable

Durable Resin for Low Friction and Wear

\$175 / L

With low modulus, high elongation, and high impact strength, Durable Resin produces parts with a smooth, glossy finish and high resistance to deformation. Use this material for applications requiring minimal friction.

Consumer packaging

Snap fits and flexures

Bushings and bearings

Living hinges



FLDUCL02

formlabs 

Prepared 01. 26 . 2018
Rev 02 01. 26 . 2018

To the best of our knowledge the information contained herein is accurate. However, Formlabs, Inc. makes no warranty, expressed or implied, regarding the accuracy of these results to be obtained from the use thereof.

Material Properties Data

	METRIC ¹	IMPERIAL ¹		METHOD
	Green ²	Post-Cured ³	Green ²	Post-Cured ³
Tensile Properties				
Ultimate Tensile Strength	18.6 MPa	31.8 MPa	2.7 ksi	4.61 ksi
Tensile Modulus	0.45 GPa	1.26 GPa	657 ksi	183 ksi
Elongation	67 %	49 %	67 %	49 %
Flexural Properties				
Flexural Stress at 5% Strain	4.06 MPa	27.2 MPa	0.59 ksi	3.95 ksi
Flexural Modulus	0.16 GPa	0.82 GPa	23.4 ksi	119 ksi
Impact Properties				
Notched IZOD	130.8 J/m	109 J/m	2.46 ft-lbf/in	2.05 ft-lbf/in
Temperature Properties				
Heat Deflection Temp. @ 0.45 MPa	< 30 °C	43.3 °C	< 86 °F	110 °F
Thermal Expansion (23 to 50° C)	117.0 µm/m/°C	145.1 µm/m/°C	65.0 µin/in/°F	80.6 µin/in/°F

¹Material properties can vary with part geometry, print orientation, print settings, and temperature.

²Data was obtained from green parts, printed using Form 2, 100 µm, Durable settings, without additional treatments.

³Data was obtained from parts printed using Form 2, 100 µm, Durable settings and post-cured with 2.5 mW/cm² of 405 nm LED light for 120 minutes at 60°C.

Solvent Compatibility

Percent weight gain over 24 hours for a printed and post-cured 1x1x1 cm cube immersed in respective solvent:

Mechanical Properties	24 hr weight gain (%)	Mechanical Properties	24 hr weight gain (%)
Acetic Acid, 5 %	1.3	Hydrogen Peroxide (3 %)	1
Acetone	sample cracked	Isooctane	<1
Isopropyl Alcohol	5.1	Mineral Oil, light	<1
Bleach, ~5 % NaOCl	<1	Mineral Oil, heavy	<1
Butyl Acetate	7.9	Salt Water (3.5 % NaCl)	<1
Diesel	<1	Sodium hydroxide (0.025 %, pH = 10)	<1
Diethyl glycol monomethyl ether	7.8	Water	<1
Hydrolic Oil	<1	Xylene	6.5
Skydrol 5	1.3	Strong Acid (HCl Conc)	distorted

Appendix C: Formlabs Nylon 12 Sintering Powder

SLS POWDERS

formlabs

Nylon 12 Powder

SLS Powder For Strong, Functional Prototypes and End-Use Parts

With high tensile strength, ductility, and environmental stability, Nylon 12 Powder is suitable for creating complex assemblies and durable parts with minimal water absorption.

Nylon 12 Powder is specifically developed for use on Fuse Series printers.

V1 FLP12G01 * May not be available in all regions

Prepared 08 . 19. 2020 To the best of our knowledge the information contained herein is accurate. However, Formlabs, Inc. makes no warranty, expressed or implied, regarding the accuracy of these results to be obtained from the use thereof.
Rev. 01 08 . 19. 2020

MATERIAL PROPERTIES DATA

Nylon 12 Powder

	METRIC ¹	IMPERIAL ¹	METHOD
Mechanical Properties			
Ultimate Tensile Strength	50 MPa	7252 psi	ASTM D638 Type 1
Tensile Modulus	1850 MPa	268 ksi	ASTM D638 Type 1
Elongation at Break (X/Y)	11%	11%	ASTM D638 Type 1
Elongation at Break (Z)	6%	6%	ASTM D638 Type 1
Flexural Properties			
Flexural Strength	66 MPa	9572 psi	ASTM D 790-15
Flexural Modulus	1600 MPa	232 ksi	ASTM D 790-15
Impact Properties			
Notched Izod	32 J/m	0.60 ft-lb/in	ASTM D256-10
Thermal Properties			
Heat Deflection Temp. @ 1.8 MPa	87 °C	189 °F	ASTM D648
Heat Deflection Temp. @ 0.45 MPa	171 °C	340 °F	ASTM D648
Vicat Softening Temperature	175 °C	347 °F	ASTM D1525
Other Properties			
Moisture Content (powder)	0.25%	0.25%	ISO 15512 Method D
Water Absorption (printed part)	0.66%	0.66%	ASTM D570

Samples printed with Nylon 12 Powder have been evaluated in accordance with ISO 10993-1:2018, and has passed the requirements for the following biocompatibility risks:

ISO Standard	Description ^{3,4}
ISO 10993-5:2009	Not cytotoxic
ISO 10993-10:2010/(R)2014	Not an irritant
ISO 10993-10:2010/(R)2014	Not a sensitizer

Flammability Properties

Testing Standard	Rating
UL 94 Section 7	HB *

* Thickness of the sample tested ~ 3.00mm

¹ Material properties may vary with part geometry, print orientation and temperature.

² Parts were printed using Fuse 1 with Nylon 12 Powder. Parts were conditioned at 50% relative humidity and 23 °C for 7 days before testing.

³ Material properties may vary based on part design and manufacturing practices. It is the manufacturer's responsibility to validate the suitability of the printed parts for the intended use.

⁴ Nylon 12 was tested at NAMSA World Headquarters, OH, USA.

SOLVENT COMPATIBILITY

Percent weight gain over 24 hours for a printed 1 x 1 x 1 cm cube immersed in respective solvent:

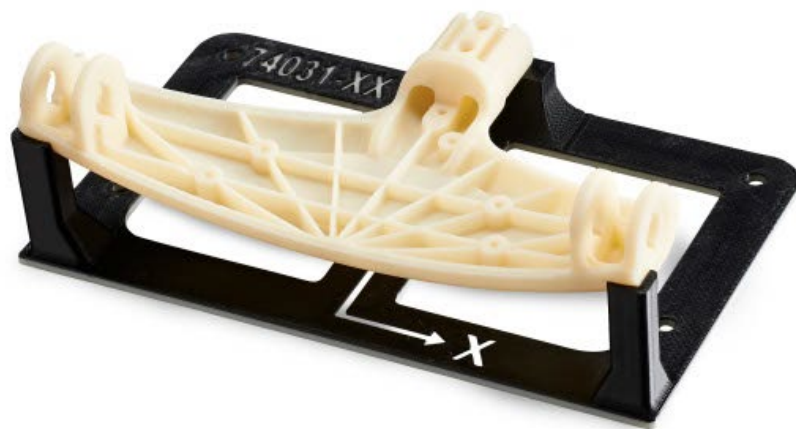
Solvent	24 hr weight gain, %	Solvent	24 hr weight gain, %
Acetic Acid 5%	0.1	Mineral oil (Heavy)	0.7
Acetone	0.1	Mineral oil (Light)	0.5
Bleach ~5% NaOCl	0.2	Salt Water (3.5% NaCl)	0.2
Butyl Acetate	0.2	Skydrol 5	0.6
Diesel Fuel	0.4	Sodium Hydroxide solution (0.025% pH 10)	0.2
Diethyl glycol Monomethyl Ether	0.5	Strong Acid (HCl conc)	0.8
Hydraulic Oil	0.6	Tripropylene glycol monomethyl ether	0.3
Hydrogen peroxide (3%)	0.2	Water	0.1
Isooctane (aka gasoline)	<0.1	Xylene	0.1
Isopropyl Alcohol	0.2		

Appendix D: Stratasys ABS Filament

ences



FDM Thermoplastic Filament



Overview

ABS-M30™ filament combines the design freedom of FDM® technology with the versatility and capability of ABS (acrylonitrile butadiene styrene). ABS is characterized by its strength and toughness, while being lightweight and resilient, suitable for most general-purpose 3D printing use cases.

Contents:

Ordering Information	3
Physical Properties	5
Mechanical Properties	6
Appendix	9



Ordering Information

Table 1. Printer and Support Material Compatibility

Printer	Model Tip (Slice)	Support Material	Support Tip
F120™	F123 Head (7, 10, 13 slice)	SR-30 (soluble)	F123 Head (all slices)
F170™	F123 Head (5, 7, 10, 13 slice)	QSR Support™ (soluble)	F123 Head (all slices)
F270™	F123 Head (5, 7, 10, 13 slice)	QSR Support (soluble)	F123 Head (all slices)
F370™	F123 Head (5, 7, 10, 13 slice)	QSR Support (soluble)	F123 Head (all slices)
F770™	F123 Head (7, 10, 13 slice)	SR-30 (soluble)	F123 Head (all slices)
Fortus 450mc™	T10 (5 slice) T12 (7 slice)	T16 (10 slice) T20 (13 slice)	SR-30 / 35 (soluble)
Fortus 900mc™/F900™	T12 (7 slice) T16 (10 slice) T20 (13 slice)	SR-20 / 30 / 35 (soluble)	T12SR20 / 30 (all slices)

Build Sheet

Low Temperature

- 0.02 x 26 x 38 in. (0.51 x 680 x 965 mm)
- 0.02 x 16 x 18.5 in. (0.51 x 406 x 470 mm)

F770 Build Sheets

- 0.01 x 30 x 41 in. (0.254 x 762 x 1041 mm)

Table 2. Consumable Ordering Information

Part Number	Description
Printer Consumables	
123-00401-S	F370 Extrusion Head, all layer heights
511-10601	T10
511-10301	T12
511-10401	T16
511-10701	T20
511-10900	T12SR30
511-10901	T12SR20
123-00302-S	F120/F170 Build Tray
123-00303	F270 Build Tray, Standard
123-00304	F370 Build Tray, Standard
123-50100	F770 Build sheet, 0.01 x 30 x 41 in. (0.254 x 762 x 1041 mm), box of 20
325-00300	Low Temperature build sheet, 0.02x26x38 in. (0.51x680x965 mm)
325-00100	Low Temperature build sheet, 0.02x16x18.5 in. (0.51x406x470 mm)
310-00100	Low Temperature build sheet, 0.03x16x18.5 in. (0.76x406x470 mm)
355-00100	Low Temperature build sheet, 0.02x14x16.5 in (0.51x355x420 mm)

**Table 3. ABS-M30 Ordering Information**

Part Number	Description
Filament Canisters^{1,2}	
355-02110	ABS-M30 (Ivory), 92.3 cu in - Plus
355-02111	ABS-M30 (White), 92.3 cu in - Plus
355-02112	ABS-M30 (Black), 92.3 cu in - Plus
355-02113	ABS-M30 (Gray), 92.3 cu in - Plus
355-02114	ABS-M30 (Red), 92.3 cu in - Plus
355-02115	ABS-M30 (Blue), 92.3 cu in - Plus
355-02116	ABS-M30 (Nectarine), 92.3 cu in - Plus
355-02117	ABS-M30 (Yellow), 92.3 cu in - Plus
355-08110	ABS-M30 (Ivory), 184 cu in - Plus
355-08112	ABS-M30 (Black), 184 cu in - Plus
355-02120	ABS-M30i, 92.3 cu in - Plus
360-50110	ABS-M30 (Ivory), 500 cu in - Xtend
360-50211	ABS-M30 (Black), 500 cu in - Xtend
333-60300	ABS-M30 (Ivory), 60 cu in - F123
333-60301	ABS-M30 (Black), 60 cu in - F123
333-60302	ABS-M30 (White), 60 cu in - F123
333-60303	ABS-M30 (Red), 60 cu in - F123
333-60304	ABS-M30 (Blue), 60 cu in - F123
333-60305	ABS-M30 (Green), 60 cu in - F123
333-60306	ABS-M30 (Yellow), 60 cu in - F123
333-60307	ABS-M30 (Orange), 60 cu in - F123
333-60308	ABS-M30 (Dark Gray), 60 cu in - F123
333-90300	ABS-M30 (Ivory), 90 cu in - F123
333-90301	ABS-M30 (Black), 90 cu in - F123
333-90302	ABS-M30 (White), 90 cu in - F123
333-90308	ABS-M30 (Dark Gray), 90 cu in - F123
311-20000	ABS-M30 (Ivory) 92.3 cu in - Classic
311-20018	ABS-M30 (Natural) 184 cu in - Classic
311-20100	ABS-M30 (White) 92.3 cu in - Classic
311-20200	ABS-M30 (Black) 92.3 cu in - Classic
311-20218	ABS-M30 (Black) 184 cu in - Classic
311-20300	ABS-M30 (Gray) 92.3 cu in - Classic
311-20400	ABS-M30 (Red) 92.3 cu in - Classic
311-20500	ABS-M30 (Blue) 92.3 cu in - Classic
311-21400	ABS-M30i, 92.3 cu in - Classic
331-20307	ABS (Black), 200 cu in., long lead - F770
355-03110	SR-30 Soluble Support, 92.3 cu in - Plus
360-53110	Xtend SR-30 Soluble Support, 500 cu in - Plus
310-30500	SR-20 Soluble Support, 92.3 cu in - Classic
311-30200	SR-30 Soluble Support, 92.3 cu in - Classic
331-20200	SR-30 Soluble Support, 200 cu in - F120
331-20207	SR30 Soluble Support, 200 cu in., long lead - F770
355-03135	SR-35 Soluble Support, 92.3 cu in - Plus
311-30235	SR-35 Soluble Support, 92.3 cu in - Classic
333-63500	QSR Soluble Support, 60 cu in - F123

¹ Classic canisters are compatible with all Fortus 900mc printers prior to s/n L502.² Plus canisters are compatible with all Fortus 450mc, all Stratasys F900, and Fortus 900mc printers s/n L502 and up.

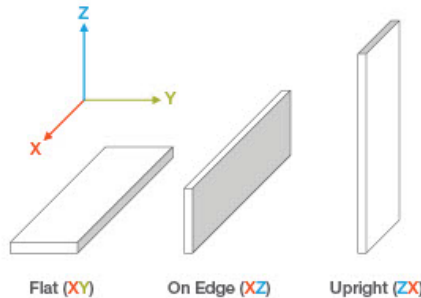


Mechanical Properties

ABS-M30 black samples were printed with 0.010 in. (0.254 mm) layer heights on the F900 and F770. For the full test procedure please see the [Stratasys Materials Test Procedure](#) (immediate download upon clicking the link).

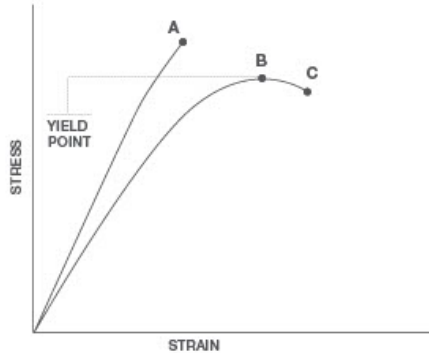
Print Orientation

Parts created using FDM are anisotropic as a result of the printing process. Below is a reference of the different orientations used to characterize the material.



Tensile Curves

Due to the anisotropic nature of FDM, tensile curves look different depending on orientation. Below is a guide of the two types of curves seen when printing tensile samples and what reported values mean.



A = Tensile at break, elongation at break (no yield point)

B = Tensile at yield, elongation at yield

C = Tensile at break, elongation at break

**Table 5. ABS-M30 Mechanical Properties (F900 - T16 Tip)**

		XZ Orientation [†]	ZX Orientation [†]
Tensile Properties: ASTM D638			
Yield Strength	MPa	30.8 (0.85)	27.5 (0.28)
	psi	4470 (120)	3990 (41)
Elongation @ Yield	%	1.8 (0.043)	1.7 (0.13)
Strength @ Break	MPa	28.1 (0.58)	26.8 (0.84)
	psi	4080 (84)	3890 (120)
Elongation @ Break	%	8.1 (1.5)	1.8 (0.31)
Modulus (Elastic)	GPa	2.40 (0.080)	2.30 (0.16)
	ksi	349 (12)	334 (23)
Flexural Properties: ASTM D790, Procedure A			
Strength @ Break	MPa	No break	47.7 (2.2)
	psi	No break	6910 (320)
Strength @ 5% Strain	MPa	58.7 (0.54)	-
	psi	8510 (78)	-
Strain @ Break	%	No break	3.4 (0.22)
Modulus	GPa	2.22 (0.037)	1.96 (0.064)
	ksi	323 (5.4)	284 (9.3)
Compression Properties: ASTM D695			
Yield Strength	MPa	88.3 (3.0)	208 (15)
	psi	12800 (440)	30100 (2200)
Modulus	GPa	2.20 (0.11)	2.16 (0.092)
	ksi	319 (17)	314 (13)
Impact Properties: ASTM D256, ASTM D4812			
Notched	J/m	101 (9.9)	32.2 (3.0)
	ft*lb/in.	1.89 (0.19)	0.603 (0.057)
Unnotched	J/m	291 (57)	103 (30)
	ft*lb/in.	5.45 (1.1)	1.93 (0.57)

(†) Values in parentheses are standard deviations.

**Table 6. ABS-M30 Mechanical Properties (F770)**

		XZ Orientation [†]	ZX Orientation [†]
Tensile Properties: ASTM D638			
Yield Strength	MPa	32.5 (1.7)	23.1 (1.3)
	psi	4720 (250)	3350 (190)
Elongation @ Yield	%	2.1 (0.1)	1.8 (0.2)
Strength @ Break	MPa	27.6 (2.4)	22.9 (1.2)
	psi	4000 (350)	3310 (170)
Elongation @ Break	%	4.5 (1.2)	1.6 (0.2)
Modulus (Elastic)	GPa	2.00 (27)	1.78 (29)
	ksi	290 (3.9)	258 (4.1)
Flexural Properties: ASTM D790, Procedure A			
Strength @ Break	MPa	No Break	37.8 (4.1)
	psi	No Break	5480 (590)
Strength @ 5% Strain	MPa	58.1 (2.2)	-
	psi	8430 (320)	-
Strain @ Break	%	No Break	2.2 (0.3)
Modulus	GPa	2.17 (0.03)	1.84 (0.06)
	ksi	315 (4.9)	267 (8.1)
Impact Properties: ASTM D256, ASTM D4812			
Notched	J/m	91.0 (17)	21.7 (3.7)
	ft ² lb/in	1.71 (0.31)	0.406 (0.07)
Unnotched	J/m	423 (96)	62.9 (134)
	ft ² lb/in	7.92 (1.8)	1.18 (0.3)

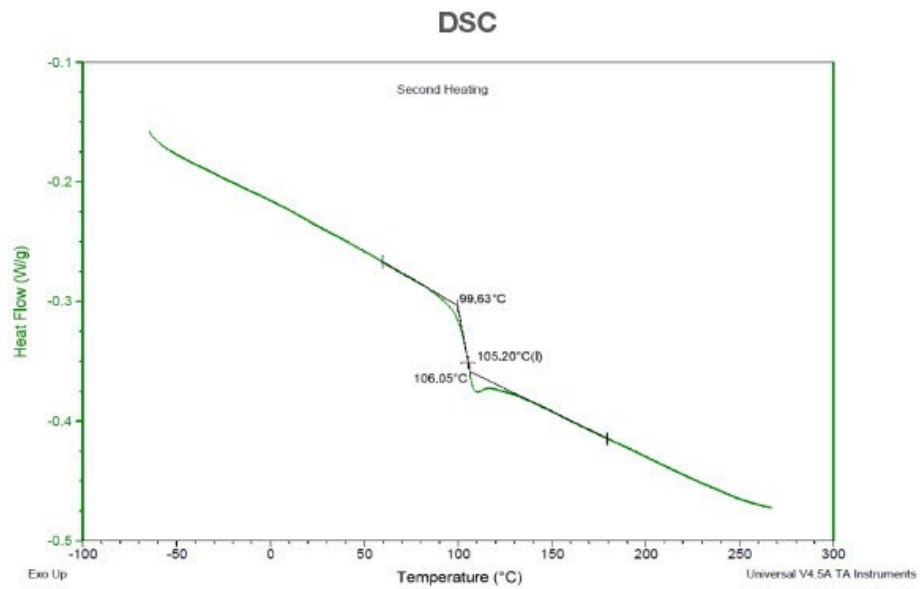
(†) Values in parentheses are standard deviations.



Appendix



Figure 1. 2nd heating scan DSC data for the ABS-M30 Black Flat (XY) sample.



10



Figure 2. Dimension change data as a function of temperature for the ABS-M30 Black Flat (XY) sample.

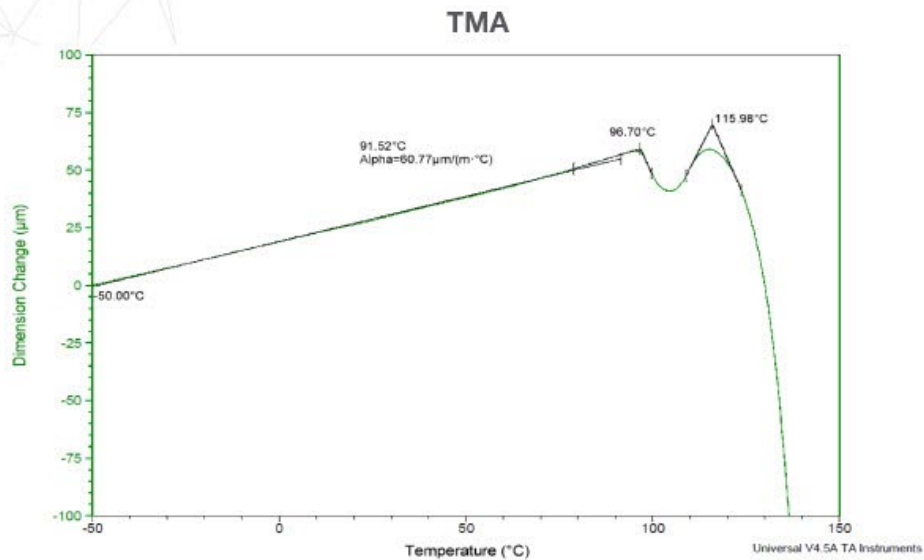


Figure 3. Dimension change data as a function of temperature for the ABS-M30 Black On Edge (XZ) sample.

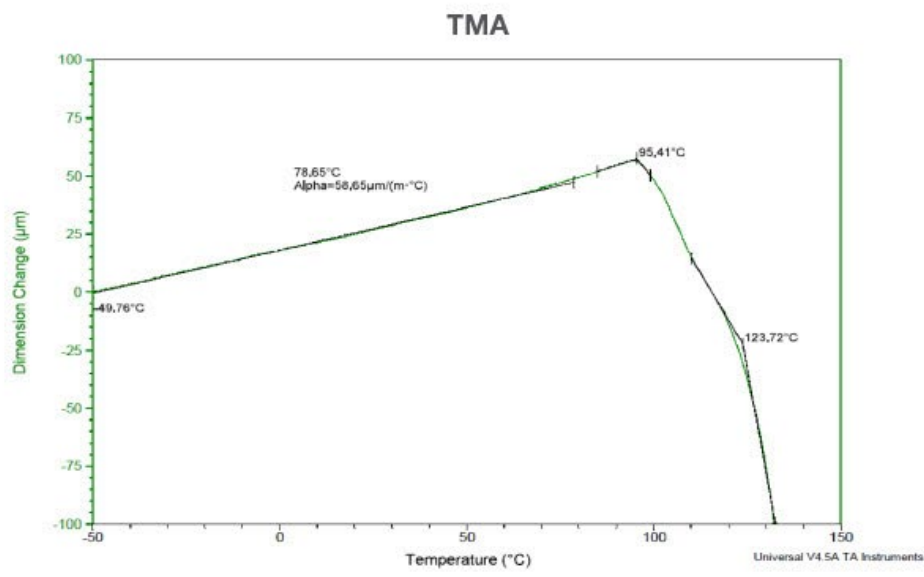
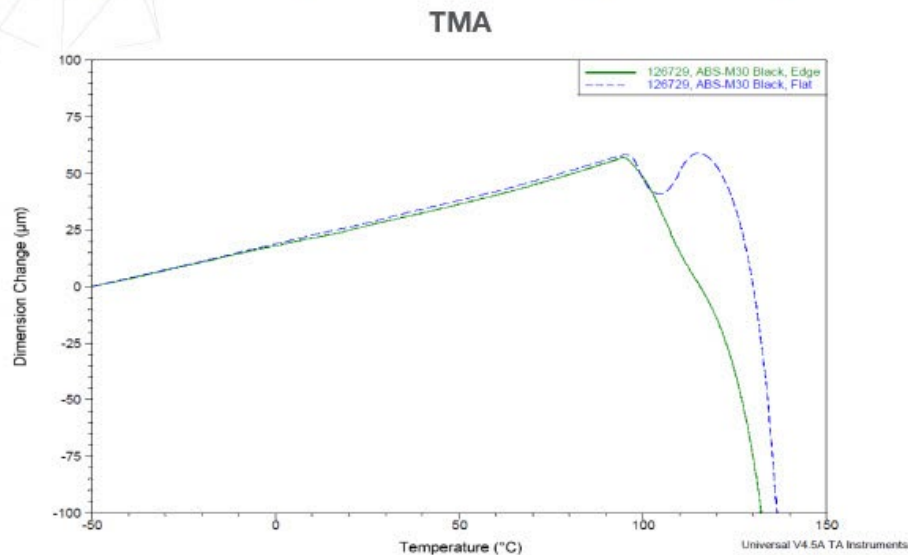




Figure 4. Overlay of the dimension change data for the Flat (XY) and On Edge (XZ) ABS-M30 Black samples.



Stratasys Headquarters

7665 Commerce Way,
Eden Prairie, MN 55344
+1 800 801 6491 (US Toll Free)
+1 952 937-3000 (Intl)
+1 952 937-0070 (Fax)

stratasys.com
ISO 9001:2015 Certified

1 Holtzman St., Science Park,
PO Box 2498
Rehovot 76124, Israel
+972 74 745 4000
+972 74 745 5000 (Fax)

© 2021 Stratasys. All rights reserved. Stratasys, the Stratasys Signet logo, FDM, and Fortus are registered trademarks of Stratasys Inc. SR-20, SR-30, SR-35, DSR Support, ABS-M30, F123 Series, F120, F170, F270, F370, F770, Fortus 450mc, Fortus 900mc and F900 are trademarks of Stratasys, Inc. All other trademarks are the property of their respective owners, and Stratasys assumes no responsibility with regard to the selection, performance, or use of these non-Stratasys products. Product specifications subject to change without notice.
MDS_FDM_ABS-M30_0921a



Appendix E: Stratasys PC-ABS Filament

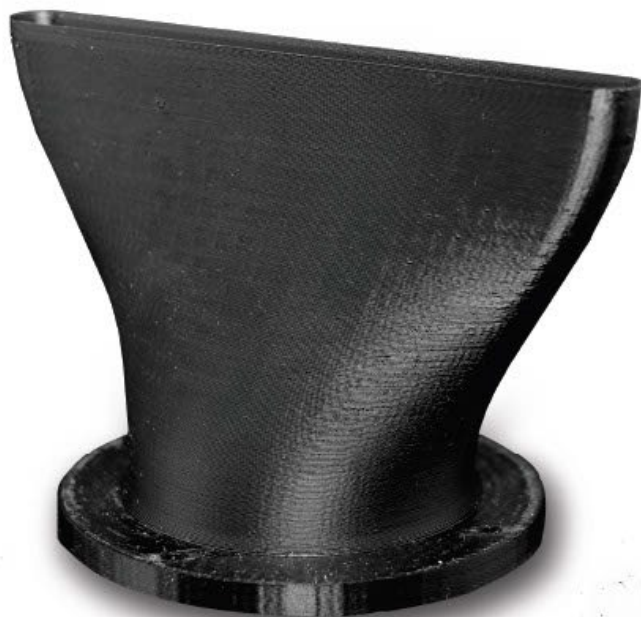


PC-ABS



FDM Thermoplastic Filament

2



Overview

PC-ABS is a blend of polycarbonate (PC) and acrylonitrile butadiene styrene (ABS) thermoplastics. The result is an FDM filament that exhibits optimal characteristics of each – excellent strength, high toughness and heat resistance, and good flexural strength. Choose PC-ABS when you need the strength of PC but the impact resistance of ABS.

PC-ABS is suitable for a variety of applications that include prototyping, tooling and low-volume production. Available colors are black, white and red.

Contents:

Ordering Information	3
Physical Properties	5
Mechanical Properties	6
UV Aging	7
Appendix	8



Ordering Information

Table 1. Printer and Support Material Compatibility

Printer	Model Tip (Slice)	Support Material	Support Tip
F370™	F123 Head (5, 7, 10, 13 slice)	QSR Support (soluble)	F123 Head (all slices)
F370®CR	F123 Head (5, 7, 10, 13 slice) T10 (5 slice)	QSR Support (soluble)	F123 Head (all slices)
Fortus 450mc™	T12 (7 slice) T16 (10 slice) T20 (13 slice)	SR-110™ (soluble)	T12SR100 (all slices)
Fortus 900mc™/F900®	T12 (7 slice) T16 (10 slice) T20 (13 slice)	SR-110 (soluble)	T12SR20 / 100 (all slices)

PC-ABS red is only available on the Fortus 450mc and F900 with the T16 model tip and SR-110 support material.

Build Sheet

Low Temperature

- 0.02 x 26 x 38 in. (0.51 x 660 x 965 mm)
- 0.02 x 16 x 18.5 in. (0.51 x 406 x 470 mm)

F370/F370CR Standard Build Trays

**Table 2. PC-ABS Filament Ordering Information**

Part Number	Description
Filament Canisters^{1,2}	
355-02260	PC-ABS (black), 92.3 cu in - Plus
310-20500	PC-ABS (black), 92.3 cu in - Classic
333-90701	PC-ABS (black), 90 cu in - F123
333-60701	PC-ABS (black), 60 cu in - F123
333-60700	PC-ABS (white), 60 cu in - F123
355-70070	PC-ABS (red), 92.3 cu in - Plus
310-30500	SR-20 Soluble Support, 92.3 cu in - Classic
355-03130	SR-110 soluble support, 92.3 cu in - Plus
333-63500	QSR soluble support, 60 cu in - F123
Printer Consumables	
511-10601	T10 tip, 0.005 (0.127 mm) layer height
511-10301	T12 tip, 0.007 (0.178 mm) layer height
511-10401	T16 tip, 0.010 in. (0.254 mm) layer height
511-10701	T20 tip, 0.013 (0.330 mm) layer height
511-10901	T12SR20 tip, all layer heights
511-10100	T12SR100 tip, all layer heights
123-00402-S	F123 Standard Head (all layer heights)
325-00300 ³	Low Temperature build sheet, 0.02x26x38 in. (0.51x660x965 mm)
325-00100 ⁴	Low Temperature build sheet, 0.02x16x18.5 in (0.51x406x470 mm)
123-00304	F370 / F370CR Build Tray, Standard

¹ Classic canisters are compatible with all Fortus 900mc printers prior to s/n L502.² Plus canisters are compatible with all Fortus 450mc, all Stratasys F900, and Fortus 900mc printers s/n L502 and up.³ Compatible with Fortus 900mc and F900.⁴ Compatible with Fortus 450mc, Fortus 900mc and F900.



Physical Properties

Values are measured as printed. XY, XZ, and ZX orientations were tested. For full details refer to the [Stratasys Materials Test Report](#) (immediate download upon clicking the link). DSC and TMA curves can be found in the Appendix.

Table 3. PC-ABS Physical Properties

Property	Test Method	Typical Values	
		XY	XZ/ZX
HDT @ 66 psi	ASTM D648 Method B	117.9 °C (244.2 °F)	126.1 °C (259.0 °F)
HDT @ 264 psi	ASTM D648 Method B	107.5 °C (225.5 °F)	112.0 °C (233.6 °F)
Molded HDT @ 66 psi	ASTM D648 Method B	125.0 °C (257.1 °F)	
Molded HDT @ 264 psi	ASTM D648 Method B	102.9 °C (217.2 °F)	
Tg	ASTM D7426 Inflection Point	105.3 °C (221.6 °F)	
Mean CTE	ASTM E831 (-50 °C to 95 °C)	72.96 $\mu\text{m}/[\text{m}^{\circ}\text{C}]$ (40.53 $\mu\text{in}/[\text{in}^{\circ}\text{F}]$)	
	ASTM E831 (-50 °C to 35 °C)	59.87 $\mu\text{m}/[\text{m}^{\circ}\text{C}]$ (33.26 $\mu\text{in}/[\text{in}^{\circ}\text{F}]$)	-
	ASTM E831 (35 °C to 50 °C)	0.4816 $\mu\text{m}/[\text{m}^{\circ}\text{C}]$ (0.2876 $\mu\text{in}/[\text{in}^{\circ}\text{F}]$)	-
	ASTM E831 (50 °C to 90 °C)	-61.76 $\mu\text{m}/[\text{m}^{\circ}\text{C}]$ (-34.31 $\mu\text{in}/[\text{in}^{\circ}\text{F}]$)	-
Volume Resistivity	ASTM D257	> 6.84*10^14 $\Omega\cdot\text{cm}$	
Dielectric Constant	ASTM D150 1 kHz test condition	2.62	2.74
	ASTM D150 2 MHz test condition	2.74	2.88
Dissipation Factor	ASTM D150 1 kHz test condition	0.001	0.002
	ASTM D150 2 MHz test condition	0.002	0.001
	Specific Gravity @23 °C	1.10	

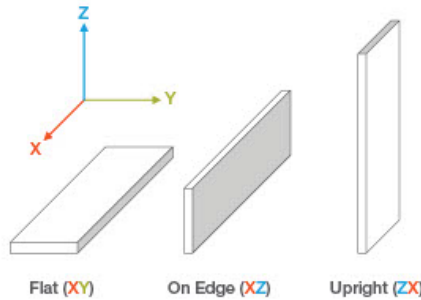


Mechanical Properties

PC-ABS samples were printed with 0.010 in. (0.254 mm) layer heights on the F900. For the full test procedure please see the [Stratasys Materials Test Procedure](#) (immediate download upon clicking the link).

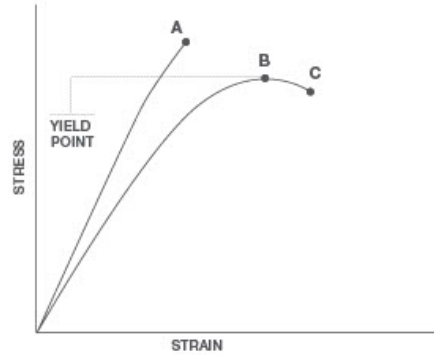
Print Orientation

Parts created using FDM are anisotropic as a result of the printing process. Below is a reference of the different orientations used to characterize the material.



Tensile Curves

Due to the anisotropic nature of FDM, tensile curves look different depending on orientation. Below is a guide of the two types of curves seen when printing tensile samples and what reported values mean.



A = Tensile at break, elongation at break (no yield point)

B = Tensile at yield, elongation at yield

C = Tensile at break, elongation at break

**Table 4. PC-ABS Mechanical Properties (F900 - T16 Tip)**

		XZ Orientation ¹	ZX Orientation ¹
Tensile Properties: ASTM D638			
Yield Strength	MPa psi	36.5 (0.73) 5300 (110)	No yield No yield
Elongation @ Yield	%	3.0 (0.083)	No yield
Strength @ Break	MPa psi	34.7 (0.83) 5040 (120)	25.9 (1.6) 3760 (230)
Elongation @ Break	%	4.7 (0.75)	1.8 (0.22)
Modulus (Basic)	GPa ksi	1.99 (0.038) 288 (5.5)	1.87 (0.19) 270 (27)
Berular Properties: ASTM D790, Procedure A			
Strength @ Break	MPa psi	No break No break	46.2 (2.0) 6700 (290)
Strength @ 5% Strain	MPa psi	61.9 (1.2) 8970 (170)	- -
Strain @ Break	%	No break	3.51 (0.30)
Modulus	GPa ksi	1.86 (0.14) 269 (20)	1.68 (0.069) 244 (10)
Compression Properties: ASTM D695			
Yield Strength	MPa psi	96.5 (3.6) 14000 (530)	172 (13) 25000 (1900)
Modulus	GPa ksi	2.14 (0.19) 310 (27)	1.85 (0.050) 269 (7.3)
Impact Properties: ASTM D256, ASTM D4812			
Notched	J/m ft*lb/in.	241 (40) 4.52 (0.75)	34.0 (6.0) 0.637 (0.11)
Unnotched	J/m ft*lb/in.	655 (127) 12.3 (2.4)	101 (23) 1.89 (0.43)

¹Values in parentheses are standard deviations.

UV Aging

PC-ABS was tested before and after UV exposure. Ten ASTM D638 upright (ZX) dogbones were tested in tensile after UV exposure and an additional ten ASTM D638 ZX dogbones were the control (no UV exposure). The UV exposed samples were cycled in the QUV chamber per ASTM G154 (Standard Practice for Operating Fluorescent UV Light Apparatus for Exposure of Nonmetallic Materials) for 1,000 hours, alternating for eight hours at 60 °C (140 °F) and 4 hours at 50 °C (122 °F) with humidity and condensation. The increase in stress at break is from the control samples. For more information see the Impact of UV Exposure on PDM Materials white paper.

Table 5. PC-ABS UV Exposure Test Results

Material	Conditioning	Yield Strength		Stress at Break		Elongation at break (%)	Increase in Stress at Break (%)	Modulus	
		(psi)	(MPa)	(psi)	(MPa)			(ksi)	(GPa)
PC	No UV Exposure	3880	26.7	3870	26.7	2.4		224	1.54
	UV Exposure	3710	25.6	3720	25.7	2.1	-3.80%	230	1.59

PC-ABS coupons were built on the F370 using the F123 head.



Appendix

Validated Materials

Stratasys Validated Materials are developed by Stratasys or a third-party provider, meet Stratasys quality standards, and have received basic reliability testing for use with Stratasys FDM printer. For the test procedure please see [Stratasys Materials Test Procedure](#) (immediate download upon clicking the link).

Table 6. Mechanical Properties of PC-ABS Red, Fortus 450mc, T16

		XZ Orientation	ZX Orientation
Tensile Properties: ASTM D638			
Yield Strength	MPa	37.5 (0.43)	29.9 (1.6)
	psi	5440 (62)	4330 (230)
Elongation @ Yield	%	3.2 (0.06)	2.0 (0.17)
Strength @ Break	MPa	35.3 (0.64)	30.2 (1.3)
	psi	5120 (93)	4380 (190)
Elongation @ Break	%	6.0 (0.99)	2.0 (0.14)
Modulus (Elastic)	GPa	1.73 (0.017)	1.75 (0.015)
	ksi	251 (2.5)	253 (2.2)

Values in parentheses are standard deviations.

Table 7. Mechanical Properties of PC-ABS Red, F900, T16

		XZ Orientation	ZX Orientation
Tensile Properties: ASTM D638			
Yield Strength	MPa	32.7 (0.46)	26.9 (0.60)
	psi	4740 (67)	3900 (87)
Elongation @ Yield	%	3.3 (0.070)	2.1 (0.030)
Strength @ Break	MPa	31.0 (0.50)	26.3 (0.59)
	psi	4500 (72)	3820 (85)
Elongation @ Break	%	9.8 (1.0)	2.4 (0.17)
Modulus (Elastic)	GPa	1.65 (0.020)	1.63 (0.035)
	ksi	240. (3.0)	237 (5.1)

Values in parentheses are standard deviations.

9



Figure 1. 2nd heating scan DSC data for the PC-ABS Flat (XY) sample.

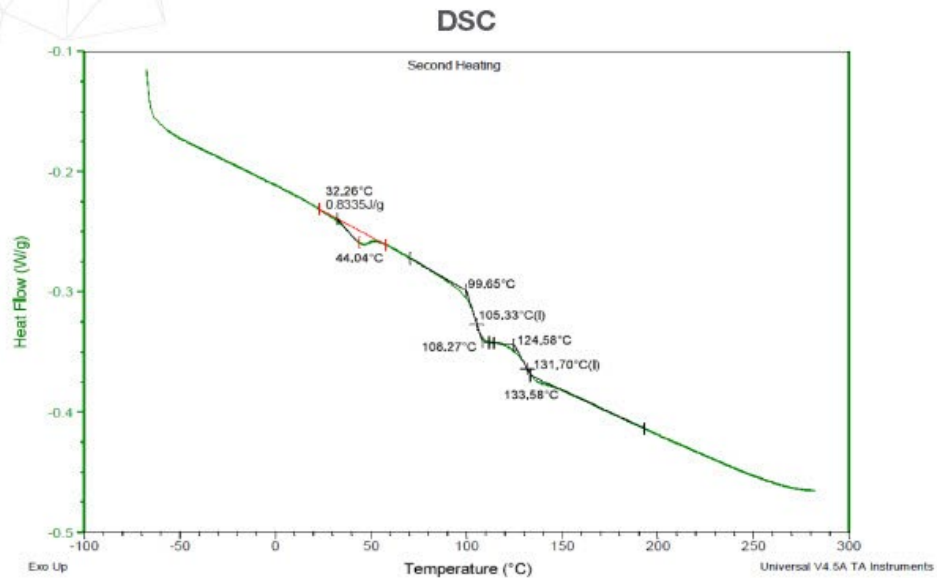


Figure 2. Dimension change data as a function of temperature for the PC-ABS Flat (XY) sample.

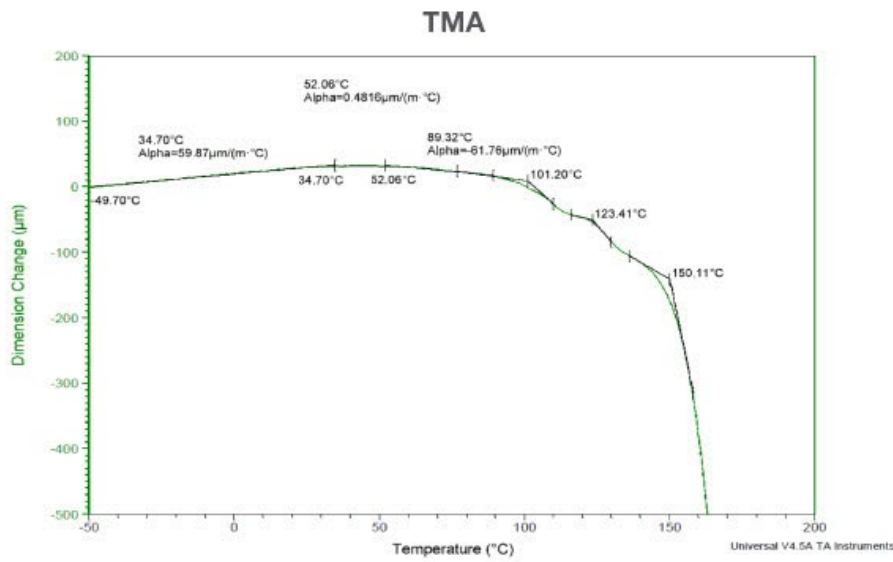




Figure 3. Dimension change data as a function of temperature for the PC-ABS On Edge (XZ) sample.

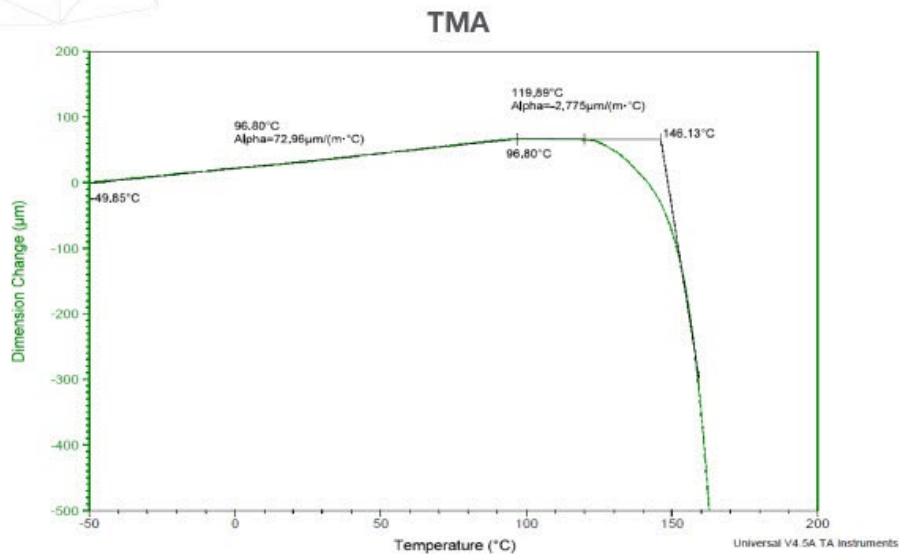
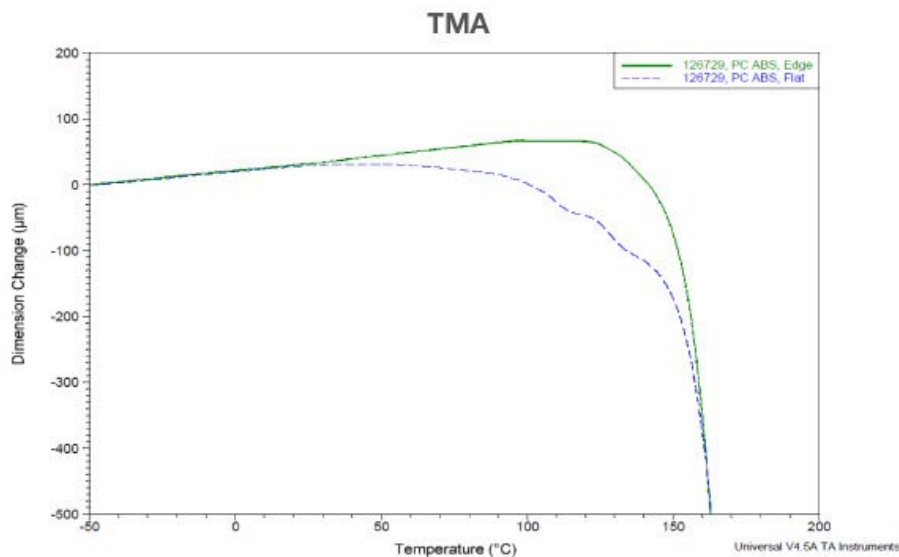


Figure 4. Overlay of the dimension change data for the Flat (XY) and On Edge (XZ) PC-ABS samples.



11

**Stratasys Headquarters**

7665 Commerce Way,
Eden Prairie, MN 55344
+1 800 801 6491 (US Toll Free)
+1 952 937-3000 (Intl)
+1 952 937-0070 (Fax)

stratasys.com

ISO 9001:2015 Certified

1 Holtzman St., Science Park,
PO Box 2496
Rehovot 76124, Israel
+972 74 745 4000
+972 74 745 5000 (Fax)

Appendix F: Stratasys ABS-CF10 Filament

1



ABS-CF10



Carbon Fiber Filled ABS FDM Thermoplastic Filament

ABS-CF10 Data Sheet

The information presented are typical values intended for reference and comparison purposes only.
They should not be used for design specifications or quality control purposes.



Overview

Stratasys ABS-CF10 combines standard ABS (acrylonitrile butadiene styrene) material with 10% chopped carbon fiber by weight. The result is a low moisture-sensitive FDM® thermoplastic 50% stiffer and 15% stronger than standard ABS 3D printing material. Typical applications include manufacturing tools, jigs, fixtures and end effectors that benefit from the combination of increased stiffness and reduced weight.

Contents:

Product and Ordering Information	3
Physical Properties	4
Mechanical Properties	5
Appendix	7



Product Information

Table 1. Printer Compatibility

Printer	Model Tip (Slice)	Support Material	Support Tip
F170™	F123 Head (7, 10, 13 slice)	QSR™	F123 Head (7, 10, 13 slice)
F190™CR	F123 Head (7, 10, 13 slice)	QSR	F123 Head (7, 10, 13 slice)
F270™	F123 Head (7, 10, 13 slice)	QSR	F123 Head (7, 10, 13 slice)
F370™	F123 Head (7, 10, 13 slice)	QSR	F123 Head (7, 10, 13 slice)
F370®CR	F123 Head (7, 10, 13 slice)	QSR	F123 Head (7, 10, 13 slice)

Support Material

- QSR soluble support

Build Tray

- F170 build tray
- F270/F190CR build tray
- F370/F370CR build tray

Table 2. ABS-CF10 Ordering Information

Part Number	Description
Filament Canisters	
333-90310	ABS-CF10, 90 cu. in.
333-63500	QSR Soluble Support, 60 cu. in. - F123
Printer Consumables	
123-00803-S	ABS-CF10 Hardened Head - Recommended (Light Gray Cover)
123-00601-S	ABS-CF10 Head (Green Cover)
123-00402-S	Standard Extrusion Head (Black Cover)
123-00302-S	F170 Build Tray, Standard
123-00303-S	F270/F190CR Build Tray, Standard
123-00304	F370/F370CR Build Tray, Standard



Physical Properties

Values are measured as printed. XY, XZ, and ZX orientations were tested. For full details refer to the [Stratasys Materials Test Report](#) (immediate download upon clicking the link). DSC and TMA curves can be found in the Appendix.

Table 3. ABS-CF10 Physical Properties

Property	Test Method	Typical Values	
		XY	XZ/ZX
HDT @ 66 psi	ASTM D648 Method B	100 °C (212 °F)	
HDT @ 264 psi	ASTM D648 Method B	99 °C (210 °F)	
Tg	ASTM D7428 Inflection Point	104 °C (219 °F)	
Mean CTE	ASTM E831 (-50 °C to 100 °C)	19 $\mu\text{m}/[\text{m}^{\circ}\text{C}]$ (11 $\mu\text{in}/[\text{in}^{\circ}\text{F}]$)	78 $\mu\text{m}/[\text{m}^{\circ}\text{C}]$ (42 $\mu\text{in}/[\text{in}^{\circ}\text{F}]$)
Volume Resistance	ASTM D257	$4.6 \times 10^{12} \Omega\cdot\text{cm}$	
Specific Gravity	ASTM D257 @23 °C	1.0972	
Dielectric Constant	ASTM D150 1 kHz test condition	2.26	11.1
Dielectric Constant	ASTM D150 2 MHz test condition	2.16	-0.001
Dissipation Factor	ASTM D150 1 kHz test condition	0.000	-0.011
Dissipation Factor	ASTM D150 2 MHz test condition	10.18	-0.014

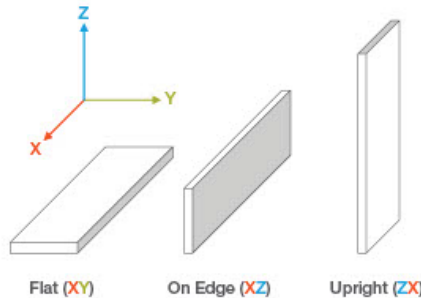


Mechanical Properties

ABS-CF10 samples were printed with a 0.010 in. (0.254 mm) layer height on the F370. For the full test procedure please see the [Stratasys Materials Test Procedure](#) (immediate download upon clicking the link).

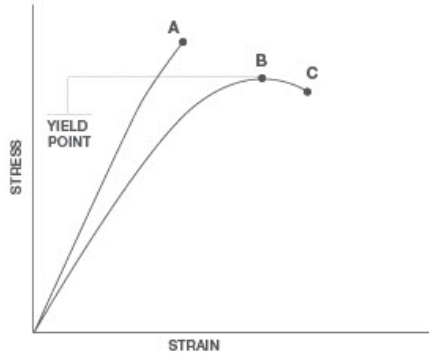
Print Orientation

Parts created using FDM are anisotropic as a result of the printing process. Below is a reference of the different orientations used to characterize the material.



Tensile Curves

Due to the anisotropic nature of FDM, tensile curves look different depending on orientation. Below is a guide of the two types of curves seen when printing tensile samples and what reported values mean.



A = Tensile at break, elongation at break (no yield point)

B = Tensile at yield, elongation at yield

C = Tensile at break, elongation at break

**Table 4. ABS-CF10 Mechanical Properties**

0.010 in layer height		XZ Orientation	ZX Orientation
Tensile Properties: ASTM D638			
Yield Strength	MPa	No yield	21.2 (0.48)
	psi	No yield	3080 (69)
Elongation @ Yield	%	No yield	1.49 (0.08)
Strength @ Break	MPa	37.7 (1.38)	21.3 (0.48)
	psi	5465 (200)	3100 (70)
Elongation @ Break	%	2.70 (0.20)	1.49 (0.09)
Modulus (Basisic)	GPa	3.342 (0.12)	1.958 (0.028)
	ksi	484.6 (18)	283.9 (4.1)
Flexural Properties: ASTM D790, Procedure A			
Strength @ Break	MPa	69.0 (2.4)	29.2 (0.86)
	psi	10000 (350)	4240 (120)
Strain @ Break	%	2.45 (0.11)	1.89 (0.08)
Modulus	GPa	3.76 (0.099)	1.75 (0.051)
	ksi	545 (14)	254 (7.5)
Compression Properties: ASTM D695			
Yield Strength	MPa	No yield	No yield
	psi	No yield	No yield
Peak Strength	MPa	73.2 (4.5)	94.8 (2.56)
	psi	10620 (650)	13740 (370)
Modulus	GPa	2.129 (0.093)	1.917 (0.063)
	ksi	309 (13.6)	278 (9.2)
Impact Properties: ASTM D256, ASTM D4812			
Notched	J/m	51.4 (1.9)	20.3 (2.8)
	ft ² lb/in	0.962 (0.04)	0.381 (0.05)
Unnotched	J/m	212 (25)	47.0 (6.4)
	ft ² lb/in	3.97 (0.47)	0.881 (0.12)

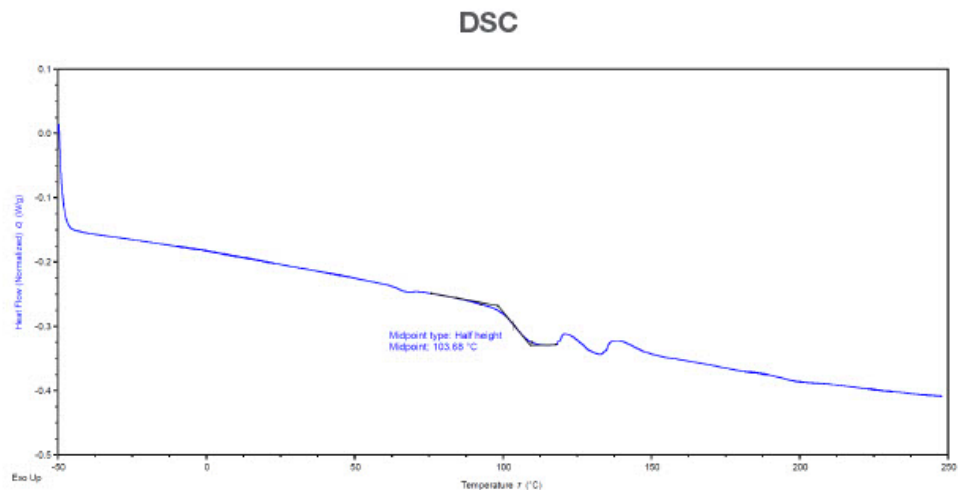
(1) Values in parentheses are standard deviations.



Appendix



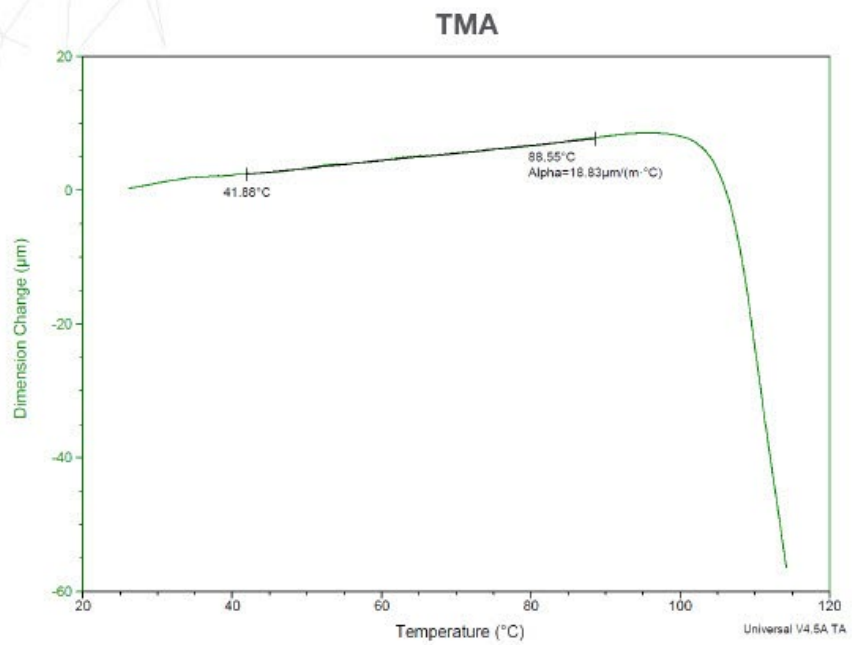
Figure 1. DSC data for the ABS-CF10 sample.



8



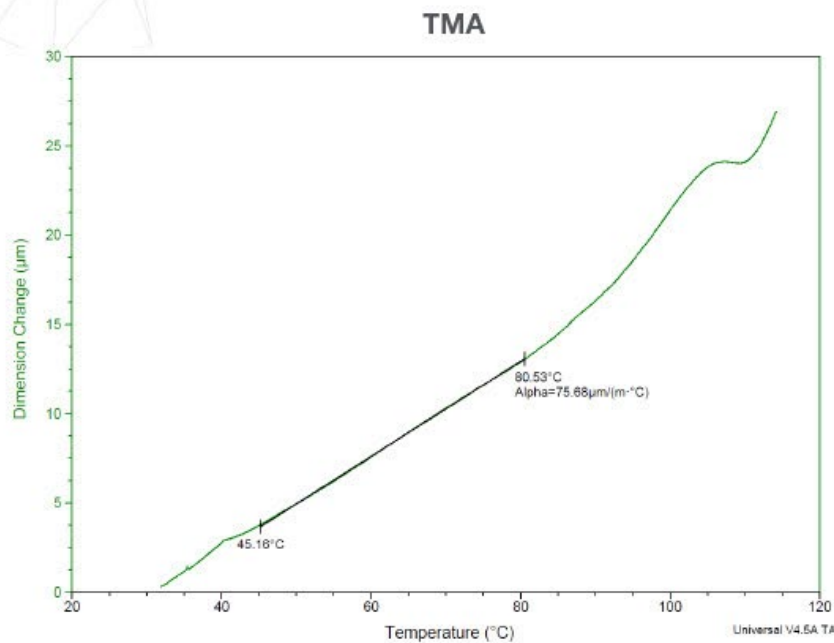
Figure 2. Dimension change data as a function of temperature for ABS-CF10 Flat (XY) sample.



9



Figure 3. Dimension change data as a function of temperature for ABS-CF10 On Edge (XZ) sample.



Stratasys Headquarters

7665 Commerce Way,
Eden Prairie, MN 55344
+1 800 801 6491 (US Toll Free)
+1 952 937-3000 (Intl)
+1 952 937-0070 (Fax)

1 Holtzman St., Science Park,
PO Box 2498
Rehovot 76124, Israel
+972 74 745 4000
+972 74 745 5000 (Fax)

stratasys.com

ISO 9001:2015 Certified



Appendix G: Ceramic Sleeving

THERMEEZ™ CERAMIC TAPES, SLEEVING AND CLOTHS Strong and Durable Use to 1100°F

Thermeez Woven, Hi-Strength, Ceramic Fiber Products are ideal for thermal insulators, padding, gaskets, flexible curtains, liquid metal splash protection, expansion joints, sleeving for flexible wire insulation, hoses, thermocouples, induction coils. They are woven from industrial grade, asbestos free, ceramic fibers and are usable up to 1100°F.

Thermeez Fabrics are durable, dimensionally and chemically stable and have excellent electrical resistance. They are user friendly and, unlike fiberglass, non-irritating to the skin. Non-Toxic, meets OSHA requirements and will not burn. They are resistant to molten metal sparks and splashes, most chemicals and solvents.

Use Woven Tapes and Adhesive Backed Pressure Sensitive Tapes for pipes, hoses, cables, exhaust systems, equipment wrapping, door gaskets, strip curtains, personal protection of tools, forceps, hot working tools, etc.

Use Sleeving for hi-temp. tubing, hose and wire insulation, protection, resilient gasketing, etc. Just select the I.D. required to slide over tubes, hoses, cables etc.

Use Rope for gaskets, packing, seals, doors, access ports fabrication tadpole gaskets, etc.

WOVEN SLEEVING

395TM-0-3.....	1/8" x 3'
395TM-0-5.....	1/8" x 5'
395TM-0-25.....	1/8" x 25'
395TM-0-50.....	1/8" x 50'
395TM-0-100.....	1/8" x 100'
395TM-1-3.....	1/4" x 3'
395TM-1-10.....	1/4" x 10'
395TM-1-25.....	1/4" x 25'
395TM-1-100.....	1/4" x 100'
395TM-2-3.....	3/8" x 3'
395TM-2-5.....	3/8" x 5'
395TM-2-25.....	3/8" x 25'
395TM-2-100.....	3/8" x 100'
395TM-3-3.....	1/2" x 3'
395TM-3-5.....	1/2" x 5'
395TM-3-25.....	1/2" x 25'
395TM-3-100.....	1/2" x 100'
395TM-4-3.....	3/4" x 3'
395TM-4-5.....	3/4" x 5'
395TM-4-25.....	3/4" x 25'
395TM-4-100.....	3/4" x 100'
395TM-5-3.....	1" x 3'
395TM-5-5.....	1" x 5'
395TM-5-25.....	1" x 25'
395TM-5-100.....	1" x 100'
395TM-6-3.....	1 1/2" x 3'
395TM-6-5.....	1 1/2" x 5'
395TM-6-25.....	1 1/2" x 25'
395TM-6-100.....	1 1/2" x 100'
395TM-7-3.....	2" x 3'
395TM-7-5.....	2" x 5'
395TM-7-25.....	2" x 25'
395TM-7-100.....	2" x 100'

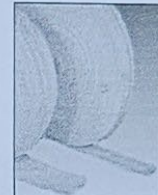
Wall Thickness is 1/16"



THERMEEZ	395
Melting Point °F	2800
Max. Continuous Service °F	1100
Density (# / ft³)	30
Specific Heat (BTU / #°F)	0.25
Dielectric Strength (volts/mil.)	450
Thermal Conductivity (BTU in / Hr °F ft²)	
@ 500°F	0.48
@ 1000°F	0.90

WOVEN TAPE

395-21.....	1/32" x 1" x 100'
395-22.....	1/32" x 2" x 100'
395-23.....	1/32" x 3" x 100'
395-41.....	1/16" x 1" x 100'
395-42.....	1/16" x 2" x 100'
395-43.....	1/16" x 3" x 100'
395-81.....	1/8" x 1" x 100'
395-82.....	1/8" x 2" x 100'
395-83.....	1/8" x 3" x 100'



ADHESIVE BACKED TAPE

395PS-21.....	1/32" x 1" x 50'
395PS-22.....	1/32" x 2" x 50'
395PS-23.....	1/32" x 3" x 50'
395PS-41.....	1/16" x 1" x 50'
395PS-42.....	1/16" x 2" x 50'
395PS-43.....	1/16" x 3" x 50'
395PS-81.....	1/8" x 1" x 50'
395PS-82.....	1/8" x 2" x 50'
395PS-83.....	1/8" x 3" x 50'



WOVEN CLOTH

395C-6.....	1/16" x 6" x 25'
395C-1.....	1/16" x 40" x 5'
395C-2.....	1/16" x 40" x 15'
395C-5.....	1/8" x 40" x 25'

THIS SUBSTANCE IS NOT CLASSIFIED ACCORDING TO THE GLOBALLY HARMONIZED SYSTEM (GHS).

HEALTH HAZARD DATA**

Currently there are no known chronic health effects in humans from long term exposure to these refractory ceramic fibers. This product may contain minor amounts of binders which burn out during the first heat up. Use adequate ventilation during this first exposure to heat.

SAFE WORK PRACTICE and PROTECTIVE EQUIPMENT

Long sleeve, loose fitting clothing and barrier cream. Dust respirator in compliance with OSHA Standard currently 29 CFR 1910.134 (NIOSH Approved) when required.

Material does not appear on NTP and/or LAC lists of reports for carcinogens.

** Extracted from MSDS



McMaster Carr Supply Company

Thermeez 397 (1500°F), Custom Sizes and Fabrication Services are Available Upon Request

COTRONICS
CORPORATION
718-788-5533

8. Computational Model Code

Appendix A: MATLAB Code

```

1 clear;
2 close all;
3
4 %% Pressure must be between 35 and 155 psi
5 %% Next step is to include head losses and convective losses
6
7 %% Fluid Constants for Prototype
8 R = 287; %specific gas constant for dry air in J/(kg K)
9 cp = 1.01e3; %specific heat of air in standard conditions in J/(kg K)
10 gamma = 1.4; %ratio of specific heats for air, assume constant
11 cv = 700; %specific heat of air in standard conditions in J/(kg K)
12 g = 9.81; %gravitational acceleration
13
14 %% Setup Constants for Prototype
15 T_0 = 295; %temperature of air in standard conditions in K
16 p_0 = 6895; %1 psi in pascals
17 p_0 = 150*p_0; %100 psi in pascals
18 rho_0 = p_0/(R*T_0); %density of air using P=rhoRT;
19 p_1 = p_0; %constant pressure assumptions
20 p_e = 1.01e5; %exit pressure = ambient pressure in pascals for perfectly expanded flow
21 initial_volume = .028; %cubic foot in cubic meters
22 initial_mass = initial_volume*rho_0; %initial mass
23 num_radii = 8; %number of throat radii plotted
24 r_throat = [0.3,0.4,0.5,0.6,0.7,0.8,0.9,1]; %throat radius in mm (1mm = 0.04in)
25 r_throat = r_throat/1000; %throat radius in m
26 A_throat = pi*r_throat.^2; %throat area in m^2
27 r_pipe = 2.67e-3; %pipe radius in m (0.165 in)
28 A_pipe = pi*r_pipe.^2; %pipe area in m^2
29 L = 1; %pipe length in m
30 q = 150; %total heat addition
31 disp(rho_0);
32
33 %% Solving for Mass Flowrate and Heating Numerically
34 myfun = @(x,a,b,c,d) a*x^4 + b*x^3 + c*x^2 + d;
35 T_1 = zeros(1,num_radii);
36
37 alpha = (A_throat/1.577)*sqrt(gamma*R/1.2);
38 beta = alpha*cp*p_1/R;
39 zeta = alpha.^3*p_1^3/(2*A_pipe^2*R^3);
40
41 for i=1:num_radii
42     a = beta(i)*zeta(i)*R^2/p_1^2;
43     b = -q;
44     c = -beta(i)*T_0;
45     d = -zeta(i)/p_0^2;
46     fun = @(x) myfun(x,a,b,c,d);
47     x_0 = sqrt(5*T_0);
48     x = fzero(fun,x_0);
49     T_1(i) = x.^2;
50 end
51
52 rho_1 = p_1./(R*T_1);
53 mdot = rho_1.*A_throat/1.577.*sqrt(gamma*R*T_1/1.2);
54
55 %% Solving for Exit and Throat Conditions
56 p_t = 0.528*p_1;
57 rho_t = 0.634*rho_1;
58 T_t = 0.833*T_1;
59
60 Ratios = IdealAreaRatio(p_1,p_e); %Ideal Ratios for fully expanded flow
61
62 AreaRatio = Ratios(1);
63 Mach = Ratios(2);
64 DensityRatio = Ratios(3);
65 TemperatureRatio = Ratios(4);
66
67 A_e = A_throat*AreaRatio; %exit area
68 rho_e = rho_1/DensityRatio; %exit density
69 T_e = T_1/TemperatureRatio; %exit temperature
70
71 c = sqrt(gamma*R*T_e); %exit sound speed
72 v = Mach*c; %exit velocity
73 burntime = initial_mass./mdot;
74 Thrust = mdot.*v; %Thrust array
75 Isp = v/g;
76 disp(v);
77
78 %% Solving for Area Ratios Based on Inlet Pressures
79 num_p = 12;
80 p_in_psi = [40,50,60,70,80,90,100,110,120,130,140,150]; %psi
81 p_in = p_in_psi*6895; %pascals
82 ARatios = zeros(1,num_p);
83 for i=1:num_p
84     Ratios2 = IdealAreaRatio(p_in(i),p_e);
85     ARatios(i) = Ratios2(1);
86 end
87
88 %% Plots
89
90 plot(r_throat,burntime);
91 xlabel('Throat Radius (m)');

```

```

91 ylabel('Burn Time (s)');
92 figure;
93 plot(_throat,Thrust);
94 xlabel('Throat Radius (m)');
95 ylabel('Thrust (N)');
96 %set(gca,'fontsize',16,'fontweight','bold');
97 %grid on;
98
99 figure;
100 plot(_throat,Isp);
101 xlabel('Throat Radius (m)');
102 ylabel('Isp (s)');
103 %set(gca,'fontsize',16,'fontweight','bold');
104 %grid on;
105
106 figure;
107 plot(p_in_psi,ARatios);
108 xlabel('Initial Pressure (psi)');
109 ylabel('Area Ratio');
110 %set(gca,'fontsize',16,'fontweight','bold');
111 %grid on;
112
113 figure;
114 plot(_throat,mdot);
115 xlabel('Throat Radius (m)');
116 ylabel('Mass Flowrate (kg/s)');
117
118 figure;
119 plot(_throat,T_e);
120 xlabel('Throat Radius (m)');
121 ylabel('Exit Temperature (K)');
122
123 figure;
124 plot(r_throat,rho_e);
125 xlabel('Throat Radius (m)');
126 ylabel('Exit Density (kg/m^3)');
127
128 x = 1:4;
129
130 figure;
131 hold on;
132 for i=1:num_radii
133 y = [T_0,T_1(i),T_t(i),T_e(i)];
134 plot(x, y,'DisplayName', string(1000*r_throat(i)) + 'mm Throat Radius')
135 end
136 xlabel('Temperature (K)');
137 set(gca, 'XTick',1:5, 'XTickLabel',{'Initial' 'Post Heating' 'Throat' 'Exit'});
138 legend('NumColumns',1);
139 %set(gca,'fontsize',16,'fontweight','bold');
140 %grid on;
141
142 figure;
143 hold on;
144 for i=1:num_radii
145 y = [rho_0,rho_1(i),rho_t(i),rho_e(i)];
146 plot(x, y,'DisplayName', string(1000*r_throat(i)) + 'mm Throat Radius')
147 end
148 ylabel('Density (kg/m^3)');
149 set(gca, 'XTick',1:5, 'XTickLabel',{'Initial' 'Post Heating' 'Throat' 'Exit'});
150
151 legend;
152
153 figure;
154 y = [p_0,p_1,r_t,p_e];
155 plot(x, y);
156 xlabel('Pressure (N/m^2)');
157 set(gca, 'XTick',1:5, 'XTickLabel',{'Initial' 'Post Heating' 'Throat' 'Exit'});
158
159 disp("Area Ratio:")
160 disp(AreaRatio);
161 disp("Mach:")
162 disp(Mach);

```

```

1 function Ratios = IdealAreaRatio(pin,pout)
2 Ratios = zeros(1,4);
3
4 PressureRatios = [2.189,3.094,3.891,4.648,5.406,6.300,7.128,7.824,9.145,9.888,10.69,132.8,142.0];
5 AreaRatios = [1.011,1.104,1.204,1.301,1.397,1.507,1.606,1.687,1.837,1.919,2.005,9.799,10.25];
6 Machs = [1.120,1.380,1.540,1.660,1.760,1.860,1.940,2.000,2.100,2.150,2.200,3.900,3.950];
7 DensityRatios = [1.750,2.241,2.639,2.996,3.338,3.723,4.067,4.347,4.859,5.138,5.433,32.85,34.46];
8 TemperatureRatios = [1.251,1.381,1.474,1.551,1.620,1.692,1.753,1.800,1.882,1.924,1.968,4.042,4.120];
9
10 PressureRatio = pin/pout;
11 j = 1;
12 while (PressureRatio > PressureRatios(j))
13 j=j+1;
14 end
15 a = j;
16 b = (PressureRatio-PressureRatios(a-1))/(PressureRatios(a)-PressureRatios(a-1));
17
18 Ratios(1) = AreaRatios(a-1) + b*(AreaRatios(a)-AreaRatios(a-1));
19 Ratios(2) = Machs(a-1) + b*(Machs(a)-Machs(a-1));
20 Ratios(3) = DensityRatios(a-1) + b*(DensityRatios(a)-DensityRatios(a-1));
21 Ratios(4) = TemperatureRatios(a-1) + b*(TemperatureRatios(a)-TemperatureRatios(a-1));
22 end

```

9. Other Software Code

Appendix A: Load Cell Arduino Code

```
/*
-----
----- HX711_ADC
----- Arduino library for HX711 24-Bit Analog-to-Digital Converter for Weight Scales
----- Olav Kallhovd sept2017
-----
*/
#include <Arduino.h>
#include <HX711_ADC.h>

HX711_ADC::HX711_ADC(uint8_t dout, uint8_t sck) //constructor
{
    doutPin = dout;
    sckPin = sck;
}

void HX711_ADC::setGain(uint8_t gain) //value should be 32, 64 or 128*
{
    if(gain < 64) GAIN = 2; //32, channel B
    else if(gain < 128) GAIN = 3; //64, channel A
    else GAIN = 1; //128, channel A
}

//set pinMode, HX711 gain and power up the HX711
void HX711_ADC::begin()
{
    pinMode(sckPin, OUTPUT);
    pinMode(doutPin, INPUT);
    setGain(128);
    powerUp();
}

//set pinMode, HX711 selected gain and power up the HX711
void HX711_ADC::begin(uint8_t gain)
{
    pinMode(sckPin, OUTPUT);
    pinMode(doutPin, INPUT);
    setGain(gain);
```

```
powerUp();  
}  
  
/* start(t):  
* will do conversions continuously for 't' +400 milliseconds (400ms is min.  
settling time at 10SPS).  
* Running this for 1-5s in setup() - before tare() seems to improve the tare  
accuracy */  
void HX711_ADC::start(unsigned long t)  
{  
    t += 400;  
    lastDoutLowTime = millis();  
    while(millis() < t)  
    {  
        update();  
        yield();  
    }  
    tare();  
    tareStatus = 0;  
}  
  
/* start(t, dotare) with selectable tare:  
* will do conversions continuously for 't' +400 milliseconds (400ms is min.  
settling time at 10SPS).  
* Running this for 1-5s in setup() - before tare() seems to improve the tare  
accuracy. */  
void HX711_ADC::start(unsigned long t, bool dotare)  
{  
    t += 400;  
    lastDoutLowTime = millis();  
    while(millis() < t)  
    {  
        update();  
        yield();  
    }  
    if (dotare)  
    {  
        tare();  
        tareStatus = 0;  
    }  
}  
  
/* startMultiple(t): use this if you have more than one load cell and you want  
to do tare and stabilization simultaneously.
```

```

* Will do conversions continuously for 't' +400 milliseconds (400ms is min.
settling time at 10SPS).
* Running this for 1-5s in setup() - before tare() seems to improve the tare
accuracy */
int HX711_ADC::startMultiple(unsigned long t)
{
    tareTimeoutFlag = 0;
    lastDoutLowTime = millis();
    if(startStatus == 0) {
        if(isFirst) {
            startMultipleTimeStamp = millis();
            if (t < 400)
            {
                startMultipleWaitTime = t + 400; //min time for HX711 to be
stable
            }
            else
            {
                startMultipleWaitTime = t;
            }
            isFirst = 0;
        }
        if((millis() - startMultipleTimeStamp) < startMultipleWaitTime) {
            update(); //do conversions during stabilization time
            yield();
            return 0;
        }
        else { //do tare after stabilization time is up
            static unsigned long timeout = millis() + tareTimeout;
            doTare = 1;
            update();
            if(convRslt == 2)
            {
                doTare = 0;
                convRslt = 0;
                startStatus = 1;
            }
            if (!tareTimeoutDisable)
            {
                if (millis() > timeout)
                {
                    tareTimeoutFlag = 1;
                    return 1; // Prevent endless loop if no HX711 is connected
                }
            }
        }
    }
}

```

```

        }
    }
    return startStatus;
}

/* startMultiple(t, dotare) with selectable tare:
 * use this if you have more than one load cell and you want to (do tare and)
stabilization simultaneously.
* Will do conversions continuously for 't' +400 milliseconds (400ms is min.
settling time at 10SPS).
* Running this for 1-5s in setup() - before tare() seems to improve the tare
accuracy */
int HX711_ADC::startMultiple(unsigned long t, bool dotare)
{
    tareTimeoutFlag = 0;
    lastDoutLowTime = millis();
    if(startStatus == 0) {
        if(isFirst) {
            startMultipleTimeStamp = millis();
            if (t < 400)
            {
                startMultipleWaitTime = t + 400; //min time for HX711 to be
stable
            }
            else
            {
                startMultipleWaitTime = t;
            }
            isFirst = 0;
        }
        if((millis() - startMultipleTimeStamp) < startMultipleWaitTime) {
            update(); //do conversions during stabilization time
            yield();
            return 0;
        }
        else { //do tare after stabilization time is up
            if (dotare)
            {
                static unsigned long timeout = millis() + tareTimeout;
                doTare = 1;
                update();
                if(convRslt == 2)
                {
                    doTare = 0;
                    convRslt = 0;
                }
            }
        }
    }
}

```

```

        startStatus = 1;
    }
    if (!tareTimeoutDisable)
    {
        if (millis() > timeout)
        {
            tareTimeoutFlag = 1;
            return 1; // Prevent endless loop if no HX711 is connected
        }
    }
    else return 1;
}
return startStatus;
}

//zero the scale, wait for tare to finish (blocking)
void HX711_ADC::tare()
{
    uint8_t rdy = 0;
    doTare = 1;
    tareTimes = 0;
    tareTimeoutFlag = 0;
    unsigned long timeout = millis() + tareTimeOut;
    while(rdy != 2)
    {
        rdy = update();
        if (!tareTimeoutDisable)
        {
            if (millis() > timeout)
            {
                tareTimeoutFlag = 1;
                break; // Prevent endless loop if no HX711 is connected
            }
        }
        yield();
    }
}

//zero the scale, initiate the tare operation to run in the background (non-blocking)
void HX711_ADC::tareNoDelay()
{
    doTare = 1;
}

```

```
tareTimes = 0;
tareStatus = 0;
}

//set new calibration factor, raw data is divided by this value to convert to
//readable data
void HX711_ADC::setCalFactor(float cal)
{
    calFactor = cal;
    calFactorRecip = 1/calFactor;
}

//returns 'true' if tareNoDelay() operation is complete
bool HX711_ADC::getTareStatus()
{
    bool t = tareStatus;
    tareStatus = 0;
    return t;
}

//returns the current calibration factor
float HX711_ADC::getCalFactor()
{
    return calFactor;
}

//call the function update() in loop or from ISR
//if conversion is ready; read out 24 bit data and add to dataset, returns 1
//if tare operation is complete, returns 2
//else returns 0
uint8_t HX711_ADC::update()
{
    byte dout = digitalRead(doutPin); //check if conversion is ready
    if (!dout)
    {
        conversion24bit();
        lastDoutLowTime = millis();
        signalTimeoutFlag = 0;
    }
    else
    {
        //if (millis() > (lastDoutLowTime + SIGNAL_TIMEOUT))
        if (millis() - lastDoutLowTime > SIGNAL_TIMEOUT)
        {
            signalTimeoutFlag = 1;
        }
    }
}
```

```
        }
        convRslt = 0;
    }
    return convRslt;
}

// call the function dataWaitingAsync() in loop or from ISR to check if new data
is available to read
// if conversion is ready, just call updateAsync() to read out 24 bit data and
add to dataset
// returns 1 if data available , else 0
bool HX711_ADC::dataWaitingAsync()
{
    if (dataWaiting) { lastDoutLowTime = millis(); return 1; }
    byte dout = digitalRead(doutPin); //check if conversion is ready
    if (!dout)
    {
        dataWaiting = true;
        lastDoutLowTime = millis();
        signalTimeoutFlag = 0;
        return 1;
    }
    else
    {
        //if (millis() > (lastDoutLowTime + SIGNAL_TIMEOUT))
        if (millis() - lastDoutLowTime > SIGNAL_TIMEOUT)
        {
            signalTimeoutFlag = 1;
        }
        convRslt = 0;
    }
    return 0;
}

// if data is available call updateAsync() to convert it and add it to the
dataset.
// call getData() to get latest value
bool HX711_ADC::updateAsync()
{
    if (dataWaiting) {
        conversion24bit();
        dataWaiting = false;
        return true;
    }
    return false;
}
```

```

}

float HX711_ADC::getData() // return fresh data from the moving average dataset
{
    long data = 0;
    lastSmoothedData = smoothedData();
    data = lastSmoothedData - tareOffset ;
    float x = (float) data * calFactorRecip;
    return x;
}

long HX711_ADC::smoothedData()
{
    long data = 0;
    long L = 0xFFFFF;
    long H = 0x00;
    for (uint8_t r = 0; r < (samplesInUse + IGN_HIGH_SAMPLE + IGN_LOW_SAMPLE);
r++)
    {
        #if IGN_LOW_SAMPLE
        if (L > dataSampleSet[r]) L = dataSampleSet[r]; // find lowest value
        #endif
        #if IGN_HIGH_SAMPLE
        if (H < dataSampleSet[r]) H = dataSampleSet[r]; // find highest value
        #endif
        data += dataSampleSet[r];
    }
    #if IGN_LOW_SAMPLE
    data -= L; //remove lowest value
    #endif
    #if IGN_HIGH_SAMPLE
    data -= H; //remove highest value
    #endif
    //return data;
    return (data >> divBit);
}

void HX711_ADC::conversion24bit() //read 24 bit data, store in dataset and start
the next conversion
{
    conversionTime = micros() - conversionStartTime;
    conversionStartTime = micros();
    unsigned long data = 0;
}

```

```

uint8_t dout;
convRslt = 0;
if(SCK_DISABLE_INTERRUPTS) noInterrupts();

for (uint8_t i = 0; i < (24 + GAIN); i++)
{   //read 24 bit data + set gain and start next conversion
    digitalWrite(sckPin, 1);
    if(SCK_DELAY) delayMicroseconds(1); // could be required for faster
mcu's, set value in config.h
    digitalWrite(sckPin, 0);
    if (i < (24))
    {
        dout = digitalRead(doutPin);
        data = (data << 1) | dout;
    } else {
        if(SCK_DELAY) delayMicroseconds(1); // could be required for faster
mcu's, set value in config.h
    }
}
if(SCK_DISABLE_INTERRUPTS) interrupts();

/*
The HX711 output range is min. 0x800000 and max. 0x7FFFFF (the value rolls
over).
In order to convert the range to min. 0x000000 and max. 0xFFFFFFFF,
the 24th bit must be changed from 0 to 1 or from 1 to 0.
*/
data = data ^ 0x800000; // flip the 24th bit

if (data > 0xFFFFFFFF)
{
    dataOutOfRange = 1;
    //Serial.println("dataOutOfRange");
}
if (reverseVal) {
    data = 0xFFFFFFF - data;
}
if (readIndex == samplesInUse + IGN_HIGH_SAMPLE + IGN_LOW_SAMPLE - 1)
{
    readIndex = 0;
}
else
{
    readIndex++;
}

```

```
if(data > 0)
{
    convRslt++;
    dataSampleSet[readIndex] = (long)data;
    if(doTare)
    {
        if (tareTimes < DATA_SET)
        {
            tareTimes++;
        }
        else
        {
            tareOffset = smoothedData();
            tareTimes = 0;
            doTare = 0;
            tareStatus = 1;
            convRslt++;
        }
    }
}

//power down the HX711
void HX711_ADC::powerDown()
{
    digitalWrite(sckPin, LOW);
    digitalWrite(sckPin, HIGH);
}

//power up the HX711
void HX711_ADC::powerUp()
{
    digitalWrite(sckPin, LOW);
}

//get the tare offset (raw data value output without the scale "calFactor")
long HX711_ADC::getTareOffset()
{
    return tareOffset;
}

//set new tare offset (raw data value input without the scale "calFactor")
void HX711_ADC::setTareOffset(long newoffset)
{
    tareOffset = newoffset;
```

```
}

//for testing and debugging:
//returns current value of dataset readIndex
int HX711_ADC::getReadIndex()
{
    return readIndex;
}

//for testing and debugging:
//returns latest conversion time in millis
float HX711_ADC::getConversionTime()
{
    return conversionTime/1000.0;
}

//for testing and debugging:
//returns the HX711 conversions ea seconds based on the latest conversion time.
//The HX711 can be set to 10SPS or 80SPS. For general use the recommended setting
//is 10SPS.
float HX711_ADC::getSPS()
{
    float sps = 1000000.0/conversionTime;
    return sps;
}

//for testing and debugging:
//returns the tare timeout flag from the last tare operation.
//0 = no timeout, 1 = timeout
bool HX711_ADC::getTareTimeoutFlag()
{
    return tareTimeoutFlag;
}

void HX711_ADC::disableTareTimeout()
{
    tareTimeoutDisable = 1;
}

long HX711_ADC::getSettlingTime()
{
    long st = getConversionTime() * DATA_SET;
    return st;
}
```

```
//override the number of samples in use
//value is rounded down to the nearest valid value
void HX711_ADC::setSamplesInUse(int samples)
{
    int old_value = samplesInUse;

    if(samples <= SAMPLES)
    {
        if(samples == 0) //reset to the original value
        {
            divBit = divBitCompiled;
        }
        else
        {
            samples >>= 1;
            for(divBit = 0; samples != 0; samples >>= 1, divBit++);
        }
        samplesInUse = 1 << divBit;

        //replace the value of all samples in use with the last conversion value
        if(samplesInUse != old_value)
        {
            for (uint8_t r = 0; r < samplesInUse + IGN_HIGH_SAMPLE +
IGN_LOW_SAMPLE; r++)
            {
                dataSampleSet[r] = lastSmoothedData;
            }
            readIndex = 0;
        }
    }
}

//returns the current number of samples in use.
int HX711_ADC::getSamplesInUse()
{
    return samplesInUse;
}

//resets index for dataset
void HX711_ADC::resetSamplesIndex()
{
    readIndex = 0;
}
```

```
//Fill the whole dataset up with new conversions, i.e. after a reset/restart
//(this function is blocking once started)
bool HX711_ADC::refreshDataSet()
{
    int s = getSamplesInUse() + IGN_HIGH_SAMPLE + IGN_LOW_SAMPLE; // get number
of samples in dataset
    resetSamplesIndex();
    while ( s > 0 ) {
        update();
        yield();
        if (digitalRead(doutPin) == LOW) { // HX711 dout pin is pulled low when a
new conversion is ready
            getData(); // add data to the set and start next conversion
            s--;
        }
    }
    return true;
}

//returns 'true' when the whole dataset has been filled up with conversions, i.e.
after a reset/restart.
bool HX711_ADC::getDataSetStatus()
{
    bool i = false;
    if (readIndex == samplesInUse + IGN_HIGH_SAMPLE + IGN_LOW_SAMPLE - 1)
    {
        i = true;
    }
    return i;
}

//returns and sets a new calibration value (calFactor) based on a known mass
input
float HX711_ADC::getNewCalibration(float known_mass)
{
    float readValue = getData();
    float exist_calFactor = getCalFactor();
    float new_calFactor;
    new_calFactor = (readValue * exist_calFactor) / known_mass;
    setCalFactor(new_calFactor);
    return new_calFactor;
}

//returns 'true' if it takes longer time then 'SIGNAL_TIMEOUT' for the dout pin
to go low after a new conversion is started
```

```
bool HX711_ADC::getSignalTimeoutFlag()
{
    return signalTimeoutFlag;
}

//reverse the output value (flip positive/negative value)
//tare/zero-offset must be re-set after calling this.
void HX711_ADC::setReverseOutput() {
    reverseVal = true;
}
```

Appendix B: Load Cell Library

```
/*
-----
HX711_ADC
Arduino library for HX711 24-Bit Analog-to-Digital Converter for Weight Scales
Olav Kallhovd sept2017
-----
*/
#ifndef HX711_ADC_h
#define HX711_ADC_h

#include <Arduino.h>
#include "config.h"

/*
Note: HX711_ADC configuration values has been moved to file config.h
*/

#define DATA_SET      SAMPLES + IGN_HIGH_SAMPLE + IGN_LOW_SAMPLE // total samples
in memory

#if (SAMPLES != 1) & (SAMPLES != 2) & (SAMPLES != 4) & (SAMPLES != 8) &
(SAMPLES != 16) & (SAMPLES != 32) & (SAMPLES != 64) & (SAMPLES != 128)
    #error "number of SAMPLES not valid!"
#endif

#if (SAMPLES == 1) & ((IGN_HIGH_SAMPLE != 0) | (IGN_LOW_SAMPLE != 0))
    #error "number of SAMPLES not valid!"
#endif

#if      (SAMPLES == 1)
#define   DIVB 0
#elif    (SAMPLES == 2)
#define   DIVB 1
#elif    (SAMPLES == 4)
#define   DIVB 2
#elif    (SAMPLES == 8)
#define   DIVB 3
#elif    (SAMPLES == 16)
#define   DIVB 4
#elif    (SAMPLES == 32)
```

```

#define      DIVB 5
#elif      (SAMPLES == 64)
#define      DIVB 6
#elif      (SAMPLES == 128)
#define      DIVB 7
#endif

#define SIGNAL_TIMEOUT 100

class HX711_ADC
{
public:
    HX711_ADC(uint8_t dout, uint8_t sck);           //constructor
    void setGain(uint8_t gain = 128);                //value must be 32, 64 or
128*
    void begin();                                     //set pinMode, HX711 gain and
power up the HX711
    void begin(uint8_t gain);                        //set pinMode, HX711 selected
gain and power up the HX711
    void start(unsigned long t);                     //start HX711 and do tare
    void start(unsigned long t, bool dotare);        //start HX711, do tare if
selected
    int startMultiple(unsigned long t);              //start and do tare,
multiple HX711 simultaneously
    int startMultiple(unsigned long t, bool dotare); //start and do tare
if selected, multiple HX711 simultaneously
    void tare();                                    //zero the scale, wait for
tare to finnish (blocking)
    void tareNoDelay();                            //zero the scale, initiate
the tare operation to run in the background (non-blocking)
    bool getTareStatus();                         //returns 'true' if
tareNoDelay() operation is complete
    void setCalFactor(float cal);                 //set new calibration factor,
raw data is divided by this value to convert to readable data
    float getCalFactor();                         //returns the current
calibration factor
    float getData();                             //returns data from the
moving average dataset

    int getReadIndex();                          //for testing and debugging
    float getConversionTime();                  //for testing and debugging
    float getSPS();                            //for testing and debugging
    bool getTareTimeoutFlag();                 //for testing and debugging
    void disableTareTimeout();                //for testing and debugging

```

```

long getSettlingTime();                                //for testing and debugging
void powerDown();                                    //power down the HX711
void powerUp();                                     //power up the HX711
long getTareOffset();                                //get the tare offset (raw)
data value output without the scale "calFactor")    //set new tare offset (raw
    void setTareOffset(long newoffset);               //if conversion is ready;
data value input without the scale "calFactor")     //checks if data is available
    uint8_t update();                                //read available data and add
read out 24 bit data and add to dataset             //override number of samples
    bool dataWaitingAsync();                         //returns current number of
to read (no conversion yet)                        //resets index for dataset
    bool updateAsync();                            //Fill the whole dataset up
to dataset                                         with new conversions, i.e. after a reset/restart (this function is blocking once
    void setSamplesInUse(int samples);              started)
in use                                              bool getDataSetStatus();           //returns 'true' when the
    int getSamplesInUse();                          whole dataset has been filled up with conversions, i.e. after a reset/restart
samples in use                                       float getNewCalibration(float known_mass); //returns and sets a new
    void resetSamplesIndex();                      calibration value (calFactor) based on a known mass input
    bool refreshDataSet();                         bool getSignalTimeoutFlag();        //returns 'true' if it takes
with new conversions, i.e. after a reset/restart (this function is blocking once
started)                                           longer time then 'SIGNAL_TIMEOUT' for the dout pin to go low after a new
    void setReverseOutput();                       conversion is started
                                                //reverse the output value

protected:
    void conversion24bit();                        //if conversion is ready:
returns 24 bit data and starts the next conversion //returns the smoothed data
    long smoothedData();                           value calculated from the dataset
value calculated from the dataset
        uint8_t sckPin;                            //HX711 pd_sck pin
        uint8_t doutPin;                           //HX711 dout pin
        uint8_t GAIN;                             //HX711 GAIN
        float calFactor = 1.0;                     //calibration factor as given
in function setCalFactor(float cal)
    float calFactorRecip = 1.0;                  //reciprocal calibration
factor (1/calFactor), the HX711 raw data is multiplied by this value
    volatile long dataSampleSet[DATA_SET + 1];   // dataset, make volatile if
interrupt is used
    long tareOffset = 0;

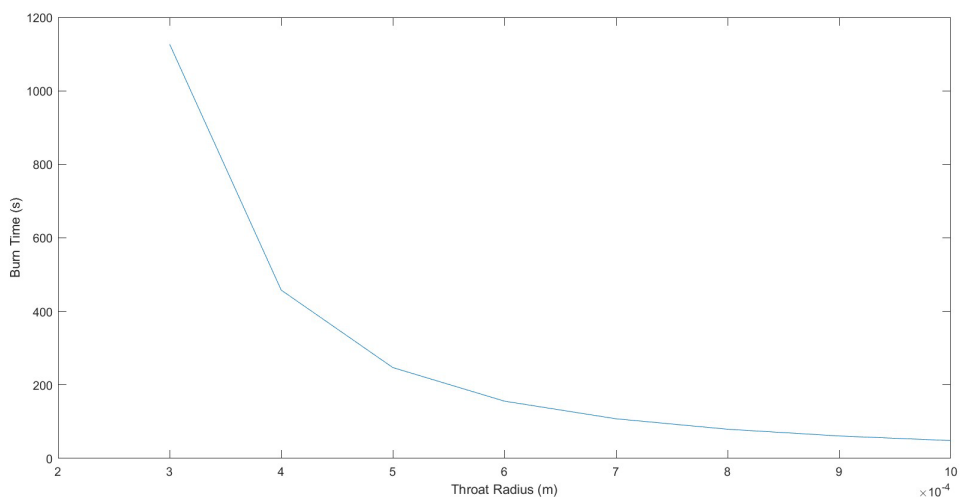
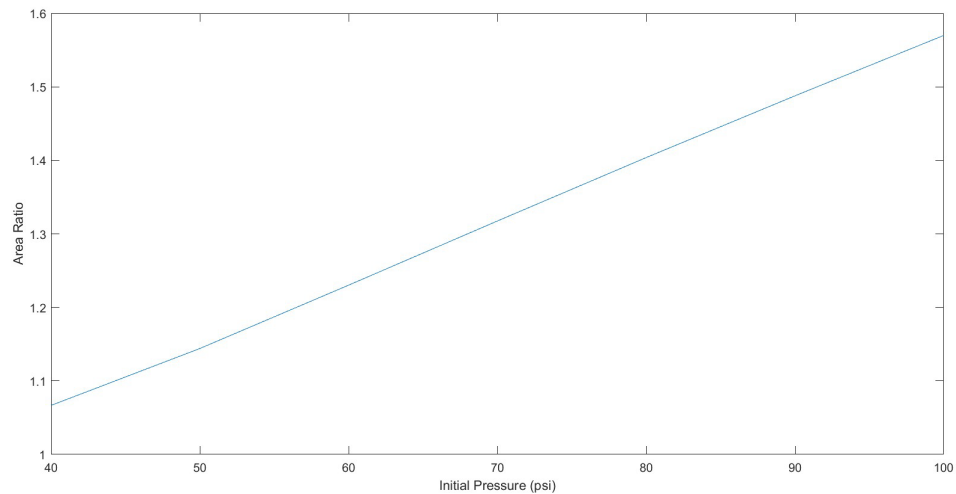
```

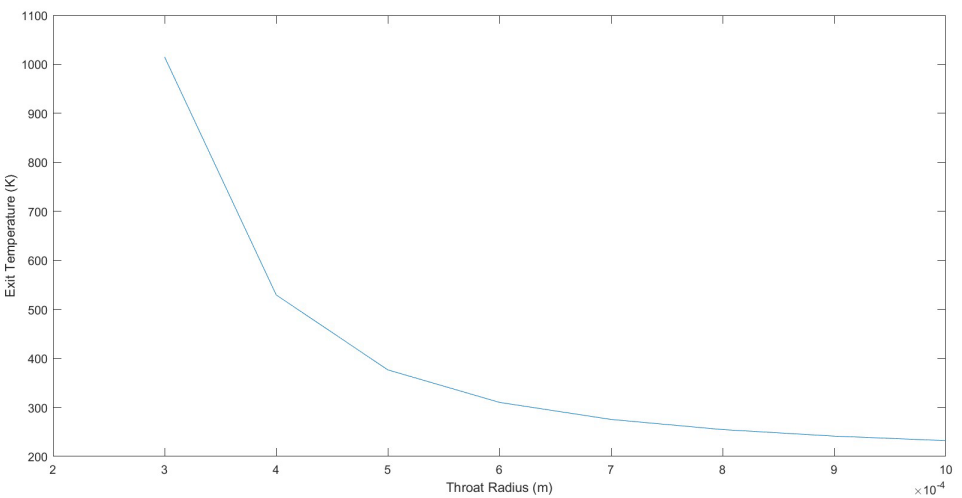
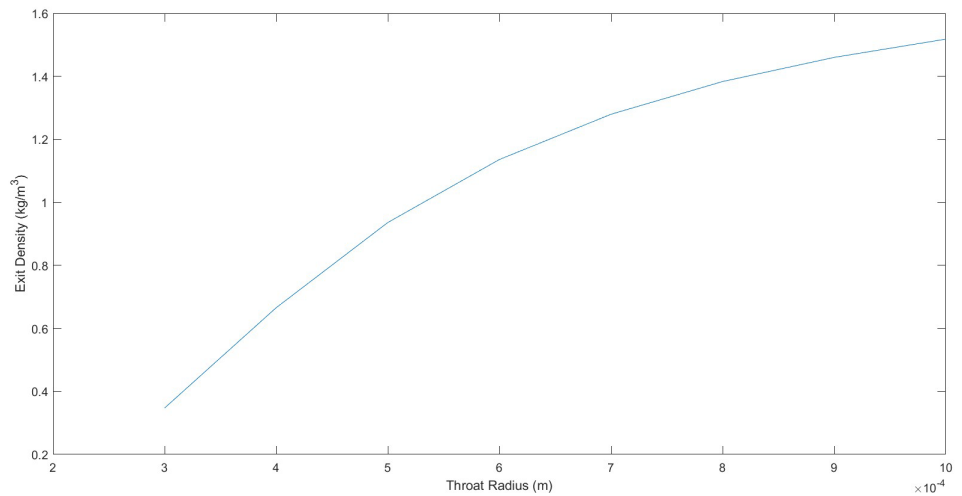
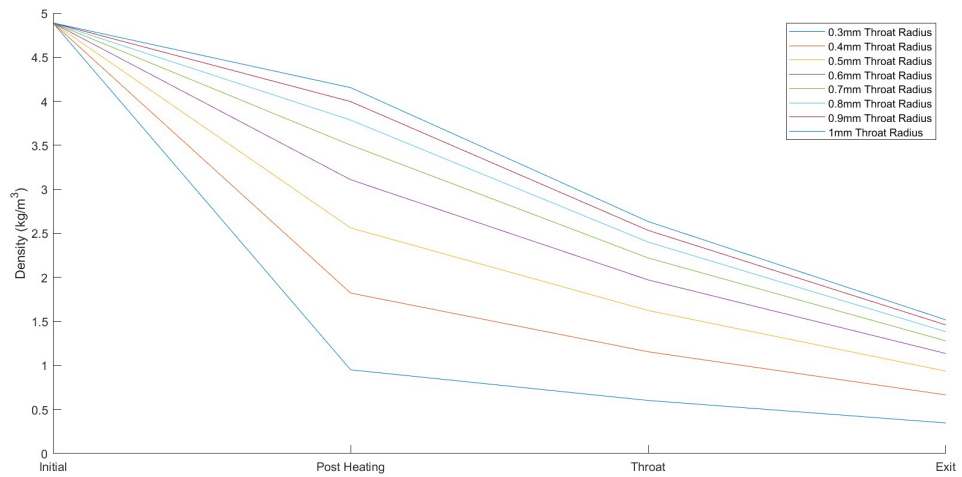
```
int readIndex = 0;
unsigned long conversionStartTime = 0;
unsigned long conversionTime = 0;
uint8_t isFirst = 1;
uint8_t tareTimes = 0;
uint8_t divBit = DIVB;
const uint8_t divBitCompiled = DIVB;
bool doTare = 0;
bool startStatus = 0;
unsigned long startMultipleTimeStamp = 0;
unsigned long startMultipleWaitTime = 0;
uint8_t convRslt = 0;
bool tareStatus = 0;
unsigned int tareTimeOut = (SAMPLES + IGN_HIGH_SAMPLE + IGN_HIGH_SAMPLE)
* 150; // tare timeout time in ms, no of samples * 150ms (10SPS + 50% margin)
bool tareTimeoutFlag = 0;
bool tareTimeoutDisable = 0;
int samplesInUse = SAMPLES;
long lastSmoothedData = 0;
bool dataOutOfRange = 0;
unsigned long lastDoutLowTime = 0;
bool signalTimeoutFlag = 0;
bool reverseVal = 0;
bool dataWaiting = 0;
};

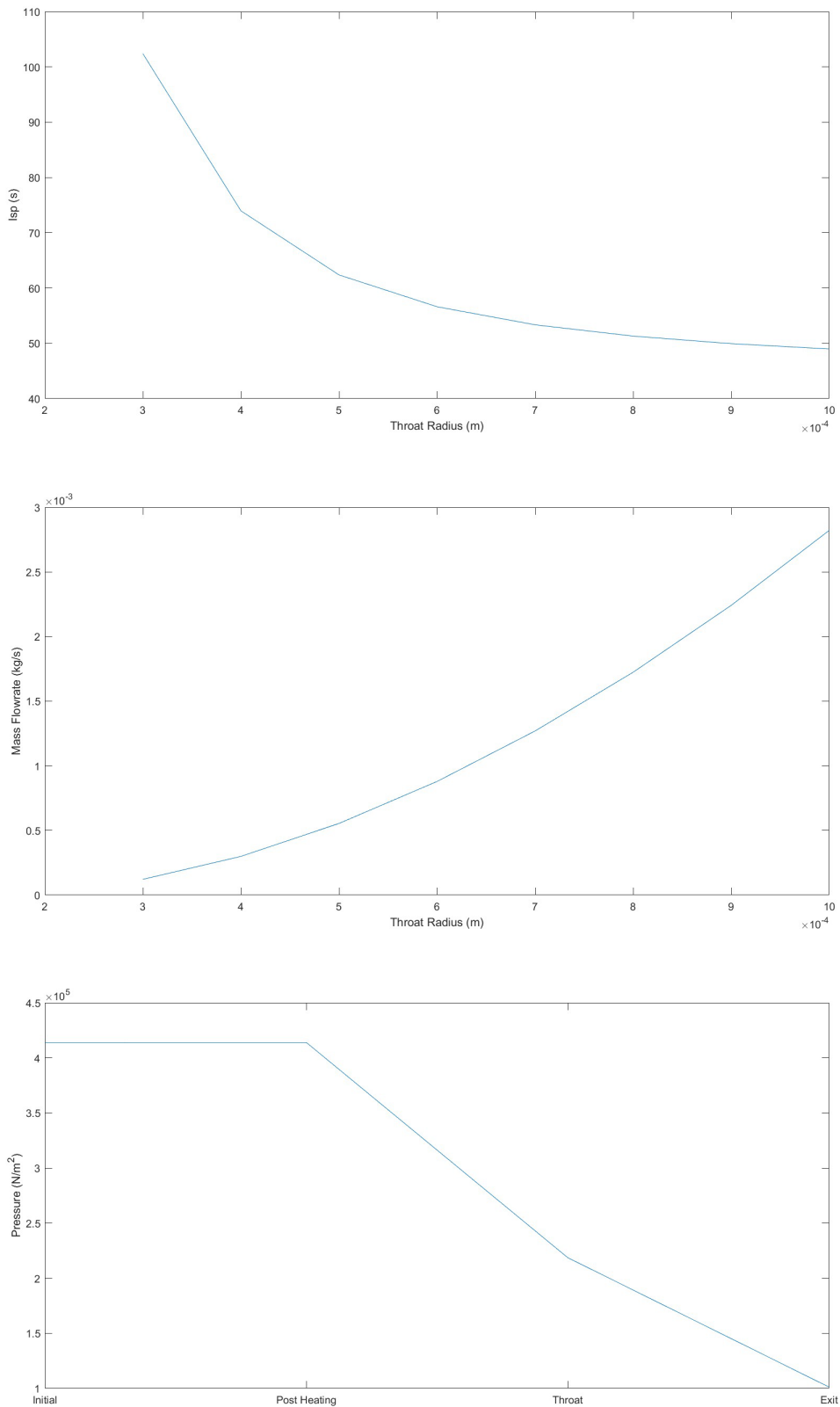
#endif
```

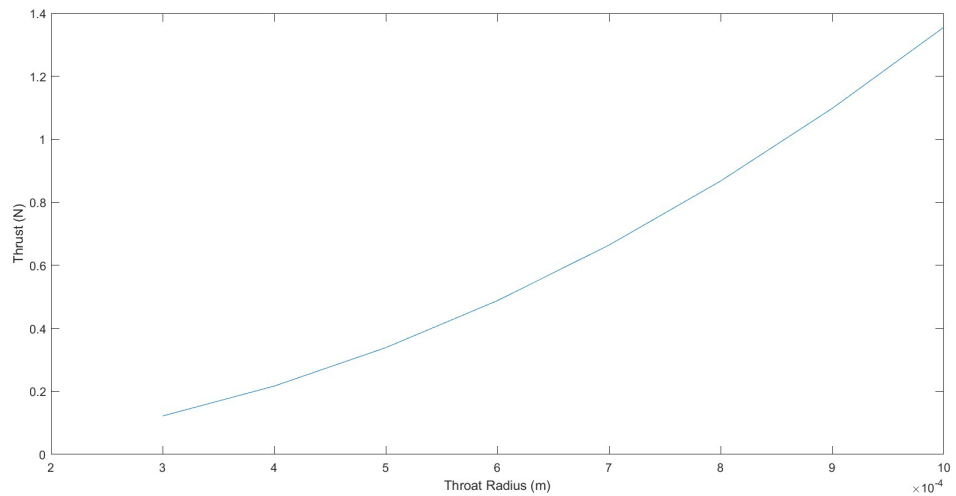
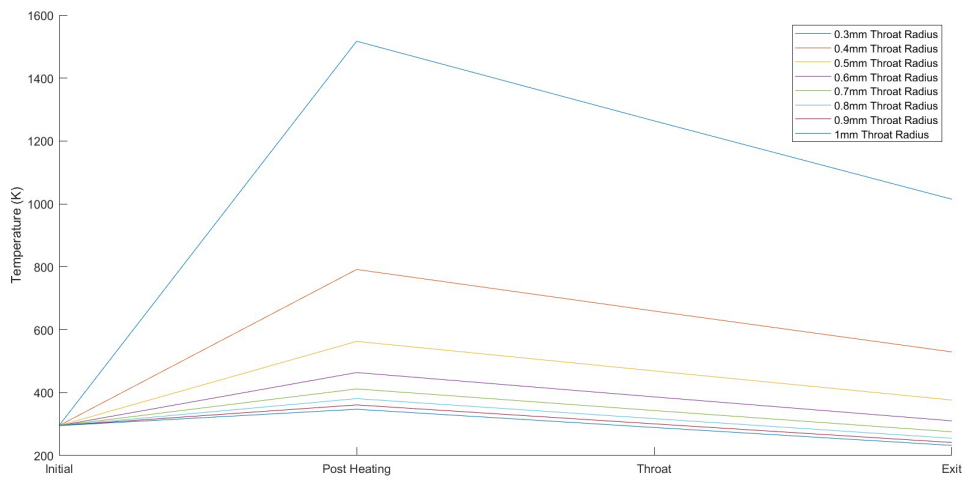
10. Analysis Supplements

Appendix A: MATLAB Plots









Appendix B: Heating Calculations

Heat Transfer Calculations

We assume 1d, steady-state, incompressible. These are poor assumptions but will hopefully give us an order of magnitude estimate.

We also assume perfect insulation on the outer layer (for now). We know that

$$q_r = \frac{\Delta T}{R}$$

so ΔT across each layer can be calculated with

$$\Delta T_{\text{FLUID}} = q R_{\text{FLUID}} \quad \Delta T_{\text{STEEL}} = q R_{\text{STEEL}} \quad \Delta T_{\text{CERAMIC}} = q R_{\text{CERAMIC}}$$

where

$$R_{\text{FLUID}} = \frac{1}{2\pi r_1 h}, \quad R_{\text{STEEL}} = \frac{\ln(r_2/r_1)}{2\pi k_s L}, \quad R_{\text{CERAMIC}} = \frac{\ln(r_3/r_2)}{2\pi k_c L}$$

Everything here is known except h . To find h , we first find Reynold's Number. Assuming $r_f = 0.5\text{mm}$, $c = 400\%$, $\nu = 5 \times 10^{-6}\text{m}^2/\text{s}$ (ν varies largely with pressure, temp), $r = 3.67\text{mm}$.

$$Re_0 = \frac{UmD}{\nu} = \frac{(r_f)^2 CD}{\nu} \approx 15,000 \rightarrow 3300$$

and thermal

The flow is turbulent and has hydrodynamic entry length

$$x = 10D \approx 5\text{cm}$$

The Dittus - Boelter equation gives

$$Nu_0 = 0.023 Re_0^{4/5} Pr^{0.4} = 43.7 = \frac{hD}{k} \rightarrow h = 216 \quad \begin{matrix} \text{stainless steel} \\ \text{porcelain (very largely)} \end{matrix}$$

Using $r_1 = 3.175\text{mm}$, $r_2 = 3.969\text{mm}$, $k_s = 15$, $k_c = 2$,

$$R_{\text{FLUID}} = 0.27, \quad R_{\text{STEEL}} = 0.0018, \quad R_{\text{CERAMIC}} = 0.018$$

So for $q = 100\text{W}$, $T_{\text{fluid}} = 100^\circ\text{C} \rightarrow T_{\text{ceramic}} = 129^\circ\text{C}$

Comparing to flat plate conduction, $R_{\text{FLUID}} < 6$.

Free Convective Losses

$$Ra_0 = \frac{g\beta(T_s - T_\infty)D^3}{\nu} = 55.8(T_s - T_\infty) \approx 10,000$$

$$Nu_0 = \left\{ 0.60 + \frac{0.387 Ra_0^{1/4}}{\left[1 + (0.559 \frac{Pr}{Ra})^{2/3} \right]^{2/3}} \right\}^2 = 4.4$$

$$Nu_0 = \frac{hD}{k} \rightarrow h = 14$$

$$q = hA_s(T_s - T_\infty) = 2\pi RLh(T_s - T_\infty) \approx 0.35(T_s - T_\infty) = 50W$$

Appendix C: Computational Model Calculations

$0 \rightarrow \text{before heating}$
 $1 \rightarrow \text{after heating}$
 $t \rightarrow \text{throat of nozzle}$

Assume P_0, P_1 known!

$\textcircled{1} \quad P = \rho R T \Rightarrow \frac{P}{\rho} = RT \Rightarrow T = \frac{P}{\rho R} \Rightarrow \rho = \frac{P}{RT}$
 $m = \rho A_0 \sqrt{\gamma R T_0}$
 $R = \text{const.}$
 $A_t = A_0 \sqrt{\frac{T_1}{T_0}}$
 $T_1 = T_0 A_{1/2}$

$\textcircled{2} \quad m = \frac{\rho_0 A_0}{1.577} \sqrt{\frac{T_1}{\gamma R \cdot 1.2}} = \alpha Q_1 T_1^{1/2}, \quad \alpha = \frac{A_0}{1.577} \sqrt{\frac{\gamma R}{1.2}}$

$\textcircled{3} \quad q = m [C_V(T_1 - T_0) + \frac{P_1}{\rho_1} - \frac{P_2}{\rho_2}] + \frac{m^3}{2A^2} \left(\frac{1}{\rho_1^2} - \frac{1}{\rho_0^2} \right)$
 $q = m [C_V(T_1 - T_0) + RT_1 - RT_0] + \frac{m^3}{2A^2} \left(\frac{P_1^2}{R^2 T_1^2} - \frac{1}{\rho_0^2} \right)$
 $q = m (C_V + R)(T_1 - T_0) + \frac{m^3}{2A^2} \left(\frac{P_1^2}{R^2 T_1^2} - \frac{1}{\rho_0^2} \right) \xrightarrow[\text{flipped}]{\text{flipped}} \frac{R^2 T_1^2}{P_1^2}$
 $q = \alpha C_P R T_1^{1/2} (T_1 - T_0) + \frac{\alpha^3 Q_1^3 T_1^{3/2}}{2A^2} \left(\frac{P_1^2}{R^2 T_1^2} - \frac{1}{\rho_0^2} \right)$
 $q = \frac{\alpha C_P P_1}{R T_0^{1/2}} (T_1 - T_0) + \frac{\alpha^3 P_1^3}{2A^2 R^2 T_0^{3/2}} \left(\frac{P_1^2}{R^2 T_1^2} - \frac{1}{\rho_0^2} \right)$
 $q = \beta T_1^{1/2} - \beta T_0 T_1^{-1/2} + \xi \frac{R^2 T_1^{1/2}}{P_1^2} - \xi \frac{T_1^{-3/2}}{\rho_0^2}$
 $O = -q + \beta \hat{T} - \beta T_0 \hat{T}^{-1} + \xi \frac{R^2}{P_1^2} \hat{T} - \xi \frac{T_1^{-3}}{\rho_0^2}$
 $O = (\beta + \xi \frac{R^2}{P_1^2}) \hat{T}^4 + (-q) \hat{T}^3 + (-\beta T_0) \hat{T}^2 - \xi \frac{T_1^{-3}}{\rho_0^2}$

Solve for \hat{T} numerically, ~~$T_1 = \hat{T}^2$~~
 $\beta = \frac{\alpha C_P P_1}{R}, \quad \xi = \frac{\alpha^3 P_1^3}{2A^2 R^2}, \quad \alpha = \frac{A_0}{1.577} \sqrt{\frac{\gamma R}{1.2}}$

\hat{T} \rightarrow vector

Then, use $\textcircled{1}$ and $\textcircled{2}$ to find m and ρ .

The area-Mach number relationship is then used to find the exit mach number, and similarly the exit temperature / speed of sound is found to get velocity. Thrust = $m v_e$, $l_{sp} = \frac{1}{2} \rho g$

11. Design Documentation

All attachments in this section are provided as links to Box folders as well as being pasted in due to the length of this document causing the document editing system to crash occasionally when pasting everything in due to volume. The research done to accompany this work was mostly encompassed by the resources provided by the client (Appendix 13), other sources are covered in the main body of the paper under Engineering Analysis and References.

Appendix A: Box Folder Access

See this Box folder for ALL raw files: <https://duke.box.com/s/qz7xdvr5rl00vlhnrzg4droju7zjgjxj>

Appendix B: Meeting and Process Notes/Documentation

Box Link: <https://duke.box.com/s/6kmj6d0qqreqzhtonc655t6bd5eebac1>

This contains all meeting notes, a PowerPoint with weekly updates for the client up until March, and a final doc that summarizes the last sprint of design work and choices.

10/27 Meeting Notes

General tasks

- Heating chamber and nozzle design for 100 kW input
- Also 1 MW and 100 MW input
- Regen cooling system
- Microwave environment modeling in heating chamber → requires background research, modify results of 1 and 2 based on results here
- Prototype
- Aux systems spec
- Launch vehicle spec

NASA proposal

Rocket Thrust Summary Glenn Research Center

Known:

P_t = Total Pressure γ = Specific Heat Ratio
 T_t = Total Temperature R = Gas Constant
 P_0 = Free Stream Pressure A = Area

Mass Flow Rate: $\dot{m} = \frac{A P_t}{\sqrt{T_t}} \sqrt{\frac{\gamma}{R}} \left(\frac{\gamma+1}{2(\gamma-1)}\right)^{\frac{\gamma+1}{2(\gamma-1)}}$

Exit Mach: $\frac{A_e}{A^*} = \left(\frac{\gamma+1}{2}\right)^{\frac{\gamma-1}{2(\gamma-1)}} \frac{\left(1 + \frac{\gamma-1}{2} M_e^2\right)^{\frac{\gamma+1}{2(\gamma-1)}}}{M_e}$

Exit Temperature: $\frac{T_e}{T_t} = \left(1 + \frac{\gamma-1}{2} M_e^2\right)^{-1}$

Exit Pressure: $\frac{P_e}{P_t} = \left(1 + \frac{\gamma-1}{2} M_e^2\right)^{-\frac{\gamma}{\gamma-1}}$

Exit Velocity: $V_e = M_e \sqrt{\gamma R T_e}$

Thrust: $F = \dot{m} V_e + (P_e - P_0) A_e$

(copying from slide 10)
determine T_0 & V_{nozzle} to get \dot{m} , $V_{nozzle} > \text{Mach } 1 \rightarrow \text{get diameter & area from there} \rightarrow \text{extract thrust manually?}$

Mayer's relation allows us to deduce the value of C_V from the more easily measured (and more commonly tabulated) value of C_P :

$$C_V = C_P - nR.$$

This relation may be used to show the heat capacities may be expressed in terms of the heat capacity ratio (γ) and the gas constant (R):

$$C_P = \frac{\gamma nR}{\gamma - 1} \quad \text{and} \quad C_V = \frac{nR}{\gamma - 1},$$

Software needed

- Flow in nozzle, regen cooling passages? – Ansys
- Mechanical stresses – Solidworks?

- Microwaves in heating chamber – COMSOL Multiphysics, VsimEM?
- [Comparison of EM simulation software - Wikipedia](#)
- Start with T0 at 5700 R and p0 at 500ish (goal 800) psi
- Try at 1000 K b/c H2 density info seems to be limited to that from first pass google-ing

The units of the formulas are not making sense, pending asking questions with TA and other resources will go back and get the numbers, for now set up CAD parametrized for throat and exit dimensions (theta_n?)

3D printing the nozzle

- [3D Printed Rocket Engine Parts Survive 23 Hot-Fire Tests - NASA](#)
- [Rapid Analysis and Manufacturing Propulsion Technology - NASA](#)
- We need life constraints to know if this will even work

Manufacturer

- [Laser Directed Energy Deposition \(DED\) Services- RPM Innovations - RPM Innovations \(rpm-innovations.com\)](#) → they have Inconel 625

To read

- [2020_aiaa_ramp_t_multimetallic_compositechambers-final.pdf \(nasa.gov\)](#)

10/31 Meeting Notes

Accomplished:

Weekly Meeting Time: Tuesday, 6:30 PM

Client Meeting Time: Monday, 1:30 PM

All notes, documentation, CAD in Box

Thrust target: 1.5 lbf

What are we going to speak with mentor about next week

Mathematical modeling of system

Present results

This week:

Mathematically model water to H₂ ratio

Modeling thrust, pressure

Decide about simulation software

Ask Harry Xu?

TO DO:

Dadmehr: finish up Maple, consider E&M simulation

Swetha: Engine nozzle params

11/6 Meeting Notes

Meeting with Mr. Hickman

As you use a composite Cp, need a composite R that varies too

Swetha using equations provided by Hickman to find possible nozzle key dimensions

Density = pressure/(RT)

- Does ideal gas law apply here?
- Probably close enough
- Other equations that we've been using are built on ideal gas law

Swetha's dimension estimates look fairly accurate

- Higher pressure --> smaller throat diam
- Increase temp --> increase ISP and exhaust velocity, decrease pressure

These things are fairly small since thrust level is so low

Typical Microwaves are about 60% efficient

Be wise to think in small steps, then progress. Need to make it as practical as possible

Fused quartz windows holds up to high temperatures

Microwave company: RFHIC

Pick a temperature below the melting point of the material so we don't have to deal with regenerative cooling

- What happens to the tensile strength of the material at operating temperature

TO DO:

- Validate equations – Send to Mr. Hickman, he will check to see if we're going in the right direction. Numbers look good!
- Implement MATLAB function to sweep through engine parameters
- Microwave heat characterization experiment. What is the absorption rate of microwaves into water?

What kind of other component-level tests could we do? Nozzle flow test? Heat absorption? Pressure burst test? Something else?

4 phase testing approach;

- Phase 1 is our prototype
- Phase 2-4 is NASAs money, higher powers

Part of the proposal: currently available microwaves. To make technology realistic, this is what microwave technology would need to be developed

Manufacturing methods

- 3D printed – Noah talk to Pat
- Lathe for nozzle

11/07/23

- Set up a Gantt chart to establish timeline
- Decide point people, person who reaches out to testing engineering
 - Aerospace Corporation --> Alejandro Assael
 - RFIT (Korea) --> Derrick Roseman
- Look into software for E&M simulation
- Shane to communicate to Robert about point of references
- Work on project memo due this Friday
- Focus on researching core subsystems of a rocket engine
 - Split subsystems amongst the team
- Write up an email to Harry about moving forward with the project (Shane)
- Make system level diagram for engine
- Noah to sweep through parameters from Swetha's calculations
- Find further resources on rocket engine design

Preliminary Gantt Chart

- Submit design to the Aerospace Corp by the end of the year/semester (Dec.20)
 - Status presentation for senior design – Dec.7
 - Include what we're making and what we are planning to test

11/14

To Do:

- Talk about newest bob email
 - What new technologies will improve ERTP?
 - Which one is most realistic?
 - Has ERTP been used at scale?
 - ERTP vs. Microwave Propulsion (DPTP)
 - Development subgroup ideas?
 - No, put down large idea first
 - Creating a presentation for 11/20 (volunteers?)
 - Anyone not here on monday for fall break?
- Greg Twiss email – Shane Send it DONE

11/28/2023

- Continue working on presentation for Robert, including all the findings we have made so far in both propulsion methods
- Work on design criteria
- Start working on calculations to determine efficiency of our nozzle design

Make a decision on which ERTP method we want to move forward with:

- 1.) Use the exhaust heat from the Radioisotope Thermoelectric Generator (RTG) to heat up our propellant and produce desired thrust
- 2.) Use both the exhaust heat and electricity produced by the RTG to produce desired thrust
- 3.) Heat from the RTG (liquid hydrogen is heated up) and chemical reaction is produced from dual propellant system

12/4

Meeting Agenda for Delagrammatikas/Twiss Call

1. Summarize proposal
 - a. Design main propulsion system to transport humans from Earth orbit to Mars
 - b. Complete analysis work for Dual Propellant Microwave Electro Thermal Propulsion (DPMETP) concept proposed by client, Robert Hickman
 - c. Create in-depth system design, including analysis on propulsion system key parameters, materials requirements, and modeling of microwave propagation + heat transfer
 - d. Develop relationships with two companies to provide microwave generator and testing facilities for full system test
 - e. **Deliverable: submit a proposal in May 2024 to NASA with analysis and path toward a prototype**
2. Progress
 - a. Team has learned a great deal about in-space propulsion methods, including DPMETP
 - b. Met with Robert Hickman 5 times to discuss learning, roadblocks, etc.
 - c. Discovered implausibility in DPMETP system concept, pivoting to Electric Resistance Thermal Propulsion (ERTP)
3. Big questions
 - a. How should we scope this project? It is unrealistic to create a fully-fledged propulsion system given our time, money, and resource limitations
 - b. What do you think is an appropriate deliverable for this project?
 - i. We are aware that we are required to produce a physical product – how can we drive our work toward this while also focusing on the full system design?
 - ii. Any novel design cannot be physically prototyped (material, cost constraints)
 1. Is a proof of concept with inferior materials sufficient?
4. Secondary Questions (if time allows)
 - a. How much time should we dedicate to each stage of development?
 - b. How long does the certification process take (NASA proposal)?

NOTES

- 1) Twiss --> Objectively it is a very difficult problem to scope. Try breaking it down to subsystems and showing the feasibility of a subsystem (maybe try the heat converter). This subset should be functional or semi-functional.
- 2) Twiss --> Try a non-functional mock-up of what a complete system could look like --> at different temperature and pressure. It should prove that we considered tradeoffs. Modelling, machining, 3D Printing.
- 3) Both of these have their own challenges
- 4) Dr. D --> we have a very large vision that is absolutely unachievable in the time and money given. Our goal is not to go to mars, but to show the feasibility of a potential technology/technique. Look for “some deflection somewhere, some thrust somewhere, anything that shows an output for the technology” OR that it does not work and that it is not-feasible
- 5) Noah --> is it better to go for a scaled-down but complete system or to go after a small subsystem and get that to work
- 6) Dr. D --> Start with a subsystem and try to make it work. If it doesn't work, you can make more of a “mock” subsystem and if it does you can expand your design to another subsystem
- 7) Dr. Twiss --> A prototype does not have to function, it just has to clarify the engineering problems in a given problem. Yes it is satisfying to build something and make it work, but there is work you can do that moves the technical ball forward that does not actually function.
- 8) Noah --> We are not familiar with what kind of packaging constraints we would have. For example, we do not know the dimensions of our final build. We have no way of saying if what we design would work.
- 9) Dr. Twiss --> yes but whatever you do will be enhanced by analysis and it will be complimented with little test results and data collected along the way. WHITEPAPER OR PAPER STUDY are very common and they do make progress finding the technical challenges and issues with a design/problem. However, you need to balance this with doing work that satisfies you as a team of engineers. We want you to be excited to work on this. There will be empirical testing, analytical solutions, design work, a blend of all these elements.
- 10) Noah --> two logistical questions. A) what is the budget? (\$2000) and B) regarding criteria, are we looking to set those for the whole thing or for each individual subsystem? How do we know how to measure or define the work we've done?
- 11) Twiss --> you can spend weeks finding the perfect scope and defining perfect criteria, but at this point I would pick something that you collectively think is interesting and you commit to it.
- 12) Dadmehr --> how novel does what we do have to be?
- 13) Both professors --> you don't have to invent anything; it does not have to be novel. Given your scope, there will be lots of pure reuse of past designs and technologies. The novel part can be its application in this technology.

Path

- Large scale architecture
- Small scale architecture
- Small scale design - jan
- Small scale manufacturing - feb
- Small scale testing - march

1/19

- Make the schedule the enemy for the scope
- Generally keep the client in the loop as much as possible on scheduling, time, and progress made each week
- End of last semester feedback
 - o Scope had cleaned up pretty well
 - o Make sure to review it and make sure it's still doable with fresh eyes
 - Confirm that client is on board with the scope and schedule
 - o Clarify what the full-scale system architecture
- Not a bad idea to consider just the heat exchanger/resistive heater
- Talk to Santillan about space for building the prototype
 - o Make it as compressible as possible
- Revise the Gantt chart as needed
- Have the scope written out clean and clear so that we can say it off the top of our heads
-

To dos

- Report 1 (Feb 2nd)
- Hammer out the scope
 - o Maybe constrain to test bed for the heat exchanger
- Figure out how much time we want to devote to this project
 - o Noah – unknown
 - o Shane – after spring break is really busy
 - o Ale – mostly free
 - o Swetha – about same as a regular class, but flexible
 - o Daniel and Derrick – a little bit more than class commitment
 - Productivity based on engagement
- Set a workday meeting
 - o Thursday 5-9 at the colab

1/25

FAST Diagram

Convey functional requirements – don't determine design outcome

Tank system

- Charge tank
- Bleed tank
- Build pressure

HX

- Combust
 - Microwave
 - Contain pressure
- Nozzle system
- Create sonic conditions at throat
- Sensors
- Voltage/current for heating element
 - Gas pressure/temp
 - Tank pressure
- Valves
- No back flow

Burn time

- Look at reasonable working pressure from commercial tanks
- Then look at volumes that are available
- OPTION 1: What's available/will fit in workspace?
 - Buy it: safer
 - Pat has compressed helium
- OPTION 2: Or – need certain amount of seconds, how much initial volume/pressure to maintain

Heating elements → expensive commercially, build it

Client meeting

Proposal: Part A (3 page, high level)

Physical Product:

- 1N
- 30s burn
- Buy tanks, buy heating element
- Design and manufacture the heat exchanger
- Design and manufacture test stand
- How to measure thrust?
 - Aerospace corp. uses pendulum with everything on the platform
- Combine pressure tank, HX, nozzle for thrust test
- Assume release to ambient
 - In reality it would release to vac

2/15

PLAN GOING FORWARD

We will divide into two groups:

1. Focused on modeling
 - a. Dadmehr
 - b. Shane
 - c. Derrick
2. Focused on building
 - a. Noah
 - b. Swetha
 - c. Ale

Continue full team meetings on Thursday

- Catch up on progress
- Work on reports

Each system will meet at least once a week separate from the rest of the team

Location:

- We have a key to Hotz's lab
- Prefer to move to Garage lab. Is there a compressed air hookup?
 - o Swetha will check if there is compressed air

Deliverables:

- "Engine" that produces thrust
- Test stand capable of measuring thrust, pressure, temperature
- Model with correlation to test data

Key Dates

- Final Report: 4/22
- Presentations 4/15
- All data collected and model complete by 4/1
 - o Based on 3/4 data and correlation, make changes to build final setup
 - o Thrust measurement test stand
 - o Conduct testing and collect all data
- Presentation 3/4
 - o Present pressure, temperature data from current test setup
 - o Present preliminary with correlation to data we're getting
 - o Calculate theoretical thrust from current setup, and state what changes we'll make to hit our thrust target if there are any
- All initial data by late night Sunday 2/25

- 2/22
 - o Test Setup Complete
 - Thermocouple plug problem
 - Analog sensors for this setup to have steady state data
 - o Modeling
 - Generic computational model of system
 - MATLAB file that can keep track of key variables given design parameters and test parameters

Ideas to calculate volumetric flow rate

- Fill a balloon over a known period of time
- Buy an airflow sensor
- Buy a car airflow sensor
- Use a piece of sawdust with a ruler, put it in the flow stream, analyze video to measure airspeed
- Sensitive force meter right in front of the air flow

Ways to measure thrust

- Pendulum
- System on wheeled cart. String to force gauge. Measure pulling force
- System on scale. Fire engine up, measure increase in weight
- Beam bending

First Test Testing Plan

Three stage testing plan to investigate

Stage 1: Proof of concept for data collection

- *Source of gas*
- *Way of measuring initial pressure*
- *Way to measure temp and pressure at exit*
- *Measure flow rate*
- *Can this setup stand up to higher temp and pressure?*

Stage 2: Introduce the Nozzle

Stage 3: Introduce heating

Set gas --> compressed air

Get properties: R, rho, specific heat ratio

Set temperature difference across the heating section

Figure out how much power and heating coil temperature for coil to make the temp difference

Coil can take 1500 W, 2100 F ~ 1420 K (rounded down)

Set operating pressure in heating section (capable of 4 bar gage)

Further calcs/modeling to find temp, pressure, Q anywhere in the system (Dani's MATLAB)

Sensing

- Thermocouple before heating
 - ~~Pressure before heating~~
 - Flow meter before heating
 - Thermocouple after heating
 - Pressure after heating – done but check for temp
- Make CAD of the setup for future reference – side job

Force measurement from the jet (until nozzle machined/printed)

Spitballing considerations

- 2 4-way Swagelok junctions?
- Flowmeter acquisition
- Nozzle params reacquire
 - Pending constraints:
 - Fluid
 - Operating pressure before nozzle
 - Operating temperature before nozzle
 - VOLUMETRIC/MASS FLOW RATE
- BACKFLOW SENSORY CAPABILITY
- Eyeballed volumetric flow

2/22

Goals from last week

- Test setup completed – NOT met
- Generic model complete – met

Things to do to actually get the two physical tests done
(heated test without nozzle, nonheated with nozzle)

- Thermocouple and DAQ
- Various nozzles printed

Modeling next steps

- Figure out density change across heating section

Worked on report 2 for the rest of the time – brainstorming report

3/7

Agenda:

- 2 week plan for build and modeling
- ~~Geometry thing for the nozzle~~
- Aerospike consideration
- Send the current nozzle out for machining via Xometry? -- NO
- ~~Report 3 planning~~

Next deliverables

- Transients on the computational model?
- High temperature part replacement
- Nozzle building plan
- Thrust measurement plan locked in
- ~~Rao nozzle length equation applied to conical nozzle~~

New idea: pulsed heating and release – not implemented

3/21

Objectives

- HEATED TEST
 - Parameters
 - Input pressure
 - Tube temp
 - Nozzle throat dia and expansion ratio
 - Measurements
 - Air speed
 - Inlet temp
 - Outlet temp
 - Wall temp
 - Optional: pressure

Things to change on build 1

- Power supply for heating system → Noah
- Metal nozzle / aerospike
 - Throat dia and expansion ratio ranges
 - Print first, then pick one and machine
 - GET AEROSPIKE CAD → due Monday
- Decide on
 - Pressure sensors, analog/digital
 - Price cap
 - Remove?
- Get rid of rubber stoppers
- Decide on FoS for heating temperature: start at 50%, move up to 75%

Testing protocol

- Go with the flow

Looking forward

- Thrust measurement
 - Direct
 - Weight offset
 - Deflection
 - Calculated from other measurements
 - Which one is the most practical and FASTEST
 - Make sure it's robust
- 7/16-20 for female end? of the Swagelok, figure out adapters needed to fit thermocouple in

Timeline

- Power supply for heating system → Noah

- End of meeting 3/28
- All nozzles printed by Apr → Swetha
 - 1st Email by 3/22
 - 4/2 EOD
- Thrust measurement decision → Ale
 - EOD 3/28
- Nozzle candidate STLs
 - Wall temp modeling by 3/28 → modeling
 - Maybe start up and shutdown times?
- Ordering new thermocouples + appropriate fittings?
 - 3/22

Last Sprint

- Decided on analog sensors due to time constraints
- Manufactured two sets of nozzles (v3 and v4) on high temp resin, found major error in CAD that led to dimensions not linking up to equations which led to the v4 nozzles print
- Threw out the aerospike based on time constraints
- Decided on horizontal frictionless movement system for thrust measurement
- Power supply for heating developed and implemented
- Thrust stand manufactured and implemented
 - T slot sleeve bearings replaced with linear rails for less friction
 - New mating plate designed for these and implemented
 - This still was not enough, so the back of the stand was lifted up to put the entire system at an angle sufficient to allow free sliding (~8 degrees)
- Modeling checking height change effects, cleaning up the model for report out

Appendix C: Ideation Process CAD

Box Link: <https://duke.box.com/s/1kcbfodeaoxbwr077d6npp5xhqjdznb1>

This shows draft nozzles, which include optimized ones (Rao nozzles, which have parabolic expanding sections) instead of conical shapes, as well as first passes at a heat exchanger concept (cylinders with through holes of a set diameter).

Figure 1 shows a Rao nozzle developed by manually marking the focus of the expanded section parabola, and then connecting lines to create the outline of the curve (this is shown in Figure 2). Figure 3 shows a screenshot of an idea for the heater structure, where fuel would flow through the holes in the cylinder, and Figure 4 shows an idea for a nozzle with internal cooling channels, which ended up not being needed.

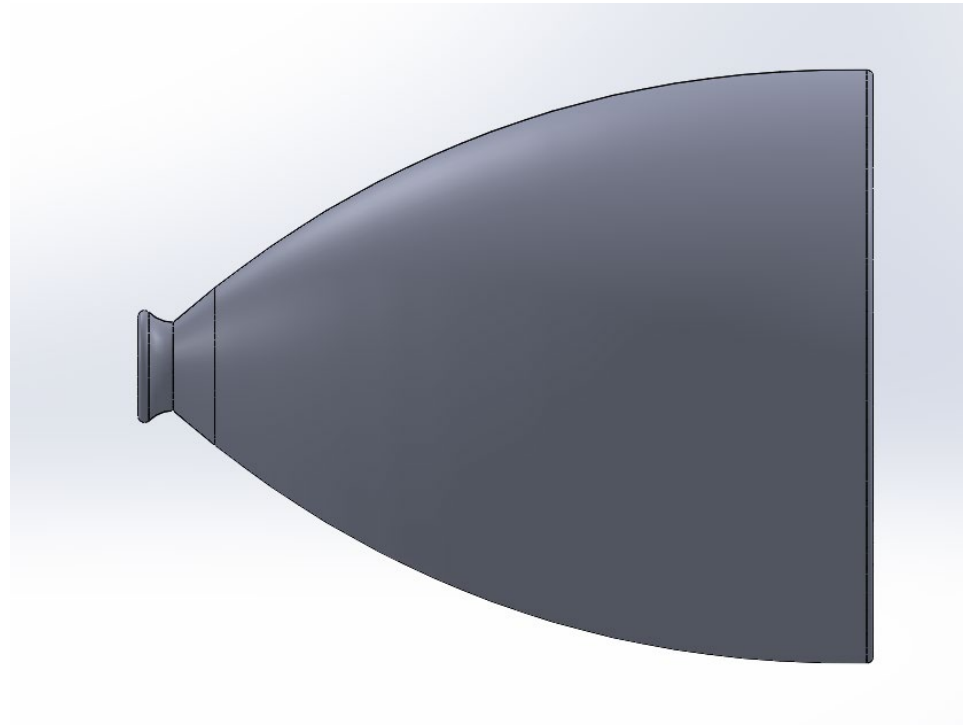


Figure 1: 13 Point Interpolation-Based Rao Nozzle

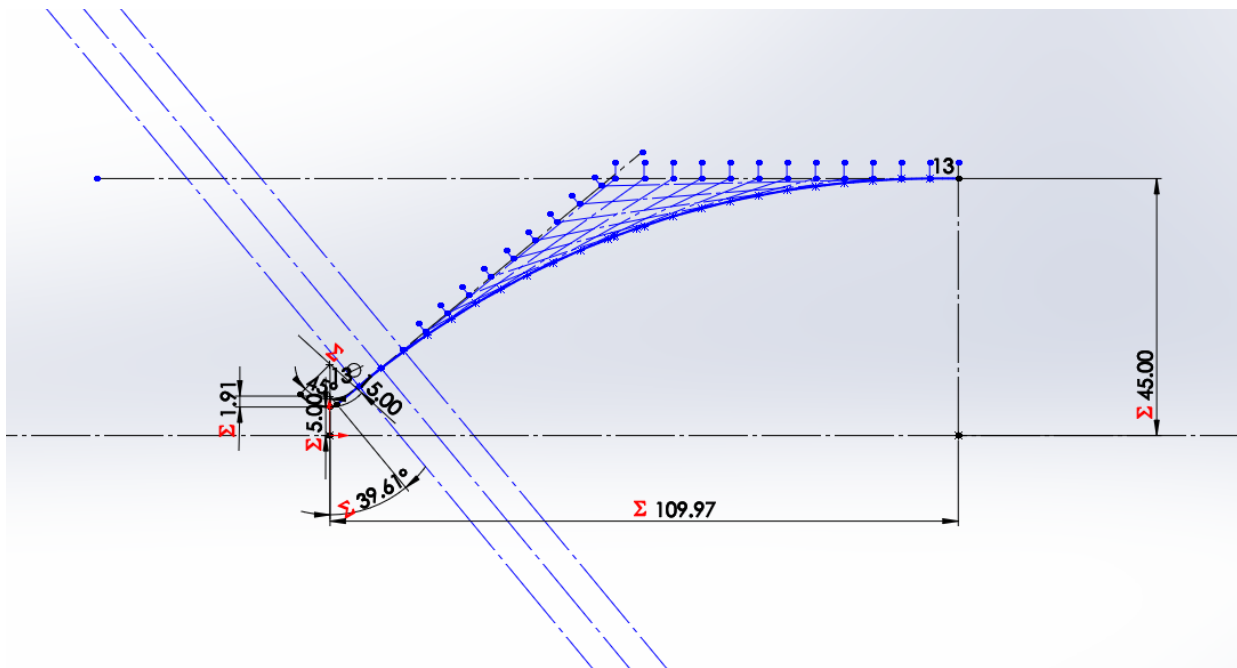


Figure 2: Sketch Basis of 13 Point Rao Nozzle

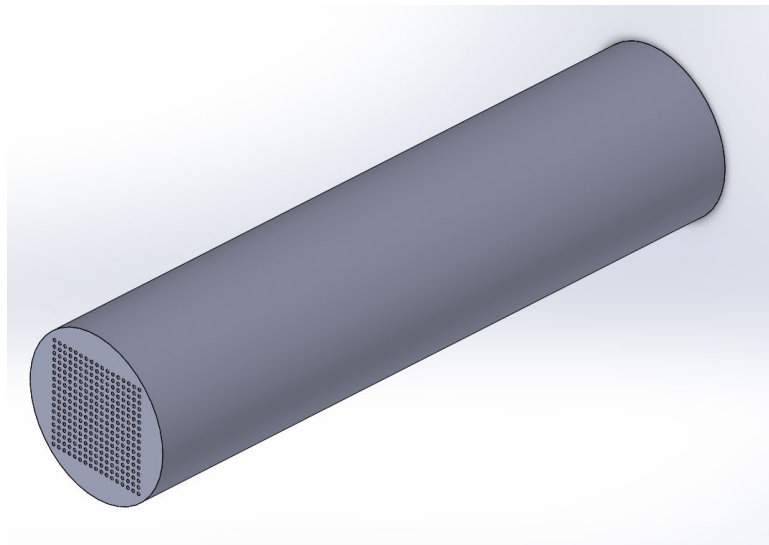


Figure 3: Draft Heater Structure

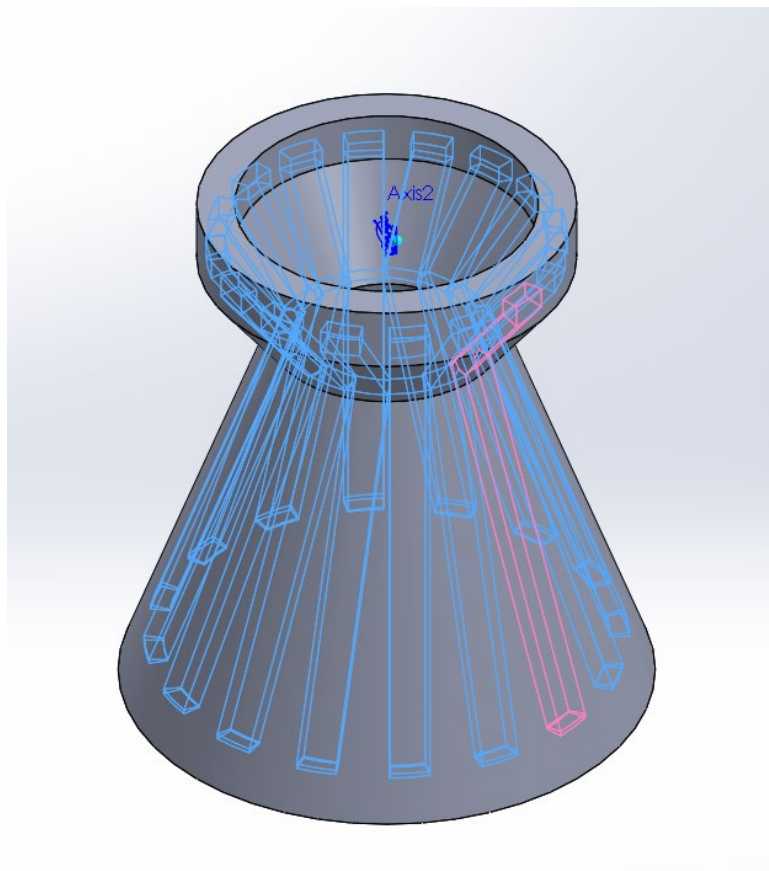


Figure 4: Draft Nozzle with Cooling Channels

Appendix D: Ideation Calculations

Box Link: <https://duke.box.com/s/6ugkou9anmaxind3ezkuqi4fsgx1rw4l>

This shows the first pass calculations done before the computational model was developed. The spreadsheet holds various calculations for Ideation CAD parameters, and the Maple worksheet shows the beginnings of the math behind the computational model.

Figure 1: Maple Worksheet

>

All units in this Maple are in metric [kg, m, sec, Kelvin, J, N, Pa]. H_r represents the heating ratio (ratio of H₂₀ to hydrogen mass flow rates)

Engine Parameters (Design Inputs)

> $F_{thrust} := 0.907188$

$$F_{thrust} := 0.907188 \quad (1)$$

> $H_{ratio} := 0.15$

$$H_{ratio} := 0.15 \quad (2)$$

> $T_{chamber} := 2500$

$$T_{chamber} := 2500 \quad (3)$$

> $P_{chamber} := 1.013 \cdot 10^6$

$$P_{chamber} := 1.013000000 \times 10^6 \quad (4)$$

> D_{nozzle} is the unknown

$$D_{nozzle} \text{ is the unknown} \quad (5)$$

> $D_{exit} := D_{nozzle} \cdot 10$

$$D_{exit} := 10 D_{nozzle} \quad (6)$$

10 here is arbitrary and should be replaced by the dimensions of the ideal nozzle

Gas Constants Modelled over Temperature

> $C_{p_H}(T) := 2.46 \cdot 10^{-3} \cdot T + 28.8$

$$C_{p_H} := T \mapsto \frac{2.46 \cdot T}{10^3} + 28.8 \quad (7)$$

> $C_{p_{H20}}(T) := 0.0922 + 3.96 \cdot 10^{-5} \cdot T - 4.18 \cdot 10^{-9} \cdot T^2$

$$C_{p_{H20}} := T \mapsto 0.0922 + \frac{3.96 \cdot T}{10^5} + \frac{(-1) \cdot 4.18 \cdot T^2}{10^9} \quad (8)$$

> $C_{p_{comb}}(T) := C_{p_H}(T) \cdot (1 - H_r) + C_{p_{H20}}(T) \cdot H_r$

$$C_{p_{comb}} := T \mapsto C_{p_H}(T) \cdot (1 - H_r) + C_{p_{H20}}(T) \cdot H_r \quad (9)$$

> $\gamma_H(T) := 1.42 - 3.46 \cdot 10^{-5} \cdot T$

$$\gamma_H := T \mapsto 1.42 + \frac{(-1) \cdot 3.46 \cdot T}{10^5} \quad (10)$$

> $\gamma_{H20}(T) := 1.33333$

$$\gamma_{H20} := T \mapsto 1.33333 \quad (11)$$

$$> \gamma_{comb}(T) := \gamma_H(T) \cdot (1 - H_r) + \gamma_{H20}(T) \cdot H_r$$

$$\gamma_{comb} := T \mapsto \gamma_H(T) \cdot (1 - H_r) + \gamma_{H20}(T) \cdot H_r \quad (12)$$

Equations Used For Determining Nozzle Diameter



Rocket Thrust Summary

Glenn
Research
Center

Known:

p_t = Total Pressure	γ = Specific Heat Ratio
T_t = Total Temperature	R = Gas Constant
p_0 = Free Stream Pressure	A = Area

Mass Flow Rate: $\dot{m} = \frac{A^* p_t}{\sqrt{T_t}} \sqrt{\frac{\gamma}{R}} \left(\frac{\gamma+1}{2} \right)^{-\frac{\gamma+1}{2(\gamma-1)}}$

Exit Mach: $\frac{A_e}{A^*} = \left(\frac{\gamma+1}{2} \right)^{\frac{\gamma+1}{2(\gamma-1)}} \frac{(1 + \frac{\gamma-1}{2} M_e)^{\frac{\gamma+1}{2(\gamma-1)}}}{M_e}$

Exit Temperature: $\frac{T_e}{T_t} = (1 + \frac{\gamma-1}{2} M_e^2)^{-1}$

Exit Pressure: $\frac{p_e}{p_t} = (1 + \frac{\gamma-1}{2} M_e^2)^{-\frac{\gamma}{\gamma-1}}$

Exit Velocity: $V_e = M_e \sqrt{\gamma R T_e}$

$$\boxed{\text{Thrust: } F = \dot{m} V_e + (p_e - p_0) A_e}$$

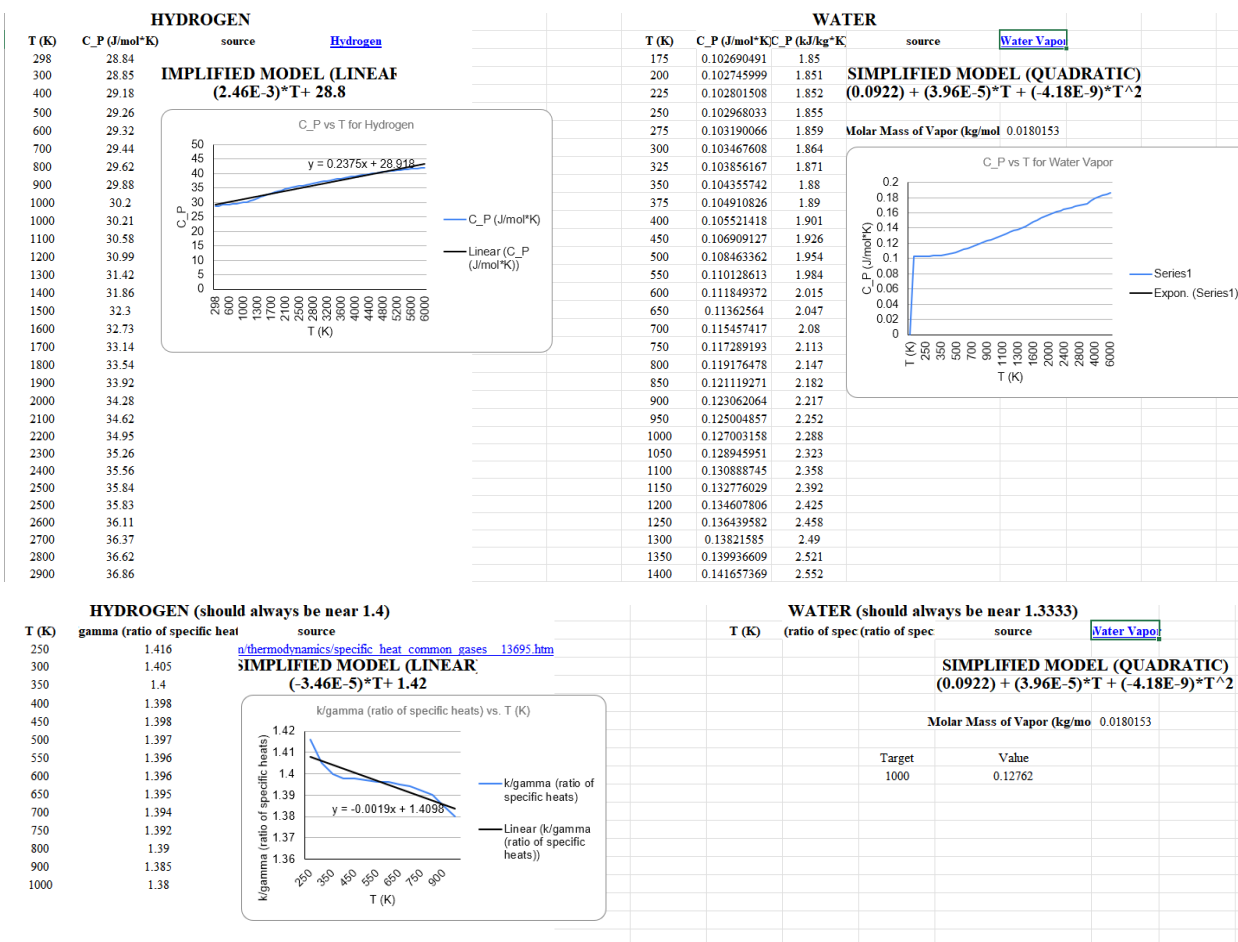
$$> m_{flow} := \frac{P_i \cdot \left(\frac{D_{nozzle}}{2} \right)^2 \cdot P_{chamber}}{\sqrt{T_{chamber}}} \quad m_{flow} := 15912.16679 D_{nozzle}^2 \quad (13)$$

$$> M_{exit_{NASA}} := \text{solve} \left(\left(\frac{P_i \cdot \left(\frac{D_{exit}}{2} \right)^2}{P_i \cdot \left(\frac{D_{nozzle}}{2} \right)^2} \right)^{-\frac{(\gamma_{comb}(T_{chamber}) + 1)}{2 \cdot (\gamma_{comb}(T_{chamber}) - 1)}} \right. \\ = \left(\frac{(\gamma_{comb}(T_{chamber}) + 1)}{2} \right) \cdot \left(1 \right. \\ \left. + \left(\frac{(\gamma_{comb}(T_{chamber}) - 1)}{2} \right) \cdot M_{exit}^2 \right)^{-\frac{(\gamma_{comb}(T_{chamber}) + 1)}{2 \cdot (\gamma_{comb}(T_{chamber}) - 1)}} \cdot \left(\frac{1}{M_{exit}} \right), M_{exit} \right)$$

$$\begin{aligned}
 M_{exit_{NASA}} &:= RootOf\left(-\left(\frac{4667}{4000} - \frac{17H_r}{200000}\right) - \frac{-233350 + 17H_r}{2(-33350 + 17H_r)} \left(1 + \frac{667}{4000} - Z^2\right. \right. \\
 &\quad \left. \left. - \frac{17}{200000} - Z^2 H_r\right) - \frac{-233350 + 17H_r}{2(-33350 + 17H_r)} + 100 - Z\right) \quad (14) \\
 > V_{exit_{mach_{NASA}}} &:= \\
 &\text{Error, invalid assignment} \\
 > V_{exit_{mach_{NASA}}} &:=
 \end{aligned}$$

Figure 2: Nozzle Design Parameters – Spreadsheet Screenshots

Heating volume	0.347303	m ³		L	2	m		
q_dot	1511.648	W/m ³		D_all	0.5	m		
Temp diff achievable	143.9665	K		d	0.01	m		
Power required	7658.033	W		Power	525	W		
Current required	106337.6	A		Temp difference	2100	K	hypothetical goal, assuming 1000 to 3100	
Voltage required	0.072016	V		number of tubes	289			
				k of heating volume	21	W/(m ² *K)	HfC, estimate	Ablation resistance and thermal conductivity of carbon/carbon composites containing hafnium carbide - ScienceDirect what-is-hafnium-carbide.pdf (langenfeldmetallic.com)
				Resistivity	0.00000195	Ohm meters	HfC, estimate	
				Mass flow rate	0.0001	kg/s	estimate, fill in manually	



12. Final Budget

Appendix A: Purchased Materials Budget

Table 1: Compiled Purchases

Item Description	Use Case	Price	Amount	Total Cost	URL
Dry Moly Lube	Used with the linear sleeve bearings to try and lower friction, ended up not being used with the linear rails that replaced the bearings	\$15.29	1	\$15.29	CRC 3084 Dry Moly Lube, (Net Weight: 11 oz.) Dark Gray, Original Version: Power Tool Lubricants: Amazon.com: Industrial & Scientific
T Slot Sleeve Linear Bearings	First attempt at making low friction linear motion in the thrust stand, replaced later with linear rails	\$64.85	4	\$259.40	T-Slotted Framing, Sleeve Bearing for 1" High Rail, 1 Flange, 1-7/8" Long, Silver McMaster-Carr
Fiberglass Insulation Sheet	Acquired to address natural convection and radiation heat losses from the nichrome wire, not used	\$31.68	1	\$31.68	Fiberglass Insulation Sheet, for Ovens and Furnaces, 1" Thick x 24" Wide x 8 Feet Long McMaster-Carr
JB Weld	Attempt at sealing wood blocks from having air go through the grains, wood was being used to pre-emptively address concerns of excess conduction through the stainless steel pipe	\$8.68	4	\$34.72	Amazon.com: J-B Weld High Heat Epoxy Syringe, Dark Grey : Industrial & Scientific
Kiln Furnace Coil Wire	Failed first attempt at buying coiled wire off the shelf	\$16.49	1	\$16.49	uxcell Heating Element Coil Wire AC220V 1500W / AC110V 375W Kiln Furnace Heater Wire 5.8mm*560mm 5PCS - Amazon.com
3/8" Ceramic Sleeving	Planned to be used to limit heat transfer from the coils to the environment, decided not to use	\$20.89	1	\$20.89	No-Irritation Ceramic High-Temperature Sleeving, 3/8" ID McMaster-Carr
1/4" Ceramic Sleeving	Used to insulate the coils from the pipe so that the current doesn't short straight through the stainless steel pipe	\$19.38	1	\$19.38	No-Irritation Ceramic High-Temperature Sleeving, 1/4" ID McMaster-Carr
Screw-in Thermocouples	To measure temperature at the beginning and end of the heating section, screw-in required to be able to effectively seal the joint where thermocouples are introduced to the system	\$52.74	1	\$52.74	EGT Thermocouple for Exhaust Gas Temp Probe with Exposed Tip & Connector K Type: Amazon.com:

					<u>Industrial & Scientific</u>
Nichrome 80 wire, 20 gauge	Used as a resistive heating element to convert electrical power supplied by the variac into thermal energy to be supplied to the fluid	\$9.99	1	\$9.99	Nichrome 80-50' - 20 Gauge Wire - 50ft - 0.81mm - 0.032in - Made in USA - Master Wire Supply: Amazon.com: Tools & Home Improvement
Gusset Corner Bracket	Used as a 90 degree connector for t-slots rails where the extra support from the gusset was needed	\$9.97	16	\$159.52	Silver Gusset Bracket, 1" Long for 1" High Rail T-Slotted Framing McMaster-Carr
Single T-Slot Rail, 1" x 1"x 6'	Actual t slot rails used to build the supporting structure for the heating rig and build the thrust stand	\$34.03	7	\$238.21	T-Slotted Framing, Single Four Slot Rail, Silver, 1" High x 1" Wide, Solid McMaster-Carr
Corner Bracket	Used as a 90 degree connector for t slot rails in tight fits as well as where the gusset wasn't needed	\$7.92	4	\$31.68	Silver Corner Bracket, 1" Long for 1" High Rail T-Slotted Framing McMaster-Carr
High Pressure Regulator	To be able to regulate pressure between 0 and 200 psi	\$43.50	1	\$43.50	Amazon.com: Viair Inline Air Pressure Regulator, 0-200 psi, Black, 90150 : Tools & Home Improvement
350 mm Linear Rails	To allow the thruster apparatus to move linear independently of the rest of the thrust stand structure with low friction	\$42.99	2	\$85.98	350MM Linear Rail 2PCS HGR15 Linear Guide Rail HGH15 Linear Slide Rail with 4PCS HGH15CA Carriage Slider Block CNC Kit: Amazon.com: Industrial & Scientific
3D Printed Nozzles, 100psi and 150 psi versions	Printed using Formlabs High Temp v2 resin, cost is based on Bluesmith printing service charges	\$23.73	1	\$23.73	Bluesmith 3D Printing Service (duke.edu)
3x3 Right Angle Surface Corner Bracket for T Slot	Used to create a flat surface for the force sensor to make contact with	\$11.60	4	\$46.40	T-Slotted Framing, Silver Corner Surface Bracket for 1" High Single Rail McMaster-Carr
Ceramic screw terminals	For connecting between the nichrome wire and the electrical power supply wires	\$1.42	2	\$2.84	uxcell 2 Way Ceramics Terminal Blocks High Temp

					<u>Porcelain Ceramic Connectors 21.5x19.5x14.2mm for Electrical Wire Cable 5 Pcs: Amazon.com: Industrial & Scientific</u>
	Running Total		\$1,092.44		-

13. Client Provided Resources

Appendix A: Rocket Science 101

The DPMP concept can be scaled to mega W power levels provided by either solar arrays or nuclear reactors. If DPMP is paired with nuclear, then the reactor can be designed with much lower operating temperatures and pressure. Then most of the reactor and DPMP components can be built with existing technology. I'm not aware of any life limiting components for the DPMP concept.

This type of propulsion system can also be used as an upper stage for lunar transport or to inject a payload into a highly elliptical orbit from LEO. I would envision a spacecraft with a large solar array or a nuclear reactor that would connect to a payload in LEO carrying the required propellant tanks and then transport the payload to the appropriate transfer orbit using DPMP. The space vehicle with the solar arrays or nuclear reactor would then return to LEO to rendezvous with the next payload. To minimize required propellant this craft could use aerobraking to transit to LEO

Designing a DPMW Thruster

Heating Chamber Design

The heating chamber should be designed to produce a resonate cavity with maximum EM concentration just ahead of the nozzle. This will depend on the design and modeling of the microwave system and the wave propagation. This will occur latter in the year. The chamber dimensions can be arbitrarily selected now and refined later.

Recent development of solid state microwave sources permit transmission of the microwaves directly to the heating chamber via coaxial cable to an antenna protruding into the heating chamber rather than by wave guides.

Nozzle Design

The area of the nozzle throat (A_t) is the most important dimension in the engine design. It is selected to produce the desired mass flowrate (m). The maximum propellant flow rate is related to the available electrical power (P) by ($m = P/c_p$) The mass flow rate m is the product of the throat area A_t times the velocity (V) and density of the propellants. We know the propellant velocity at the throat will be at Mach 1. The speed of sound $c = (g_c * k * R * T_t)^{.5}$ where g_c is the gravitational constant, k is the ratio of specific heats and T_t is the temperature at the throat in degrees R. T_t can be calculated as $T_0 / (1 + (k-1)/2) * M^2$ where M is the Mach #) and equal to 1.

The nozzle wall geometry immediately upstream of the throat determines the distribution of gas properties at the throat. Constant-radius arcs are used for the shape of the throat-approach wall. Fortunately the exact design of the curves inside the combustion chamber do not require any kind of "optimum" shape analysis. Prior to reaching the throat, the flow is relatively low speed (subsonic). A gently arcing wall with a radius of curvature of similar magnitude to the throat radius is usually sufficient to prevent excessive losses. A small radius is desirable both for minimum overall length and for minimum wall area exposed to the high heat fluxes associated with flow near Mach 1.

For a given area ratio, maximum nozzle efficiency within a given length is obtained by using a sharp-corner (zero-radius) transition between the upstream radius and the supersonic contour. A downstream wall radius 0.4 times the throat radius usually is a good compromise between fabrication difficulty and minimum nozzle length.

A more rigorous approach is needed for the design of the supersonic (diverging) section than the converging section of the nozzle to minimize separation and turbulent losses. As the nozzle area increases the temperature and pressure of the effluents will decrease while the velocity and Mach # increase. The area ratio (A_r) is the ratio of the nozzles exit area (A_e) divided by the area of the throat. The local Mach number is related to this value by

$$A_r = (((1+((k-1)/2)*M^2)/(1+((k-1)/2)))^{(k+1)/2(k-1)})/M$$

The speed of sound is decreasing with increasing nozzle area as the temperature decreases. $T = T_0/((k-1/2)* M^2)(A_t)$ The actual exit velocity can then be calculated as $V_e = M*(gc*k*R*T)^{.5}$. The following chart shows V_e as a function of A_r for a DPMW thruster.



As the area ratio is increased the Isp increases but the size and weight of the nozzle increases. The selected A_r is a compromise between the two.

One approach to the shape of the diverging nozzle is to use a conical design, as shown below. Conical nozzles expand linearly from the throat with a half-angle (α) generally ranging between 12-18 degrees. While these nozzles are relatively easy to manufacture, they have several downsides. At the nozzle exit plane a component of flow velocity is not aligned with the vehicle's thrust vector. This component is skewed by an angle of α , which decreases the overall efficiency of engine.



The efficiency for conical nozzles is plotted below. A typical 15-degree conical nozzle has an efficiency of about 98%

Rocket Science 101(condensed)

The science of rocketry stems from the laws of motion developed by Isaac Newton in 1687. The equation establishing force as the product of mass times acceleration ($F = ma$) essentially translates to you can apply force to a vehicle by accelerating mass out the backend at high speed. It wasn't until 1903 that a Russian named Konstantine Tsiolkovski developed an equation to relate Newton's laws to rockets. This has become what is known as the Rocket Equation. This will be described later under vehicle sizing.

Still there didn't seem to be many practical applications for rockets until Robert Goddard showed up. He is considered the father of modern rocketry. In 1934 he developed the first liquid fuel rocket, but perhaps more importantly, he applied a converging /diverging nozzle to the design which increased the theoretically efficiency of rockets from 2% to 95% (to be discussed later). He published papers on rocket travel through space and human travel to the moon. His work was thoroughly trashed by the New York Times who claimed Goddard didn't understand basic physics in that there's nothing to push against in a vacuum. In 1969 as Apollo 11 was on its way to the moon, the New York Times printed a correction, but the damage had been done. Despite proving the New York Times wrong by conducting experiments in a vacuum chamber, Goddard was unable to attract more research funds. Rocket science in the U.S. was effectively dead.

A young German named Werner Von Braun was next to advance rocketry. He was a big fan of Goddard and read everything he wrote. He developed the first modern rocket called the V2. After World War II, Von Braun and a large portion of his team transitioned to the U.S. where they lead many of America's rocket development efforts including the Redstone and Saturn vehicles.

All rockets generate thrust by expelling gas at high velocity. There are basically two ways of doing this. One is by generating ions that are accelerated by a magnetic field. This is known as ion propulsion. To date, it has very high efficiency in terms of specific impulse, but very low thrust.

The other is thermal propulsion. This entails heating a gas in a chamber and allowing it to expand through a converging diverging nozzle. If the back (exit) pressure is low enough in relationship to the chamber pressure the gas will accelerate through the nozzle to achieve sonic velocity (the speed of sound) at the throat of the nozzle. It can't go any faster. To achieve sonic flow at the nozzle the ratio of the chamber pressure (P_0) divided by the pressure at the throat (P_t) must be above the critical condition. This is defined as :

$$P_t/P_0 < (2/(k+1))^{(k/k-1)}$$

where k is the ratio of specific heats (c_p/c_v).

The gas will then expand in the diverging nozzle to achieve supersonic speeds. To analyze this concept a momentum analysis was performed on the control volume shown in Figure 1.

While increasing the pressure above the critical condition won't increase the velocity of the gas above Mach 1. It will increase the density of the gas and consequently the mass flow rate. This is an important factor in determining the thrust produced by the engine.

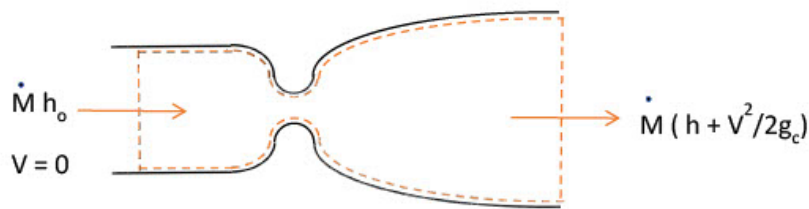


Figure 1

Assuming the flow is steady, one dimensional, and adiabatic an energy balance gives:

$$h_0 = h + V^2/2g_c$$

Assuming the fluid is a perfect gas then:

$$h - h_0 = c_p(T - T_0)$$

Where h_0 is the initial enthalpy in the chamber,

h is the enthalpy at the exit plane,

V is the velocity at the exit plane,
 c_p is the specific heat of the exhaust products in the chamber,
 T_0 is the temperature in the chamber,
 T is the temperature at the exit plane

Now, we can relate the stagnation temperature (T_0) to the temperature and velocity downstream by:

$$V = (2g_c * c_p * T_0 * (1 - T/T_0))^{.5}$$

Note: Much of the discussion is conducted in English units, however the equations should work with either English or SI units if the correct units and unit conversions are used. For example in the above equation c_p is usually expressed in Btus/lb. To use the equation c_p needs to be multiplied by 778 to convert from Btus to ft-lbs. In other words:

$$V = (2g_c * c_p * 778 * T_0 * (1 - T/T_0))^{.5}$$

Assuming, T/T_0 is small then:

$$V_{max} = (2g_c * c_p * T_0 * 778)^{.5}$$

The 778 was added to convert from BTUs to ft-lbfs.

This is the maximum exit velocity that can be achieved by the rocket with a nozzle of infinite exit area. Obviously this is not possible to build a nozzle like this, but nozzles achieving 95% of this value can be designed and built. Exhaust velocity (V_e) is the primary measure of rocket efficiency.

The exhaust velocity divided by the gravitational constant (V_e/g_c) generates a quantity known as specific impulse (isp). This term quantifies the force (lbf) that will be produced by the one

pound (lbm) of propellant in one second. The unit of measure is in secs. In SI units Isp is also measured in secs.

Different propellants will produce different levels of Isp. The most efficient propellant combination is LH₂/LO₂. At currently available temperatures it has an Isp of approximately 455 secs. Another common propellant combination is RP1/LO₂ (Isp = 340). It has the advantage over LH₂/LO₂ in that the RP1 is much denser than LH₂ permitting smaller lighter tankage. Hypergols are a class of highly toxic propellants that ignite on contact. This produces a very reliable engine particularly when multiple starts are involved. Solid rockets have low Isp (240 secs), but can generate a very high level of thrust. They are usually used to get a heavy vehicle stack moving after ignition.

There are a number of ways to heat the propellant in the chamber. We have been discussing Chemical Thermal Propulsion (CTP) in which the propellants are heated by an exothermal chemical reaction. This form of propulsion is limited by the specific heat of the exhausted propellants. LH₂/LO₂ is the best propellant combination available for CTP. The exhaust product is H₂O which has a specific heat of .75 BTU/lbm.

A much higher exhaust velocity can be achieved with a propellant with a higher c_p . Hydrogen gas has the highest c_p and can achieve an exhaust velocity of 36,000 ft./sec if heated to 6000 °R, equating to an Isp of 1129 secs. The question is how to heat the hydrogen. Arc gas thrusters have been developed using hydrogen but have very limited thrust and are not very energy efficient. The gas can alternately be heated by passing it through a nuclear reactor (Nuclear Thermal Propulsion). This approach can generate reasonably high Isp (900 sec) and high thrust levels (15,000 lbs). This requires the entire reactor to be able to withstand the temperatures and pressures of the expended propellant. In the case of NASA's latest NTP endeavor this is 5700 °R and 800 psi. This is a very challenging goal.

Another way to heat a gas is with microwaves. Microwaves can heat a gas in two ways. The first is to heat free electrons to cause a plasma discharge. The propellant is then passed through and heated by the plasma discharge. This has been the approach used on almost all Microwave electro-thermal thrusters. However, the plasma can not form if the pressure is above 30 psi. This results in a very low density effluent and consequently very low thrust. The maximum thrust that has been achieved under laboratory conditions is 250 mN.

The second way to heat a gas with microwaves is using molecular rotation resulting from dielectric heating. This is the technique used in microwave ovens. Unfortunately, this only works on polar molecules. H₂ and most other paired gasses such as O₂, N₂ are non-polar.

In the Dual Propellant Microwave Propulsion (DPMP) concept a polar gas is mixed with hydrogen allowing the composite gas to be heated with microwaves. H₂O is a polar molecule. Water can be added to the hydrogen either directly as H₂O or as LO₂ where it will combust with the hydrogen to produce water. When mixed with hydrogen it decreases the combined c_p of the gas mixture to be heated by the microwaves. If the percentage of H₂O is below 15%, Isps exceeding 1000 can still be achieved. With scalable thrust levels.

The DPMP concept was developed by Robert Hickman and patent application was submitted in 2023 (US Application 18/192,144).

The DPMP concept is shown in Figure 2. LH₂ is pumped into the heating chamber. The pressure is selected to achieve sonic flow in the throat and ensure proper expansion in the nozzle and achieve the desired thrust levelxx. The hydrogen itself can not be heated by microwaves because it is a non polar molecule. Either H₂O or LO₂ is pumped into the heating chamber through an injector where it mixes with the hydrogen. If LO₂ is used, it reacts with a portion of the hydrogen to produce water. The composite gas can be heated by microwaves.

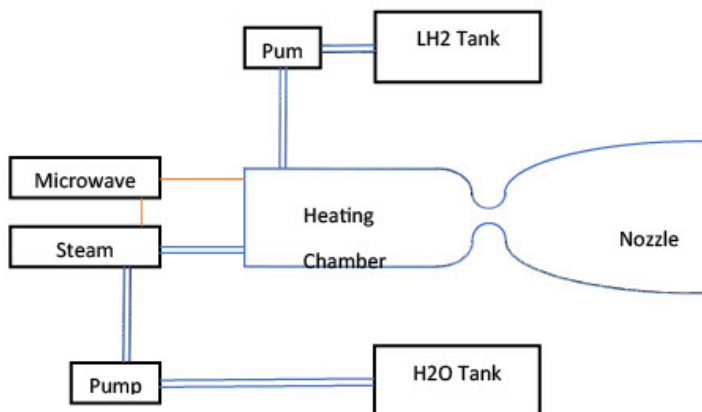


Figure 2.

The c_p for H₂ at 6500 °R is 4.5 Btu/lbm and for water the c_p at this temperature is 0.75. If O₂ is added to the H₂ as 10% of the mass then the composite c_p is 3.94. This produces a maximum exhaust velocity of 35,800 ft/sec that translates to an Isp of 1112 secs.

The table below shows how the c_p , Isp, and Thrust/Megawatt changes as the percent of O₂ increases. The Isp decreases and the thrust increases. Similar results are achieved for the percentage of H₂O, except for the values for Thrust/MW will be lower. In the case of energy from the LH₂/LO₂ reaction is heating the composite gas and reducing the amount of microwave heating required. Consequently use of O₂ results in a higher Thrust/MW as compared to H₂O.

% O ₂	10	20	30	40	50
Cp	3.94	3.48	3.03	2.575	2.11
Isp	1112	1046	975	899	815
Thrust/MW	38	43	49	57	68

This temperature was selected because it represents the upper limit in temperature that can be sustained by modern materials such as Ultra High Temperature Ceramics (UHTC). If the propellants are used to perform regenerative cooling of the heating chamber then the operating temperature could be further increased. This will result in a higher effective Isp.

The achievable thrust can easily be scaled up or down based on the available electrical power. Assuming an 80% heating efficiency and 10% O₂, 3.8 lbf of thrust can be produced with a 100 KW solar array. Using 50% O₂ the thrust would increase to 6.8 lbf

In comparison NASA was developing ion propulsion for transport to Mars. Hall thrusters provide the most capable solution in terms of available thrust. The most advanced of these appears to be the X3 program. In 2017 they conducted a test using 102 kW that generated 1.1 lbf of thrust with an Isp of 1800 secs. To date it has been difficult to scale ion thrusters above this thrust level. At a comparable power level the DPMP concept would produce 3 to 6 times the thrust to electrical power ratio.

While the Hall thruster produces better Isp than the DPMP concept, it suffers from life limiting erosion at higher power levels. The X3 was scheduled to perform a 100 hour life test in 2018. I can find no report that that was achieved. To perform a Mars mission will require thousands of hours of continuous operation for an ion engine.

It appears in Design Architecture 5, NASA has replaced Ion propulsion with NTP as their baseline.

An

engineer by the name of G.V.R. Rao came up with a design to improve upon the conical nozzle. The resulting wall contour is based on a "skewed parabola." The length of a Rao nozzle is typically defined to be 80% of the length of a 15-degree conical nozzle with the same expansion ratio. This results in a shorter and lighter nozzle. The parabolic contour reduces the flow exit angle, as compared to a conical nozzle. This helps to align the flow exit velocity with the vehicle's thrust vector and increases nozzle efficiency.

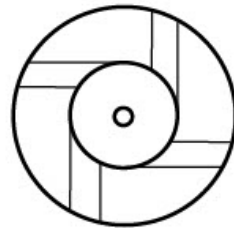
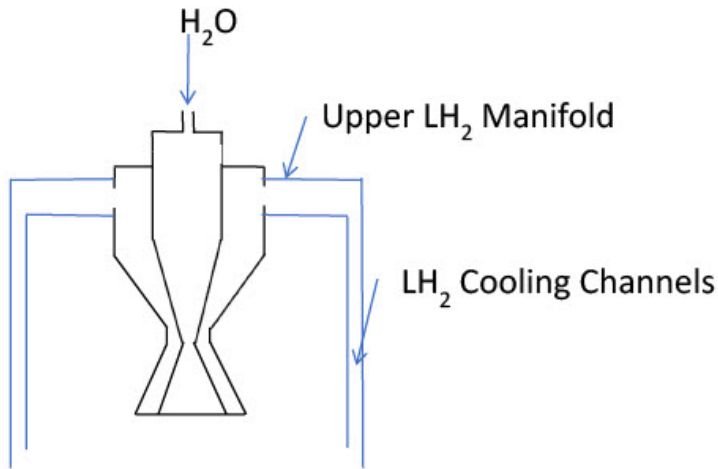
Regenerative Cooling

To achieve maximum performance of the thruster, the exhaust gas must be heated to very high temperatures exceeding the melting point of most material. For example the Space Shuttle Main Engines (SSMEs) combustion chamber and throat were constructed from NARloy-Z. This material melts at 1000 degrees Kelvin, yet the operating environment exceeds 3600 degrees Kelvin. In order to withstand this harsh environment, the combustion chamber must be constructed from a material with excellent heat conduction characteristics and a high melting point, but also incorporate a regenerative cooling system to prevent the materials from melting or losing structural integrity. Cryogenic hydrogen enters the aft manifold and flows into a set of coolant passages evenly dispersed around the nozzle and chamber's circumference.¹ As coolant flows through these channels toward the nozzle injector, thermal conductivity allows heat to pass through the walls of the chamber and be carried away by the extremely cold hydrogen. This design needs to maintain the wall at a temperature below its melting point while simultaneously increasing the enthalpy of the hydrogen as it is routed into the combustion chamber. Design of a regenerative cooling system requires a thermal analysis that simultaneously solves three equations, the transfer of heat from the exhaust gas to the channel wall, the heat transfer from the channel wall to the coolant and the heat conducted between the hot wall and cold wall. For more details on how to perform this analysis the student is referred to:

<https://www.ijert.org/research/thermal-design-and-analysis-of-regeneratively-cooled-thrust-chamber-of-cryogenic-rocket-engine-IJERTV2IS60264.pdf>

Injector Design

In the DPMW thruster the Hydrogen and water propellants must be mixed. A simple way to accomplish this is with a co-axial injector design such as shown in the following figures. The first figure shows hydrogen flowing from the regenerative cooling system up the channel walls to a manifold at the top of the heating chamber where it enters the outer chamber of the injector. The second figure is a cross section showing swirl vanes to impart a swirl to the hydrogen gas this helps mixing with the H₂ but also concentrates the hotter gasses in the center and cooler gasses near the chamber walls. H₂O is injected in the center chamber of the injector.



Vehicle Sizing

The size of a vehicle stage is determined by the required change in velocity or Delta V (D_V) produced by the stage and the propellants used. The maximum D_V velocity produced by a vehicle is established by the rocket equation as follows:

$$D_V = V_e * \ln(M_0/M_f) = Isp * g_c * \ln(M_0/M_f)$$

where:

Isp is the specific impulse in dimension of secs,
 g_c is the gravitational constant,

M_0 is the initial total mass, including propellant, a.k.a wet mass
 M_f is the final total mass without propellant, a.k.a. dry mass.

To size a vehicle stage, decide the Delta V you want the stage to produce and with the Isp of the engine you can calculate M_0/M_f . At first it would seem that you could design any number of stages to meet these conditions until you realize M_0 includes not only the wet mass of the stage but also the weight of the payload (P). M_f is equal to the weight of both the dry weight of the stage (S) and the payload (P). Without performing detailed design and structural calculations you can get a pretty good estimate of the stage mass fraction or Mass ratio (R) by looking at comparable vehicles. The mass fraction of a stage is $R = F/(S+F)$ where F is the weight of the fuel and S is the dry weight of the stage excluding the payload. For large stages using RP1/LO₂ as a fuel the mass fractions are about .93 for stages using LH₂/LO₂ the mass fraction is about .89. This is due to the lower density of LH₂. Smaller stages have lower mass fractions due to volume versus weight relationships. After a few algebraic manipulation this results in:

$$F = (P - P/C) / (1 + (1/RC) - (1/R))$$

Where C = Exp(D_v / (Isp * g_c))

Given the desired D_v, R, and P you can calculate F, M₀, M_f, S, and F.

To achieve orbit most vehicles are multi-stage. This is due to the fact that a single stage vehicle has to carry the entire dry weight of the vehicle to the final D_v while a multi-stage vehicle is dropping significant weight as it goes. To size a multi stage vehicle decide on the D_v split between the stages and then start calculating the weight of the upper stage. For the next stage the P includes both the weight of the actual payload plus the wet mass of the upper stage.

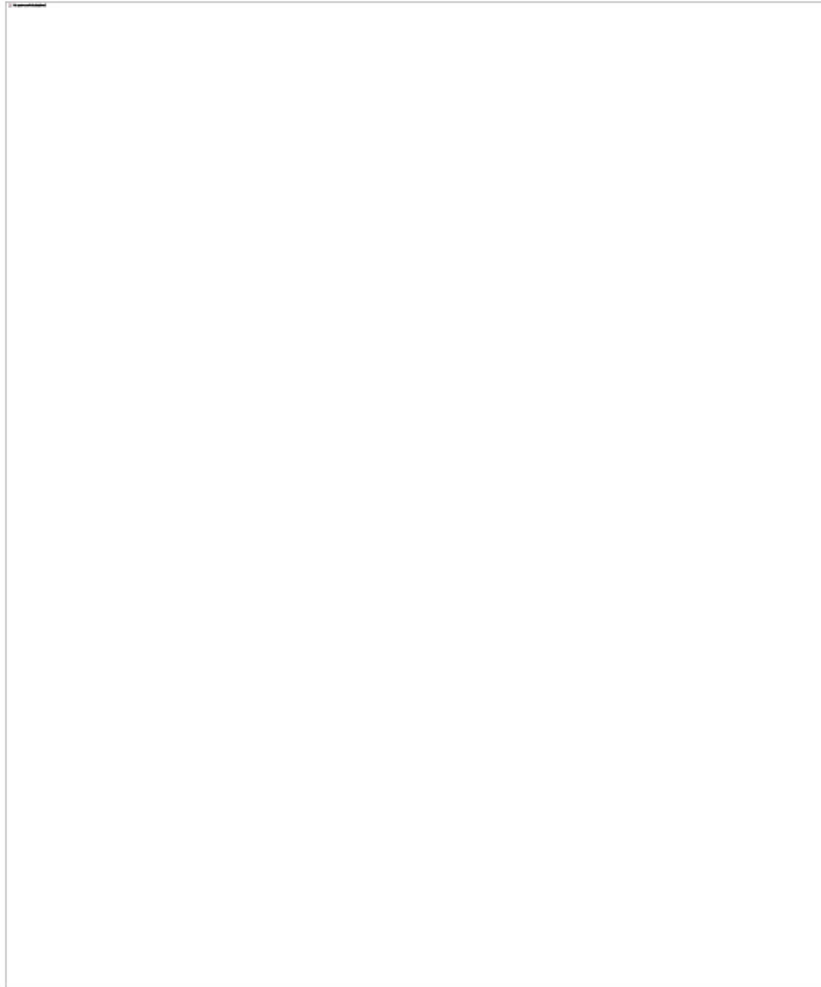
To achieve low earth orbit requires a velocity of about 25000 ft/sec. All the time the vehicle is in the atmosphere it is encountering drag. Before it reaches orbit it is fighting the pull of gravity. These losses must be made up by additional D_v. The value will depend on the aerodynamic profile of the vehicle and the trajectory flown. Typically these require an additional D_v of 5,000 ft/sec.

To leave low earth orbit and travel to the moon (Trans Lunar Injection) will require an additional 10,600 ft/sec. Mars is in an elliptical orbit relative to the Earth and its closest distance to earth varies on a 15-year cycle. At the lowest energy point, the D_v to achieve a Mar transfer orbit from LEO is about 13,000 ft/sec. The student might want to run the numbers and compare the size and weight of a stage going to Mars with a 500,000 lb payload using an Isp of 450 secs vs. 1100 secs. Don't forget you have to get back. This will require an additional 9500 ft/sec.

Conclusion

There are a few critical factors determining the design of a propulsive stage. Most of these are related to the engine design. For a thermal propulsion systems, these consist of propellant selection, gas temperature and pressure, area of the nozzle throat and the nozzle expansion ratio. The equations provided here are based on assumptions such as adiabatic conditions,

perfect gas, etc. While not completely accurate these equations provide very good approximations of the engine performance. The material presented is very top level and simplified and rocket system design can become highly analytical and quite rigorous. However the information should be sufficient to get the Mars Propulsion Team off to a good start.



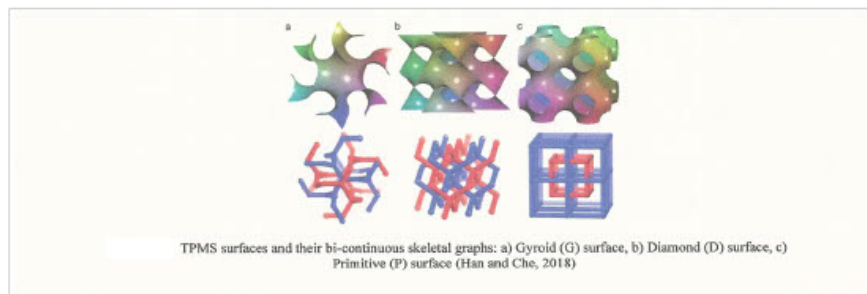
Appendix B: Rocket Science 101 Part 2

Rocket Science 101- Part 2

Congratulations. By now you should have mastered the equations in Rocket Science 101. These form the foundation of any thermal propulsion system and will apply equally as well to the discussions in Part 2. As discussed before thermal propulsion involves heating a gas in a chamber and allowing it to expand through a converging - diverging nozzle. In Rocket Science 101 a number of ways to heat the gas were discussed. One way that was not mentioned was what I'm calling Electric Resistance Thermal Propulsion (ERTP). In this approach the gas is passed through a heat exchanger that is heated by an electrical current. This is essentially the same technique used in nuclear thermal propulsion except in NTP the heat exchanger is heated by a nuclear reaction and the reactor is the heat exchanger. ERTP is an old construct that has not been considered because of past limits on the ultimate temperature and efficiency of the system. With new technologies these limitations can be removed. In this new construct the heat exchanger is built of a conducting material and is actually the heating element. Current is passed through the heat exchanger to generate heat. The temperature that the heat exchanger can produce is controlled by material properties. In recent years a new class of materials have evolved called Ultra High Temperature Ceramics (UHTC). Although they are called ceramics they are also metallic in composition and can conduct current. One of the most capable of these is Hafnium Carbide (HFC) with a melting point of 4231 °K. This would permit hydrogen passing through the heat exchanger to achieve very high temperatures and Isp. There is ongoing research to develop additive manufacturing (3D printing) capabilities with these materials.

The second new technology that can be applied is Triply Periodic Minimal Surfaces. Refer to:

<https://docs.lib.psu.edu/cgi/viewcontent.cgi?article=3392&context=iracc> for more details. These shapes have demonstrated up to 120% improvement in heat transfer coefficients compared to state of the art Printed Circuit heat exchangers and even more compared to shell & tube designs. The heat of the gas exiting the heat exchanger is dependent on the operating temperature of the heat exchanger and the efficiency of the heat exchanger.



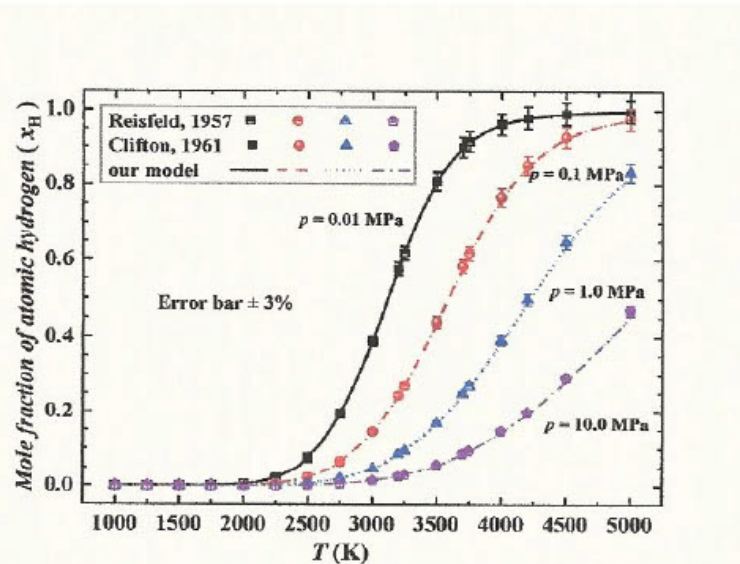
These new heat exchanger designs are enabled by additive manufacturing capabilities.

A third technology that could significantly increase the Isp of this concept is hydrogen molecular dissociation. Refer to:

www.researchgate.net/publication/360539509_Study_on_high-temperature_hydrogen_dissociation_for_nuclear_thermal_propulsion_reactor

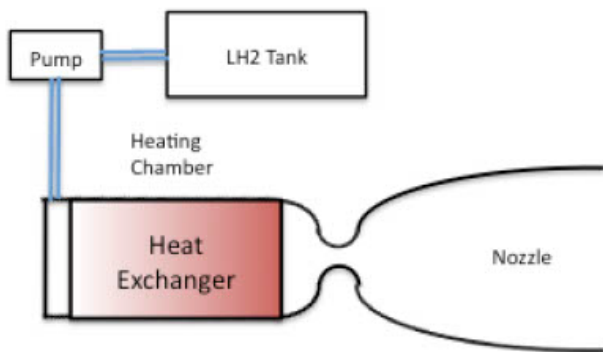
In Rocket Science 101 you learned that the ISP of a propulsion system was controlled by chamber gas temperature and specific heat. Hydrogen was said to be the gas with the best c_p . Hydrogen normally occurs as the diatomic gas H₂. There is actually a gas with a better c_p called monoatomic hydrogen or H₁. It has a c_p 44% better than H₂. This translates to a 20% increase in Isp.

As shown below, the transition of H₂ to H₁ is highly dependent on temperature. If electric resistance propulsion can reach temperatures as high as 3500°K a significant portion of the gas can be converted to H₁ with a corresponding increase in Isp. This phenomenon is not well understood. During your Senior Project you have the tools to do some calculations and speculate on the impact and propose future study and experimentation that would be done under your NASA proposal. An issue is the recombination of H₁ to H₂. When this occurs heat will be generated that effects Isp depending on where it occurs.



The Concept.

As shown below the heat exchanger would be housed in the heating chamber. The heat exchanger would be designed to generate the required conditions to heat hydrogen to the prerequisite temperatures by passing a current through the actual UHTC structure of the heat exchanger. The material thicknesses could be varied from bottom to top to produce the desired electrical resistance and temperature. Ideally the electrical resistance would be lower where the gas entered and increase toward the exit. Using a 300 $^{\circ}\text{K}$ margin between the highest operating temperatures and the melting point, a HfC heat exchanger would have a max temp of 3900 $^{\circ}\text{K}$. Assuming the gas comes out 200 $^{\circ}\text{K}$ below this value would (3700 $^{\circ}\text{K}$) the Isp would be 1185 secs if all the gas were all H₂. If 80% had been converted to H₁ the Isp would be 1362 sec.

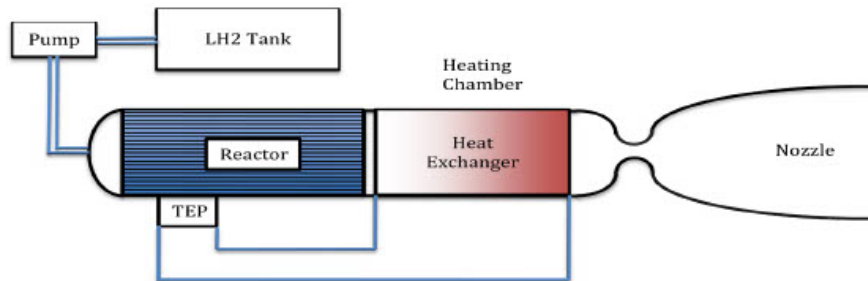


Electric Resistance Thermal Propulsion has the flexibility to be powered by either solar arrays or by a nuclear reactor. NASA is still investing in the development of nuclear electric propulsion. However the intent was to power an ion engine. Since ion propulsion really hasn't worked out, this may be a perfect alternative.

In the concept shown below an ERTP heat exchanger is used in conjunction with Nuclear Thermal Propulsion (NTP). This approach heats the gas to a hotter temperature than NTP alone. In other words it sort of acts like an afterburner. Since NTP operates below the temperature required to generate H1, this may also significantly boost the available Isp. If NASA's effort to develop NTP can't produce the prerequisite temperatures to achieve a Isp of 900 sec, ERTP would allow reactors to be designed and built that operate at a much lower temperature than currently planned.

Even if the extremely high temperatures can't be achieved, it still could be a better alternative than any other EP option.

The heat from the reactor can power a traditional electrical generation capability to power the ERTP. This required a considerable increase in system complexity. A simpler alternative would be use a Thermonic Electric Propulsion (TEP) module to convert waste heat generated by the reactor into electricity to power the ERTP unit.

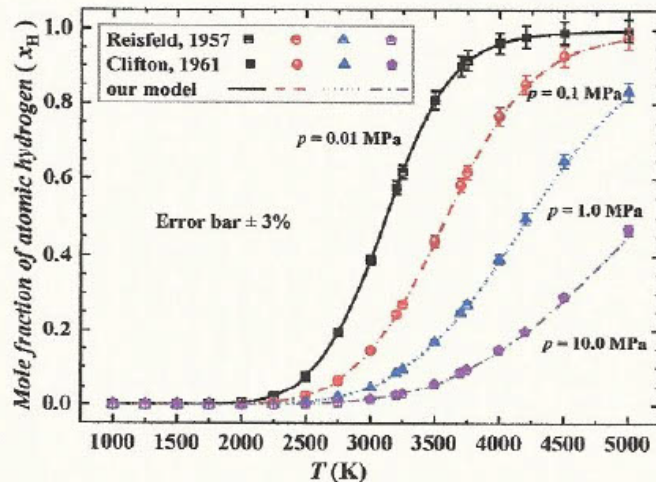


When you conduct the exercise of sizing a Mars Transfer vehicle you will find out that the low thrust of all other EP designs will require many thrusters operating for thousands of hours. I see no technical reason why ERTP solutions couldn't be sized in the same thrust class as NTP (thousands of pounds).

Appendix C: Atomic Rocket

Electric Resistance Thermal Propulsion with H₁ Or The Atomic Rocket

On earth hydrogen gas exists primarily in the form of diatomic molecules (H₂). However, when the temperature becomes high enough, dissociation of the molecule can occur and monoatomic or atomic hydrogen (H₁) can form. Based on studies from Xi'an Jiatong University, Figure 1 shows the relationship between H₁ generation vs. temperature and pressure.



Because H₂ is twice as heavy per mole as H₁, the M_f of the gas can be converted to a mass fraction (F_m) by dividing M_f by (M_f + 2 * (1 - M_f)). Using the first law of thermodynamics and the ideal gas law the specific heat of a monoatomic molecule can be calculated as:

$$5R/2 = 20.79 \text{ J Mol}^{-1} \text{ K}^{-1} \text{ or for } 20.8 \text{ kJ/Kg.}$$

where R is the universal gas constant.

For H₁ R = 8.31 J/Kg K and k is 1.66. This is significantly higher than the c_p for H₂ which varies with temperature and can be represented by $c_p = .0015*T + 13.77$. R for H₂ is 4.124 J/Kg K and k is 1.4. It has been recognized that the higher specific heat of H₁ will result in a higher Isp and better performance than for H₂. It has not been general recognized that a far more significant factor is that the heat of dissociation for hydrogen can be recovered during the thrust generation process to significantly increase Isp.

It requires approximately 4.46 EV to break the H₂ bond and create H₁. This translates to a dissociation energy (E_D) of 215 MJ/Kg of H₁ produced. The H₁ and H₂ molecules are in equilibrium with H₁ atoms being created and destroyed at the same rate and F_m represents the mass fraction of the gas that is H₁. However, if the temperature goes down or the pressure goes up, the mole fraction of H₁ will rapidly decrease. As the H₁ atoms recombine to form H₂ the energy of dissociation is released to increase the temperature of the gas. In the converging section of the nozzle the temperature drops as the gas moves toward the throat. If atomic hydrogen is present it will recombine to form H₂ and the resulting release of energy will reduce the temperature drop and increase the resulting I_{sp}. When the gas reaches the diverging portion of the nozzle the temperature and pressure will drop rapidly and any remaining atomic hydrogen will convert to diatomic hydrogen. Once again the resulting energy release will heat the gas and increase I_{sp}. The total energy released (E_R) = E_D*F_m)

To analyze the impact on exhaust velocity and I_{sp} an energy balance was performed on a control volume encompassing the nozzle. The energy entering the nozzle can be expressed as :

$$m*(h_0 + E_R + .5V_0^2)$$

where m is the mass flow rate,
 h_0 is the gas enthalpy,
 V_0 is the velocity of the gas entering the nozzle

The energy leaving the nozzle can be expressed as:

$$m*(h_1 + .5V_e^2)$$

where h_1 is the enthalpy of the gas leaving
 V_e is the exit velocity of the gas

Due to the principle of continuity we know

$$m*(h_0 + E_R + 12V_0^2) = m*(h_1 + .5V_e^2)$$

If V_0 is very small then:

$$h_0 + E_R = h_1 + .5V_e^2$$

or

$$V_e = (2*(h_0 - h_1 + E_R))^{.5}$$

Since

$$h_0 - h_1 = c_p(T_0 - T_1)$$

where c_p is the specific heat of the gas

then if T₁ is negligible

$$V_e = (2 * (c_p * T_0 + E_R))^{0.5}$$

These equations were incorporated in the attached Excel spreadsheet.

From the above chart an H1 Mole Fraction of .6 was determined given a temperature of 3700 °K and a pressure of .1MPa and were entered, in the Atomic H spreadsheet. The result was an Isp of 1822 secs. This is 4 times better than chemical propulsion and 2 times better than the planned performance of NASA's Nuclear Thermal Propulsion program.